Department of Companion Animals and Horses

University of Veterinary Medicine Vienna

Equine Surgery Unit

(Head: Univ.-Prof. Dr.med.vet. Florien Jenner, Dipl.ACVS Dipl.ECVS)

Characterization of extracellular vesicles from equine bone marrow-derived mesenchymal stem cells and their therapeutic potential

PhD thesis submitted for the fulfillment of the requirements for the degree of

DOCTOR OF PHILOSOPHY (PhD)

University of Veterinary Medicine Vienna

submitted by

Robert Soukup

Vienna, September 2023

1 Acknowledgments

I would like to express my sincere gratitude to the following individuals who have been instrumental in the successful completion of this thesis: Firstly, I would like to thank my wife, Bianca, for her unwavering support, encouragement, and motivation throughout this journey. Her constant belief in me and her patience during the ups and downs of this process have been invaluable. I would also like to extend my thanks to Iris for her scientific support, guidance, and valuable feedback throughout my research. Her expertise in the field has been instrumental in shaping this thesis. I am also grateful to my lab team, especially Sinan, for their technical support and for always being available to answer my queries. Their constant support has been crucial in ensuring the smooth progress of my research. Finally, I would like to acknowledge the contributions of my supervisors, Florien and Giovanni, for their guidance, mentorship, and for developing me as a researcher. Their insights and feedback have been invaluable in shaping the direction of my research. I am grateful to each one of you for your invaluable contributions and support, and for being a part of this journey with me.

2 Contributions

2.1 Publication list

Robert Soukup, Iris Gerner (shared first authorship), Sinan Gueltekin, Hayeon Baik, Johannes Oesterreicher, Johannes Grillari and Florien Jenner; Characterisation of extracellular vesicles from equine mesenchymal stem cells. Accepted for publication on 17 May 2022

Robert Soukup, Iris Gerner, Thomas Mohr, Sinan Gueltekin, Johannes Grillari and Florien Jenner; Mesenchymal stem cell conditioned medium modulates inflammation in tenocytes: complete conditioned medium has superior therapeutic efficacy than its extracellular vesicle fraction. Accepted for publication on 23 June 2023

2.2 Contribution

2.2.1 Experimental design

Florien Jenner, Johannes Grillari, Iris Gerner and Robert Soukup designed the experiments and defined the conditions.

2.2.2 Experiments

Experiments were performed by Robert Soukup with Sinan Gültekin providing technical assistance.

2.2.3 Data analysis

Data analysis was performed Florien Jenner, Johannes Grillari, Iris Gerner and Robert Soukup. Thomas Mohr did the computational analysis of the differential expression data.

2.2.4 Writing of the thesis

Robert Soukup wrote this thesis with the aid of Florien Jenner, Johannes Grillari and Iris Gerner who did the proofreading and the corrections.

3 Declaration

I declare that: (a) The thesis submitted for assessment is entirely my own work and has not been previously submitted for any other assessment. Furthermore, I have appropriately acknowledged all debts for words, data, arguments, and ideas used in this thesis. (b) The thesis adheres to the presentation and style guidelines outlined in the relevant documentation.

4 Table of contents

5 Summary

Tendinopathy is a common tendon disorder caused by overuse injury, resulting in chronic pain and impaired biomechanical tendon properties. Current treatments do not effectively restore tendon function, highlighting the need for better options. Regenerative medicine, which aims to restore damaged tissues and organs, offers potential solutions using approaches like stem cell therapy. Mesenchymal stem cells (MSCs) are a promising strategy due to their ability to differentiate into different cell types and secrete bioactive molecules. Recent studies suggest that the paracrine effect of MSCs, specifically their secretome (which includes growth factors, cytokines, and extracellular vesicles), plays a crucial role in tissue regeneration.

This study focuses on evaluating the therapeutic effect of the secretome of equine MSCs and its sub-fractions, extracellular vesicles (EVs), and soluble proteins, on inflamed tenocytes. The author emphasizes the need for standardized methods for isolating and characterizing EVs in order to develop EV-based regenerative therapies. The similarity between tendinopathies in horses and humans suggests that the findings may have implications for both species.

Various studies have shown the regenerative potential of MSC-conditioned media (CM) and EVs in tendon repair, promoting cell proliferation, tissue architecture restoration, and the expression of genes related to collagen and tendon matrix formation. However, the exact mechanisms of action and the specific bioactive molecules responsible for therapeutic effects remain unclear. Standardized purification and analytical methods are crucial for understanding and developing reliable EV-based regenerative therapies.

The study also highlights the importance of optimal donor cells, their preconditioning status, and the age or passage number of MSCs in the secretome's therapeutic efficacy. Allogeneic MSCs offer a cell-free, off-the-shelf treatment option with scalable and standardized manufacturing. Additionally, future studies should focus not only on quantitative parameters but also on qualitative aspects, such as the identification of specific components and their regenerative effects.

Overall, this research contributes to understanding the therapeutic potential of MSC secretomes and their sub-fractions in tendon repair, emphasizing the need for standardized methods, characterization, and dosage determination to advance EV-based regenerative therapies.

6 Zusammenfassung

Die Tendinopathie ist eine häufig auftretende Sehnenerkrankung, die durch Überlastungsverletzungen verursacht wird und zu chronischen Schmerzen sowie Beeinträchtigungen der biomechanischen Eigenschaften der Sehne führt. Aktuelle Behandlungen stellen keine effektive Wiederherstellung der Sehnenfunktion sicher, was den Bedarf nach besseren Optionen hervorhebt. Die regenerative Medizin, die darauf abzielt, geschädigtes Gewebe und Organe wiederherzustellen, bietet potenzielle Lösungen durch Ansätze wie die Stammzelltherapie. Mesenchymale Stammzellen (MSCs) sind eine vielversprechende Strategie aufgrund ihrer Fähigkeit, sich in verschiedene Zelltypen zu differenzieren und bioaktive Moleküle abzusondern. Aktuelle Studien deuten darauf hin, dass der parakrine Effekt von MSCs, insbesondere ihr Sekretom (zu dem Wachstumsfaktoren, Zytokine und extrazelluläre Vesikel gehören), eine entscheidende Rolle bei der Geweberegeneration spielt. Diese Studie konzentriert sich auf die Bewertung der therapeutischen Wirkung des Sekretoms von Pferde-MSCs und seiner Subfraktionen, extrazelluläre Vesikel (EVs) und lösliche Proteine, auf entzündete Tenocyten. Der Autor betont die Notwendigkeit standardisierter Methoden zur Isolierung und Charakterisierung von EVs, um EV-basierte regenerative Therapien zu entwickeln. Die Ähnlichkeit zwischen Tendinopathien bei Pferden und Menschen legt nahe, dass die Ergebnisse für beide Arten Bedeutung haben könnten. Verschiedene Studien haben das regenerative Potenzial von MSC-Konditionierungsmedien (CM) und EVs bei der Sehnenreparatur gezeigt, indem sie die Zellproliferation, die Wiederherstellung der Gewebearchitektur und die Expression von Genen, die mit der Kollagen- und Sehnenmatrixbildung in Verbindung stehen, fördern. Die genauen Wirkmechanismen und die spezifischen bioaktiven Moleküle, die für therapeutische Effekte verantwortlich sind, bleiben jedoch unklar. Standardisierte Reinigungs- und Analysemethoden sind entscheidend, um EV-basierte regenerative Therapien zu verstehen und zu entwickeln. Die Studie hebt auch die Bedeutung optimaler Spenderzellen, ihres Vorbedingungsstatus und des Alters oder der Passagenanzahl von MSCs für die therapeutische Wirksamkeit des Sekretoms hervor. Allogene MSCs bieten eine zellfreie, sofort verfügbare Behandlungsoption mit skalierbarer und standardisierter Herstellung. Darüber hinaus sollten zukünftige Studien nicht nur auf quantitativen Parametern, sondern auch auf qualitativen Aspekten wie der Identifizierung spezifischer Komponenten und ihrer regenerativen Wirkungen liegen. Insgesamt trägt diese Forschung dazu bei, das therapeutische Potenzial von MSC-Sekretomen und ihren Subfraktionen bei der Sehnenreparatur zu verstehen, und unterstreicht

die Notwendigkeit standardisierter Methoden, Charakterisierung und Dosierungsberechnung, um EV-basierte regenerative Therapien voranzutreiben.

7 Introduction

Tendinopathy is a tendon disorder often resulting from overuse injury, which leads to impaired biomechanical tendon properties and chronic pain. It is the most common musculoskeletal complaint for which human patients seek medical attention and is prevalent in both occupational and athletic settings, afflicting 25 % of the adult population and accounting for 30–50 % of all sports-related injuries [1]. The Achilles tendon, the largest and strongest tendon in the human body, is involved in as many as half of all sports-related injuries [2]. Tendon injuries are also a prevalent problem in horses especially in performance horses. The equine structure most at risk of suffering a tendon injury is the superficial digital flexor tendon (SDFT) with an incidence rate of up to 53 % and a re-injury rate of up to 80 % [3–10]. However, no current treatment, neither in human nor veterinary medicine, restores the functional properties of injured tendons resulting in inferior scarring repair, reduced elasticity and consequently high re-injury rates. Better treatment options are therefore highly needed.

Regenerative medicine is a multidisciplinary field that aims to restore, replace or regenerate damaged or lost tissues and organs by using different approaches such as stem cell therapy, tissue engineering, and gene therapy. Mesenchymal stem cell (MSC) therapy is one of the promising strategies in regenerative medicine because they are easy to obtain and due to their ability to differentiate into various cell types and secrete numerous bioactive molecules that modulate the immune response and promote tissue repair and regeneration [11]. Promising advances have been made in the treatment of equine tendon injuries with MSCs as therapeutic agent which resulted in a reduced reinjury rate and better tendon echogenicity [12–15]

However, the exact mechanism of how MSCs exert their therapeutic effects is still unclear. Recent studies have suggested that the paracrine effect of MSCs, specifically their secretome, may play a crucial role in tissue regeneration rather than their differentiation potential. The secretome of MSCs includes various bioactive molecules such as growth factors, cytokines, chemokines, and extracellular vesicles, which are involved in several physiological processes such as cell proliferation, differentiation, and immune modulation which bear regenerative potential. However, it is still not clear which components of the MSC secretome are responsible for its regenerative potential, whether it is the whole secretome or just fractions of it. Further studies are needed to identify the specific bioactive molecules that contribute to the therapeutic effect of MSCs.

This work evaluates the therapeutic effect of the secretome of equine MSCs and its sub-fractions, extracellular vesicles (EVs) and the soluble proteins, on inflamed tenocytes to evaluate their potential as a future therapeutic agents. This required some preliminary work in order to properly characterize equine EVs. The International Society for Extracellular Vesicles (ISEV) published a position paper to provide minimal criteria (MISEV criteria) for the isolation and characterisation of human EVs to better exchange EV data and counteract methodological inconsistency [16]. However, guidelines for equine EV work were still missing but standardised purification and analytical methods are a crucial prerequisite for the development of EV-based regenerative therapies. The importance of proper EV characterisation and standardize EV isolation methods is outlined and discussed in the first Paper of this PhD Thesis.

The second paper examined the effects of different fractions of bone marrow-derived mesenchymal stem cell (MSC) secretome on inflamed tenocytes and found that the complete conditioned media (CM) had the most potent treatment effect, while the extracellular vesicle (EV) and protein fractions showed less influence on gene expression. However, standardization, dosage, route of administration, clearance of EVs, and other factors present challenges in comparing CM and its subfractions and need to be addressed for successful translation into clinical applications of cell-free therapies.

7.1 Tendons & Tendinopathies

7.1.1 Tendon Biology

Tendons are soft connective tissue structures responsible for joint movement by transmitting forces from the muscle to the bone. The biomechanical properties of tendons depend on the specialized biophysical and biochemical composition defined by the extracellular matrix (ECM) architecture, ECM biophysics, cell-matrix interactions and molecular gradients [17]. The ECM consists of 60-80 % water, longitudinally aligned collagen fibers, proteoglycans, glycosaminoglycans, glycoproteins, elastin and other small molecules [18]. The smallest component of tendons are collagen molecules which are arranged longitudinally. Intermolecular crosslinks bind groups of five collagen molecules together to form microfibrils which further pack together, forming fibrils [19,20]. These fibrils are further stabilized by crosslinking and aggregate to form collagen fibers which are aligned longitudinally. This assures elasticity and the crimp pattern of the fibres provides additional energy storing capabilities [21]. Each fascicle, which is the largest subunit of aggregated collagen fibers, is surrounded by a connective tissue compartment called the interfascicular matrix (IFM) [22].

Collagen I which is arranged in tensile-resistant fibres is the main tendon collagen. Also, collagen types III, IV, V and VI are present [23–26] Proteoglycans (PGs), glucosaminoglycans and glycoproteins attract water and provide functional stability to the collagen structure [27]. In addition, other small leucine-rich PGs such as fibromodulin, biglycan, and lumican, together with osteoadherin, tenascin-C, proline arginine rich and leucine-rich repeat protein, optican, keratocan, epiphycan, syndecan, perlecan, agrin, fibronectin, laminin, versican, and aggrecan are present in tendon tissue [26,28,29].

The force transmission is dependent on the structural integrity between individual muscle fibers and the ECM as well as the fibrillar arrangement of the tendon which absorbs and loads energy [30–32]. Furthermore, the ECM serves as scaffold for adhesion of cell tyrosine kinase receptors [33,34]. This interaction leads to activation of intracellular signaling pathways and cytoskeletal rearrangement [35–37]. Integrin molecules link the ECM to the cytoskeleton and establish a mechanical continuum along which forces can be transmitted from the outside to the inside of the cell and the other way round [38–41]. Several studies describe the expression of ECM components and their receptors in fibroblasts under stretched or relaxed conditions *in vitro* and found out that collagen XII and tenascin-C increase their expression and synthesis when fibroblasts are stretched and are suppressed in cells that are left in a relaxed state [41,42].

7.1.2 Tendinopathy

Tendinopathy is a tendon disorder often resulting from overuse injury which leads to impaired biomechanical tendon properties and chronic pain. No current treatment restores the functional properties of injured tendons resulting in significant impact on quality of life and high socioeconomic pressure with the annual health expenditure on human tendon injuries exceeding €145 billion [43,44].

The prevalence of tendinopathies may increase due to extrinsic factors like mechanically demanding work or sports activities and intrinsic factors like age, obesity and diabetes [44]. The Achilles tendon in humans is functionally and clinically equivalent to the superficial digital flexor tendon (SDFT) which is the structure most at risk for suffering an injury in horses with an incidence of as high as 53 % and re-injury rates of up to 80 % [3–10]. Similar as in humans, horses show an age-related trend towards matrix degeneration which includes matrix fibrillation, chondroid metaplasia, chondrone formation, neovascularisation and fibroplasia [4]. The prevalence of tendinopathies is increased by the same extrinsic factors as in humans. Due to the tendon tissue's poor intrinsic healing ability, matrix micro-damage may accumulate over time, overwhelming the capacity of cells to repair structural defects before subsequent loading cycles, lead to clinical injury [45,46]. Another reason for the development of a tendinopathy is a single serious injury.

Tendinopathies are characterized by alterations in tendon structure, composition, and cellularity which leads to pain and reduced tendon elasticity resulting from the formation of fibrovascular scar tissue in an attempt to repair the injured tendon [44]. The resulting scar tissue precludes the tendon from regaining the biomechanical characteristics of normal tendons, which leads to chronic tendinopathies with an increased predisposition for mechanical failure and resulting in high re-injury rates [1,47].

7.2 Tendon healing

The repair process of tendons is highly orchestrated and can be divided into three overlapping phases characterized by specific cellular and molecular cascades involving extrinsic and intrinsic healing.

In the initial inflammatory phase inflammatory cells, at first mainly neutrophils, are directed to the injury site by pro-inflammatory cytokines like interleukin -6 (IL-6) which in turn induce cytokine and matrix metalloproteinase-1 (MMP1) expression in tenocytes [48]. Later on, macrophages represent the dominating leucocytes. The initial inflammatory response targets

the removal of necrotic tissue and the release of growth factors that induce neovascularization and further initiate chemotaxis of fibroblasts and tenocytes which pave the way for tissue repair [49]. There is growing evidence that inflammation (the first phase of the injury response), or the lack of its resolution, has a crucial role in disease progression, especially when shifting to a chronic state [2,43,44,47,50–55]. The inflammatory milieu can modify tenocyte physiology by increasing metabolic activity and inducing an activated, proinflammatory phenotype with inflammation memory and the capacity for endogenous production of inflammatory cytokines such as tumor necrosis factor-α (TNF-α) and Interleukin-1β (IL-1β) [55]. After a few days and peaking at three weeks post-injury tendon healing enters the proliferative phase.

Growth factors such as basic fibroblast growth factor (bFGF), bone morphogenetic proteins (BMPs) -5, -6 and -7, -12, -13, and -14 also known as growth and differentiation factors (GDFs), transforming growth factor beta (TGFβ), insulin-like growth factor-1 (IGF-1), platelet-derived growth factor (PDGF) and vascular endothelial growth factor (VEGF) facilitate tissue repair [56]. Tenocytes synthesize abundant ECM predominately consisting of randomly arranged collagen type III and proteoglycans.

During the remodeling phase, which begins 6-8 weeks post injury, matrix synthesis decreases and collagen type III is replaced by collagen type I. Collagen fibers align along the longitudinal axis of the tendon to enhance tensile strength and elasticity [56]. Unfortunately, the healed tendon does not regain the mechanical properties of an uninjured one which is mainly due to reduced integration of collagen fibers with a higher ratio of collagen type III to collagen type I and a lack of proper fibre alignment.

7.3 Treatments in regenerative medicine

Traditional treatments for equine and human tendon injuries include physical therapies, followed by slowly ascending exercise or anti-inflammatory drugs [57]. In human medicine severely injured tendons can additionally be treated using tendon grafts and suture anchors however with various possible complications such as rejection, adhesion or disease transmission [58–60]. Nevertheless, none of these treatments can fully restore the functional capabilities of a healthy tendon and they hence lead to the formation of biomechanically inferior scar or replacement tissue, causing high reinjury rates, degenerative disease progression and chronic morbidity. Hopes for the future lie on regenerative medicine approaches which may have the potential to improve outcomes compared to traditional therapies.

For the treatment of various musculoskeletal indications in equine medicine, multiple regenerative therapies, such as platelet-rich plasma (PRP), autologous conditioned serum (ACS), and MSCs are applied. Autologous blood products, such as PRP and ACS, exert their effect based on the secretome of the contained blood cells. The MSC secretome is the entity of released organic and anorganic molecules [61]. The secretome mirrors the ability of the parental cells to condition and program the surrounding microenvironment, influencing a variety of endogenous responses, in injured tissues. It affects neighboring cells and may have substantial potential in regenerative medicine. The secretome comprises soluble and vesicular proteins, lipids, RNA (mRNA and non-coding RNAs), and DNA [62–69].

The immunomodulatory and pro-regenerative effect of both PRP and ACS is based on growth factors and cytokines released from the platelet alpha granula, leucocytes and stem cells. The administration aims at reducing inflammation, protecting intact and newly formed tissue, recruiting cells such as MSCs, macrophages, and other pro-regenerative cells and at supporting neovascularization by supplying growth factors, cytokines, and nutrients [70]. Still, the composition of these products is subject of high variation depending on the physiological state of the patient or the sample processing technique leading to difficulties in comparing study results [71–73].

PRP is derived from anticoagulated blood through centrifugation to increase the platelet concentration. The spectrum of growth factors and cytokines of PRP includes platelet-derived growth factor (PDGF), insulin-like growth factor (IGF), transforming growth factor beta (TGF-β1), vascular endothelial growth factor (VEGF), fibroblast growths factor (FGF), platelet-derived epidermal growth factor (PDEGF), osteocalcin, osteonectin, fibronectin and thrombospondin [74].

ACS is a cell-free blood product derived from blood during and after coagulation which also contains active growth factors and cytokines similar to PRP but the concentration is different because the platelets are not enriched. Due to being a cell-free product, ACS can easily be frozen and stored as compared to PRP [75,76]

MSCs show great potential for regenerative medicine which will be explained in detail in the next chapter. Tendon treatment with MSCs has been employed in equine orthopaedics since 2003 and has yielded promising results reducing reinjury rates in the equine SDFT from 56 % to 18 % [5,14,15,77–81]. Yet, translational progress into human clinical practice so far is disappointing, partially due to the regulatory and manufacturing challenges inherent to all cell

therapies and safety concerns such as potential tumorigenicity [82]. In brief, their therapeutic effect is based on the secretion of bioactive factors, referred to as the secretome, which modulate the immune response, reduce inflammation, inhibit cell death, and induce and stimulate endogenous regeneration. However, little is known about the components and sub-fractions of the MSC secretome and whether the entire secretome, isolated membrane-bound extracellular vesicles (EVs) or soluble factors such as proteins are required to achieve a therapeutic effect. This work focuses on these open questions and tries to answer, how the secretome of MSCs and its sub-fractions, impact inflamed tenocytes.

Stem cells can be classified into two groups, embryonic and adult. Embryonic stem cells are obtained from the inner cells mass of blastocytes and are pluripotent [83]. In contrast, adult stem cells are obtained from peri-natal or post-natal sources and can be either multipotent or unipotent [83]. Adult stem cells include both hematopoietic stem cells (HSC) and MSCs [84]. A position paper by Dominici et al. was published in which the Mesenchymal and Tissue Stem Cell Committee of the International Society for Cellular Therapy proposed minimal criteria to define (human) MSCs to assure uniformity [85]. Besides their capability to differentiate toward osteoblasts, adipocytes and chondroblasts, they must be plastic-adherent when maintained under standard culture conditions, and they must be positive for the surface markers CD105, CD73 and CD90, and lack expression of CD45, CD34, CD14 or CD11b, CD79α or CD19 and HLA-DR surface molecules [85]. MSCs can be isolated from various sources like adipose tissue, bone marrow, umbilical cord matrix, peripheral blood, umbilical cord blood, synovial membrane and synovial fluid using different protocols [5,14,78,86–97].

In vivo MSCs maintain homeostasis of the organism in normal conditions by replacing damaged cells in tissues and organs [98]. Upon induction of an injury, they have immunomodulatory capacities and display several pro-regenerative characteristics like pro-angiogenic, anti-inflammatory and anti-apoptotic properties after migrating to the site of injury [99–102].

The interest in MSCs is still ongoing, and they have become a popular cell source in regenerative medicine and immune modulation [103–105]. In clinical applications, autologous and allogeneic MSCs are used to repair damaged tissues and enhance the function of damaged tissues and organs [106]. Over 1.000 clinical studies are ongoing using MSCs to treat various clinical conditions (clinicaltrials.gov; search conducted March 16th, 2022). However, the administration of cells is not free of safety concerns, which include potential tumorigenicity and

their ability to elicit an immune response [82]. Additional concerns about using MSCs for clinical applications include the lack of standardized protocols for their isolation and culture and the lack of evidence-based guidelines for the optimal delivery route and cell dosage [107,108]. Following systemic application, the vast majority of administered MSCs are trapped in the lungs of the patients and do not reach their desired target [109,110]. Upon local administration, they show low viability and poor engraftment [111–113]. Furthermore, allogeneic MSCs potentially express disease candidate genes which can be transmitted from the donor to the patient as well as other potential pathogens.

7.4 Therapeutic potential of MSCs

The efficacy of MSCs is highly donor dependent. Both ageing and disease are associated with perturbations at the genomic, epigenomic, and proteomic levels which negatively influence MSC proliferation, differentiation and paracrine signaling function and thus the therapeutic potential of cell therapies [112,114–118]. A benefit of allogeneic MSC administration is the possibility of donor selection and off-the-shelf availability - the donor cells can be isolated and expanded in advance rather than at the timepoint when an injury occurred [119,120].

In addition to donor age and disease, intrinsic properties of MSCs are highly dependent on their tissue of origin and its surrounding microenvironment, such as inflammation and disease status [5]. In juvenile MSCs, higher proliferation rates, longer lifespans, and lower immunogenicity were demonstrated compared to cells from adult donors [121–125]. On the other hand, it was recently discovered that *in vitro* expansion of adipose stem cells may affect the cells more than natural aging of their donor [126]. MSCs derived from diverse tissue sources exhibit distinct differentiative and therapeutic capabilities, a phenomenon similarly observed in their paracrine factors. Consequently, this variance contributes to the heterogeneity of MSC populations, thereby influencing their therapeutic efficacy [127–129]. One strategy to overcome this problem is the utilization of colonies derived from a single cell, however this requires optimized and standardized cell culture protocols [130]. All the influencing factors listed above need to be considered when studying the therapeutic potential of MSCs and when using them for cell therapies to ensure comparability and consistency.

In equine regenerative medicine MSCs have been used for almost two decades to treat musculoskeletal disorders like osteoarthritis and tendinopathies. Treating injuries of the SDFT with MSCs is not only a common approach but was also the first attempt of using MSC to regenerate a musculoskeletal tissue. Since then, various studies were performed using MSCs from different sources. The treatment effect of bone marrow (bmMSCs) and adipose tissue derived MSCs (ADSCs) on injured tendon tissue was evaluated in several studies with long and short-term follow up. Overall, the studies showed a considerable improvement of tendon regeneration following MCS application compared to the non-treated control group [87]. Umbilical cord blood derived MSCs (ucbMSC) were also used to treat injured tendons with similar positive effects despite their allogeneic origin [88,131]. Interestingly, other studies could not find significant differences in tendon healing between patients treated with MSCs and the serum receiving control groups [132]. However, in most studies, the re-injury rate in horses with tendon or ligament injuries treated with MSCs was significantly lower compared to horses receiving

conventional treatments [78,91]. MSC treatment seems to prevent the progression of the tendinopathies and promote a greater organization of collagen fibers, a decreased inflammatory infiltrate, higher fibroblastic density, more neovascularization, a higher echogenicity score and less collagen type III in the tendon tissue [87,133–136].

The therapeutic potential of MSCs was initially thought to be based on their capability to differentiate into resident cell types of the injured host tissue and homing at the site of injury [136]. However, more recently, it was discovered that the pro-regenerative and immunomodulatory potential of MSCs is predominantly based on to their paracrine effect. MSCs secrete bioactive factors that reduce inflammation, modulate the immune response, inhibit cell death, promote wound healing and angiogenesis, and provide significant pro-regenerative effects [62–64,137–139].

The concerns related to cell therapies like low viability, poor engraftment after injection and potential immune rejection might be bypassed by using the secretome of MSCs, which has none of those adverse effects compared to using MSCs themselves. The secretome can be produced in large quantities which are storable and administered off-the-shelf. Nevertheless, it is still unclear whether components of the secretome act synergistically or redundantly and whether the entire secretome, isolated EVs or soluble factors are required to achieve a therapeutic effect [140,141] . The mechanisms of action and the optimal timepoint of administration of each component could enhance the success of cell-free therapies.

Cell-free therapies have shown promising therapeutic and immunomodulatory potential in acute myocardial infarction (AMI) and acute kidney injury (AKI) models and were evaluated in various other conditions described below [63,142–150]. Previous studies report, that rat tenocytes experience an improvement in proliferation rate and a reduction of inflammatory markers compared to the control group upon treatment with CM from MSCs. Positive therapeutic effects of human adipose derived MSC secretome was reported on various skin cells which experienced significant mitogenic effects [151]. MSC-CM, stimulates axonal growth of neurons in rats and increased Schwann cell proliferation in humans [152,153]. Immunomodulatory effects, like reduction of immune response in inflammatory arthritis in mice upon MSC-CM treatmentand the ability of CM from embryonic stem cells to restore macrophage function in spinal cord injury, were reported [154155]. Interestingly, some studies found that the stem cell secretome is capable to reduce reactive oxygen species and oxidative stress [156,157]. In addition, it was recently discovered that human MSC-CM has anti-apoptotic abilities in hepatocytes and can

down-regulate miR143 which plays a detrimental role in cell cycle arrest [158]. Furthermore, CM of human embryonic MSCs reduces replicative senescence in adult MSCs and cardiomyocytes [159,160]. MSC-CM promotes tendon-bone healing of the rat rotator cuff via regulation of immune response [161]. It further promoted rat tenocyte proliferation via activation of extracellular signal-regulated kinase1/2 (ERK1/2) signal molecules compared to the untreated control group [162]. Similarly, MSC-CM promoted tendon-bone healing of the rat rotator cuff by inhibiting M1 and supporting M2 macrophage polarization [161]. In horses, CM of amniotic membrane-derived mesenchymal cells inhibited proliferation of PBMCs and are beneficial for tendon disease *in vivo* [163]. A study of horse amniotic membrane-derived mesenchymal cells and its CM reports that the CM decreased peripheral blood mononuclear cells (PBMCs) proliferation significantly, which suggests immunosuppressing effects of the soluble factors. In addition, MSC-CM demonstrated an immunomodulatory effect by inhibiting proliferation of PBMC *in vivo* and induced neovascularization, which was not observed before treatment and declined during progression of the healing process characterized by a decrease of vessel size and quantity in horses [163].

All these findings indicate the broad application range of CM for regenerative medicine. Characterizing the various components of the secretome and their effector molecules will contribute significantly to the understanding of the mode of actions of this promising treatment.

7.5 Extracellular Vesicles

In addition to a number of soluble factors, cells secrete various membrane-bound EVs which are categorized according to their diameter into apoptotic bodies (>1000 nm), microvesicles (100–1000 nm) and exosomes (30–150 nm) [164]. Exosomes (30-150nm) have a defined mode of biogenesis and are highly interesting for regenerative applications because they have been shown to play essential roles in intercellular communication [165,166]. EVs above that size are less homogenous in origin e.g. particles above 500 nm are either apoptotic bodies, conglomerates of proteins or other contaminants which are not desired and are characteristic for poor EV isolates [16]. The international society for extracellular vesicles (ISEV) propose additional parameters for the classification of EVs like biomarkers and cells of origin [16]. Prominent membrane-bound and cytosolic biomarker proteins found in or on exosomes are members of the tetraspanin family (CD9, CD63 and CD81), an endosomal sorting complex required for transport (ESCRT) of proteins (Alix, TSG101), integrins, heat shock proteins (Hsp) and actin [167,168].

Various studies reported that cells release large amounts of exosomes into the extracellular environment. Exosomes act as essential mediators of cell communication. Released from parental cells they have a subsequent influence on the target cell, which is highly dependent on the characteristics of the parental cell [169]. This influence is mediated through direct stimulation of target cells, transfer of activated receptors to recipient cells and epigenetic reprogramming via delivery of functional proteins, lipids, and RNAs [170]. Reports indicate that different exosome subpopulations with unique characteristics and cargo may be distinguished based on their size and surface but little is known about the underlying processes responsible for cargo selection [171,172]. Cargo sorting is possibly dependent on a combination of internal and external factors influencing the donor cell [173,174].

In addition to the properties explained above, exosomes can be further distinguished by their distinctive biogenesis pathways [174].

7.5.1 Biogenesis

Exosome biogenesis is a complex process dependent on the cellular environment, cell differentiation and maturation status [175,176] Upon formation, exosomes are released from endosomes either via inward-budding of the endosomal membrane to form intraluminal vesicles (ILVs), generating multivesicular bodies (MVBs) or via outward-budding at the plasma

membrane. Both principles function either via direct budding of the plasma membrane or through the Endosomal Sorting Complexes Required for the Transport (ESCRT)-dependent pathway and the ESCRT-independent pathway [177–180].

The best characterized mechanism involves the ESCRT machinery to ubiquitinate proteins in the early endosome [177]. Each ESCRT complex consists of multiple proteins with various functions. ESCRT-0 recruits ESCRT-I, and together with ESCRT-II, they promote inward budding by recognizing and sequestering ubiquitinated membrane proteins and initiating intraluminal membrane budding. The ESCRT-III complex completes membrane budding by sequestrating MVB proteins and actual scission of ILVs into the extracellular milieu as exosomes [181–183].

An alternative pathway of exosome formation involves synthesis of ceramide as a mechanism to induce vesicle curvature and budding [184]. The third mechanism which mediates exosome biogenesis is tetraspanin-mediated organization of specific proteins [185].

7.5.2 Exosome uptake

Recent studies suggest that exosome uptake is not a random process but rather a highly orchestrated process based on proper receptor and ligand interaction as well as on origin and status of the exosome and its donor cell, the environment, and the recipient cell's status [186–191].

Exosomes can transmit intercellular signals by direct contact via their surface ligands or internalization through direct membrane fusion or endocytosis in order to release their cargo into the target cell [192–194]. Direct contact between the exosome and recipient cell lipid bilayers can lead to membrane fusion induced by SNARE proteins [195,196]. Docking and subsequent endocytosis of exosomes are dependent on protein-protein interactions: Tetraspanins are membrane proteins that can form tetraspanin-enriched microdomains (TEMs), which mediate vesicular fusion [197].

Exosomes are internalized by the target cells via various pathways. The clathrin-mediated endocytic pathway uses transmembrane receptors and ligands which form clathrin-coated vesicles that fuse with endosomes, followed by cargo release [198]. An alternative pathway is the lipid raft-mediated endocytosis pathway which shifts the cargo into the early endosome [199]. Phagocytosis is typically involved in engulfing bacteria or dead cells but can also internalize

exosomes. It is a stepwise process during which the cell membrane encircles the particles and forms phagosomes [199].

After cellular uptake, exosomes travel along intracellular filamentous structures to the site of their destination [200]. They follow the endosomal pathway to lysosomes and eventual degradation [201,202]. However, cargoes avoid degradation by exploiting the gradual acidification through the endosomal compartments, and some cargoes can passively diffuse across the cytoplasm [203–206]. The Endoplasmic reticulum (ER) is the target site for exosomes carrying mRNA and miRNAs to unload their cargo leading to immediate translation. This route is potentially possible as ER scanning can occur after exosome sorting into the endosome trafficking circuit [207]. Micro-RNAs (miRNAs) are a class of tissue-specific, non-coding RNAs, with an average length of 22 nucleotides, that interact with the 3' untranslated region (UTR) of target messenger-RNAs (mRNAs) to negatively regulate gene expression or, under certain circumstances, activate gene expression [208,209]. Recent studies suggested that miRNAs are transported between cells and subcellular to control the rate of translation and transcription [210]. MiRNAs are therefore highly promising biomarker candidates which may be utilized to influence regulatory processes in target cells or tissues [211,212]. Another possible method of delivering exosome cargoes is nuclear envelope associated invagination which are is linked with the late endosomes allowing delivery of exosome components into the nucleoplasm [213,214]. Other possible routes of exosomes to escape lysosomal degradation include using pathways similar to viruses, redirection of exosome cargoes from endosomal pathway to trans-Golgi network through retrograde trafficking or membrane fusion between exosomes and the endosomal membrane [198,215,216].

7.5.3 Isolation methods

There are different methods to isolate exosomes from cell culture supernatants and body fluids. The most frequently performed is the differential ultracentrifugation (dUC) approach, which separates particles by sedimentation using different centrifugation forces and durations [217,218]. The conditioned cell culture media or body fluid is typically centrifuged with 300-2000 x g to remove cell debris and apoptotic cells. The resulting supernatant containing the exosomes is ultracentrifuged at 100 000 x g for 1.5-2 h, in order to pellet the desired exosomes [219,220]. Various laboratories apply slightly different centrifugation protocols, which leads to problems

concerning the reproducibility of experiments. Furthermore, the isolation process is influenced by other variables like the rotor type, the acceleration and the K-factor [218,221].

Another method to isolate exosomes is size exclusion chromatography which uses porous gel filtration as a stationary phase and a biofluid as a mobile phase for isolation. Size exclusion chromatography allows to separate exosomes of different size ranges by eluting bigger particles first, followed by smaller vesicles and finally, non-membrane-bound proteins [222].

Another popular size-based separation technique used for exosomes isolation/purification are different filtration strategies. Ultrafiltration (UF) is a fast and convenient technique to isolate exosomes from highly diluted samples using membranes with defined molecular weight cut-offs (MWCO) [223]. The drawback of this method is a high loss of Exosomes which are trapped in the membrane and the insufficient depletion of proteins [224,225]. Tangential flow filtration (TFF) enables concentration of exosomes from a fluid by tangentially flows across an UF membrane (hollow fiber membrane) but not directly through the membrane isolating only the particles within a defined MWCO [226,227]. This method is particularly suitable for large-scale EV isolation from diluted samples because in contrast to SEC, TFF concentrates the isolated exosomes [226].

In contrast to the above mentioned size-based separation techniques, charge-based techniques exploit the interaction between the negatively charged EV membrane components and an anion exchanger with positively charged functional groups or cations [228]. Examples for this principle are anion-exchange chromatography (AIEC), electrophoresis and di-electrophoresis (DEP) [229–231].

Affinity-based isolation of exosomes is also among the most popular techniques used in the field. It utilizes protein or receptor interaction of the Exosomes with antibodies. Immune-affinity capturing by employing antibodies which are covalently linked to magnetic beads via biotinylation is the most frequently used form of this approach [232].

7.5.4 Detection and characterization methods

Characterizing the exosome isolate is an important step to ensure the quality of the sample. There are various methods for visualizing exosomes such as transmission electron microscopy (TEM), scanning electron microscopy (SEM), cryo-electron microscopy (cryo-EM) or atomic force microscopy (AFM). However, these standard imaging techniques require elaborate

sample processing and fixation prior to imaging and only provide rough information about the size and the presence of the lipid-bilayer [233–237]. Another possibility is to label EVs by using fluorescent antibodies against EV membrane proteins or by using various lipophilic dyes which directly stain the lipid bilayer of the EVs [238–240]. The stained isolates can be analyzed using flow cytometry providing detailed information about the EV quantity, size distribution and characteristics regarding various exosome markers. Other fluorescent based methods to detect exosomes are digital PCR and digital enzyme-linked immunosorbent assay (ELISA) [238]. The main difference to non-digital methods is that the samples are diluted to a concentration that allows to analyze only one molecule at a time which can offer insights into exosome heterogeneity and cargo variety. Nano tracking analysis (NTA) provides accurate information about size (10 nm – 2000 nm) and concentration of exosomes by tracking the Brownian motion of each particle [241]. Moreover, NTA can detect the protein expression of EVs by measuring the fused fluorescent antibodies and incorporated fluorophores which holds additional information about the characteristics of the isolate [241].

Cargo analysis can be performed qualitatively by western blotting or quantitatively by flow cytometry, mass spectrometry, and miRNA- and RNA-sequencing [242–244]. Another strategy is to insert chemicals with fluorophores into the exosomes which provides the opportunity to track the cargo upon administration or detect miRNAs [245,246].

7.5.5 Clinical applications of exosomes

Exosomes are a promising tool for treating various diseases and clinical conditions. Upon injection, exosomes show minimal immune clearance and are efficient at entering other cells to deliver functional cargo [247].Plant- and human tissue-derived exosomes have been tested in clinical trials.

New methods and strategies are emerging to enrich therapeutically valuable exosome subpopulations based on their surface ligand presentation. Different approaches and strategies for cell cultivation, purification, and quality control of exosomes are developed in order to comply with good manufacturing practice (GMP). However, it is mandatory to discriminate between exosomes with a therapeutic and reciprocal effect. Latter ones can modify for example tumor behavior by shuttling between MSC and tumor cells leading to higher proliferation and metastasis.

The vast majority of ongoing exosome-based clinical trials aims at identifying diagnostic or prognostic biomarkers exploiting that different pathophysiological conditions release different

sets of exosome which can be used as biomarkers to diagnose various diseases [248–253]. In addition, some trials are also investigating exosomes as therapeutic agents in a wide range of diseases including cancer, neurodegeneration and infectious diseases [254–260]. Recent studies report that EV administration reduces the expression of pro-inflammatory cytokines such as IL-1β and IL-6 while the production of anti-inflammatory cytokines such as IL-10 and TGF-β1 and expression of genes related to collagen and tendon matrix formation, such as COL1a1, and SCX are increased *in vivo* [261–264]. Furthermore, MSC-EVs demonstrated their immunomodulatory capacity in a variety of tendon injury models *in vivo* by reducing macrophage NF-κB activity and the IL-1β and IFN-γ response, decreasing M1 and supporting M2 macrophage polarization and increasing the production of anti-inflammatory cytokines such as IL-4 and IL-10 [261–263,265].

EVs have a subsequent influence on the target cell, dependent on the encapsulated cargo and the origin and activation status of the donor cell and have potential benefits upon administration in horses [169,266–271]. The regenerative potential of EVs in tendon and ligament repair was shown *in vivo* in various species including mice, rats, rabbits and humans [161,261–265,272–277]. *In vitro* studies in horses have found anti-inflammatory properties of EVs and an *in vivo* study which was performed with EVs isolated from MSCs, showed reduced MMP 13 gene expression, which a marker of cartilage degradation, in chondrocytes [278–280].

MSC-EVs administered into tendon defects of rats resulted in enhanced proliferation of tendon stem/progenitor cells (TSPCs), better restoration of the tendon architecture, an improved histological score, greater expression of genes related to collagen and tendon matrix formation, including collagen (Col) type I, mohawk (MKX), scleraxis (SCX), tenomodulin (TNMD) and tissue inhibitor of metalloproteinase-3 (TIMP-3) and decreased MMP 3 expression [261,274,275,277].

In humans EVs have been shown to elicit a therapeutic effect by themselves. They have an influence on the target cell, dependent on the encapsulated cargo and the origin and activation status of the donor cell [169,266–269]. They potentially mediate inflammation between cells and have been linked to the induction of angiogenesis [270,271,281]. Furthermore, the packed miRNAs are promising biomarker candidates because they carry out critical regulatory tasks in biofluids. They are tissue-specific and transported between cells and subcellular to control the rate of translation and even transcription [210–212].

Recently, proteomic analysis provided evidence of different protein compositions between the secretome and EVs [282,283]. Several secreted proteins which exert cytoprotective and regenerative capacities were identified [50,284–292]. However, clinical trials; in which single cytokines were administered for the treatment of cardiovascular diseases; led to poor outcome [141]. Lipids were linked to various cascades like modulation and induction of cell death or immune functions [293,294]. Furthermore, lipid composition, either packed in exosomes or free floating, contributes to cell signaling and homeostasis [295].

8 Manuscripts

International Journal of
Molecular Sciences

MDPI

Article

Characterisation of Extracellular Vesicles from Equine Mesenchymal Stem Cells

Robert Soukup [1,†], Iris Gerner [1,2,†], Sinan Gültekin [1], Hayeon Baik [1], Johannes Oesterreicher [3], Johannes Grillari [2,3,4,*] and Florien Jenner [1,2,*]

[1] VETERM, Equine Surgery Unit, Department for Companion Animals and Horses, Vetmeduni, 1210 Vienna, Austria; robert.soukup@vetmeduni.ac.at (R.S.); iris.gerner@vetmeduni.ac.at (I.G.); sinan.gueltekin@vetmeduni.ac.at (S.G.); hayeon.baik@vetmeduni.ac.at (H.B.)
[2] Austrian Cluster for Tissue Regeneration, 1200 Vienna, Austria
[3] Ludwig Boltzmann Institute for Traumatology, the Research Center in Cooperation with AUVA, 1200 Vienna, Austria; johannes.oesterreicher@trauma.lbg.ac.at
[4] Institute of Molecular Biotechnology, University of Natural Resources and Life Sciences, 1090 Vienna, Austria
* Correspondence: johannes.grillari@trauma.lbg.ac.at (J.G.); florien.jenner@vetmeduni.ac.at (F.J.)
† These authors contributed equally to this work.

Abstract: Extracellular vesicles (EVs) are nanosized lipid bilayer-encapsulated particles secreted by virtually all cell types. EVs play an essential role in cellular crosstalk in health and disease. The cellular origin of EVs determines their composition and potential therapeutic effect. Mesenchymal stem/stromal cell (MSC)-derived EVs have shown a comparable therapeutic potential to their donor cells, making them a promising tool for regenerative medicine. The therapeutic application of EVs circumvents some safety concerns associated with the transplantation of viable, replicating cells and facilitates the quality-controlled production as a ready-to-go, off-the-shelf biological therapy. Recently, the International Society for Extracellular Vesicles (ISEV) suggested a set of minimal biochemical, biophysical and functional standards to define extracellular vesicles and their functions to improve standardisation in EV research. However, nonstandardised EV isolation methods and the limited availability of cross-reacting markers for most animal species restrict the application of these standards in the veterinary field and, therefore, the species comparability and standardisation of animal experiments. In this study, EVs were isolated from equine bone-marrow-derived MSCs using two different isolation methods, stepwise ultracentrifugation and size exclusion chromatography, and minimal experimental requirements for equine EVs were established and validated. Equine EVs were characterised using a nanotracking analysis, fluorescence-triggered flow cytometry, Western blot and transelectron microscopy. Based on the ISEV standards, minimal criteria for defining equine EVs are suggested as a baseline to allow the comparison of EV preparations obtained by different laboratories.

Keywords: extracellular vesicles; equine; mesenchymal stem cell; EV isolation; EV characterisation

check for updates

Citation: Soukup, R.; Gerner, I.; Gültekin, S.; Baik, H.; Oesterreicher, J.; Grillari, J.; Jenner, F. Characterisation of Extracellular Vesicles from Equine Mesenchymal Stem Cells. *Int. J. Mol. Sci.* **2022**, *23*, 5858. https://doi.org/10.3390/ijms23105858

Academic Editor: Takayoshi Yamaza

Received: 7 March 2022
Accepted: 17 May 2022
Published: 23 May 2022

Publisher's Note: MDPI stays neutral with regard to jurisdictional claims in published maps and institutional affiliations.

1. Introduction

Mesenchymal stem/stromal cells (MSCs) can be isolated from various sources such as adipose tissue, bone marrow, umbilical cord matrix, cord blood, blood or synovial fluid and have shown promising therapeutic potential for the treatment of musculoskeletal disorders such as tendinopathy and osteoarthritis in both human and equine patients [1–11]. However, the transplantation of viable replicating cells presents safety concerns and limitations regarding standardisation, quality control and donor-dependent therapeutic potential [12–15]. MSCs exert their therapeutic effect not by engraftment and differentiation but predominantly by secreting a wide range of bioactive molecules such as cytokines, enzymes and growth factors, collectively referred to as secretome, which induce and support endogenous regeneration and modulate the immune response. The secretome,

consisting of soluble and extracellular vesicle (EV) bound proteins, lipids, and nucleic acids, has proven to have equivalent therapeutic effects as the parental cells, providing the opportunity to develop cell-free regenerative therapies [16–20]. EVs alone can also achieve this regenerative potential, which offers additional advantages over the use of the whole secretome, as they protect their encapsulated or associated contents from degradation and can be stored without potentially toxic cryopreservatives [21–25].

EVs are a heterogeneous population of nanosized membrane-encapsulated particles secreted by cells into the extracellular environment. They are formed by a phospholipid bilayer originating from their parent cell and encapsulate nucleic acids, lipids and proteins [26] EVs contribute to cell-to-cell signalling in health, ageing and disease and are a promising tool for therapeutic and diagnostic applications [27–33]. Various subsets of EVs have been categorised according to their diameter as apoptotic bodies (>1000 nm), microvesicles (100–1000 nm) and exosomes (30–150 nm) [34]. The latter two are commonly referred to as extracellular vesicles. Due to their overlapping size, EVs can be further distinguished by their biogenesis pathways, their cell of origin and their cargo [35].

The functionality and hence therapeutic efficacy of EVs is determined by their cargo, which depends on the origin and activation status of the producer cell, and their surface and transmembrane molecules that govern target specificity and EV uptake by recipient cells [36–50]. The resulting heterogeneity of EVs in both content and functionality necessitates and impedes standardised, well-defined EV manufacturing processes to determine their therapeutic efficacy and achieve reliable therapeutic EV dosing in preclinical and clinical settings [38–50]. Unfortunately, the current lack of standardised isolation protocols and characterisation strategies limits the comparability and reproducibility of results obtained by different laboratories [42]. The International Society for Extracellular Vesicles (ISEV) published a position paper to provide minimal criteria (MISEV criteria) for EV isolation and characterisation to better exchange EV data and counteract methodological inconsistency when working with EVs [51]. Standardised purification and analytical methods will facilitate the discovery of functional heterogeneity and the production of EV-based regenerative therapies.

The isolation strategy for EV preparations is dependent on the volume and type of fluid from which the EVs are separated (cell culture supernatant, biological fluids such as blood plasma/serum, etc.) and needs careful consideration since it directly affects the isolated EV population and EV purity [38–50]. According to a survey from 2019, the most commonly used method to isolate EVs is differential ultracentrifugation (UC), followed by size exclusion chromatography (SEC) [52]. UC separates particles by sedimentation using different centrifugation forces and durations [52]. The EV extraction efficacy of this method is determined by a combination of acceleration, rotor type, viscosity and duration of centrifugation [46–49]. In contrast, SEC uses the biofluid as a mobile phase and the porous resin particles as a stationary phase to isolate particles of the desired size. Smaller particles enter the stationary phase's pores and elute later, while particles bigger than the isolation range flow around the resin and elute earlier from the column [38–40,50].

Each method leads to different yields and purities of EVs and is accompanied by certain advantages and disadvantages such as time efficiency, costs and sample volume [40–42]. Most researchers adopt these two methods with slight differences, which, again, leads to problems concerning the reproducibility of experiments, especially if publications lack proper documentation.

The varying degree of EV population heterogeneity and purity introduced by the choice of isolation methods also confounds the measurement of EV purity and content, which are essential determinants for EV dosing. Currently, protein concentration and particle count are the most commonly used dosing strategies; however, different EV isolation methods can, due to coisolating contaminating proteins, yield samples with up to an eightfold difference in protein content relative to particle number from the same source material. Moreover, other parameters used to quantify EVs, such as total lipid abundance, total RNA or the presence of specific molecules, do not perfectly correlate with the actual EV number,

emphasising the need for in-depth reporting of the isolation and quantification methods used in each study and for the standardisation of EV production procedures [51,53,54].

The potential benefits of administered EVs in horses have been shown in various studies [52,55,56]. However, the comparisons of different protocols for equine EV work are still vastly missing, which is also attributed to the lack of working antibodies. Therefore, in this study, we characterised EVs isolated from equine bone-marrow-derived MSCs (bmMSCs) following the ISEV guidelines and compared the two most common isolation methods, UC and SEC, with respect to EV yield, purity, cost and time efficacy, the complexity of the protocol and the need for specialised equipment. Differences in surface marker stability, size uniformity and number of particles were assessed by a Western blot, nanotracking analysis (NTA) and fluorescence-triggered flow cytometry (FT-FC).

2. Results

2.1. Cells Isolated from Equine Bone Marrow Show Distinct MSCs Characteristics

The cells isolated from the bone marrow of the three donor horses were plastic adherent and positive for the MSC markers CD90, CD44 and CD29 and negative for CD31 and Pan B (Figure 1a). The isotype controls were negative. Furthermore, the bone-marrow-derived cells showed adipogenic (Figure 1b), chondrogenic (Figure 1c) and osteogenic (Figure 1d) trilineage differentiation potential after three weeks in culture (Figure 1). The control samples, which were cultured in standard DMEM media with 10% FCS, showed no indication of differentiation.

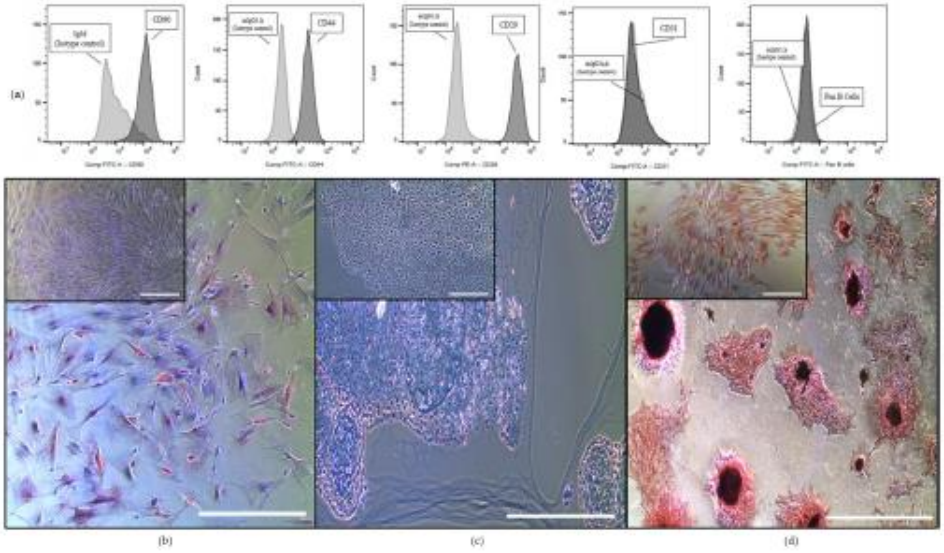

Figure 1. Characterisation of the equine bone-marrow-derived cells showing trilineage differentiation capacity and canonical surface marker expression of equine MSCs. (**a**) Bone-marrow-derived cells were stained with the indicated cell surface antigens (dark grey plots) or Immunoglobulin (Ig) isotype controls (light grey plots) and analysed by flow cytometry (one representative FT-FC experiment is shown). Cells stained positive for CD90, CD44 and CD29 and negative for CD31 and Pan B, as well as IgG isotype controls. Displayed on the x-axis is either Phycoerythrin (PE) or Fluorescein isothiocyanate (FITC) conjugated to one the previous mentioned antibodies. (**b**–**d**) Bone-marrow-derived cells showing trilineage differentiation into the adipogenic ((**b**) stained with Oil red O, scale bar: 400 µm), chondrogenic ((**c**) stained with Alcian blue, scale bar: 400 µm and 100 µm for the control) and osteogenic ((**d**) stained with von Kossa stain, scale bar: 400 µm) lineage. The corresponding controls (cells grown in expansion medium) are shown in the insert in the top left corner of each micrograph.

2.2. EV Isolation Strategy

EVs were isolated from equine bone-marrow-derived MSCs conditioned media (8×10^6 cells per replicate) of all three donors and three independent culture flasks using either SEC or UC. After 48 h (seeding density at 0 h: 4×10^6 cells per T175 flask), 22 mL serum-free medium yielded 20 mL debris-free supernatant following centrifugation, which could then be further processed in 10 mL aliquots using SEC and UC to isolate EVs (Figure 2).

Figure 2. Illustration of the experimental setup: MSCs derived from the bone marrow of 3 equine donors were cultured in serum-free DMEM for 48 h ($n = 3$ biological replicates, plus 3 technical replicates per donor). Then, 22 mL of cell-free supernatant was collected from 8×10^6 cells per replicate and centrifuged in a 50 mL falcon tube with $3000\times g$ for 20 min at 4 °C. In total, 20 mL of debris-free supernatant was recovered. Half of it was used to isolate EVs by the SEC columns, and the other half was filled into UC tubes.

2.3. Nanotracking Analysis Shows Significantly Higher EV Yield by UC Compared to SEC

The EV yield measured by NTA was significantly different ($p < 0.0021$) between the two isolation methods with UC yielding 27.7 times more EVs from 10 mL SN ($2.24\times 10^{12} \pm 1.6 \times 10^{12}$ (mean ± s.d.) particles/mL) than SEC ($8.08 \times 10^{10} \pm 4.73\times 10^{10}$ particles/mL) (Figure 3a). The size distribution between the SEC and UC was similar with no statistically significant differences (Figure 3b,c). Specifically, in the SEC isolate, the frequency of parents (FOP) of the particles ≤200 nm was 81.7% ± 2.9%, the FOP >200–500 nm was 17.5% ± 2.9% and the FOP >500 nm was 0.7% ± 0.5%. In the UC isolates, the FOP of the particles ≤200 nm 84.8% ± 7.9%, FOP >200–500 nm was 14.6% ± 7.3% and the FOP >500 nm was 1.4% ± 0.5%.

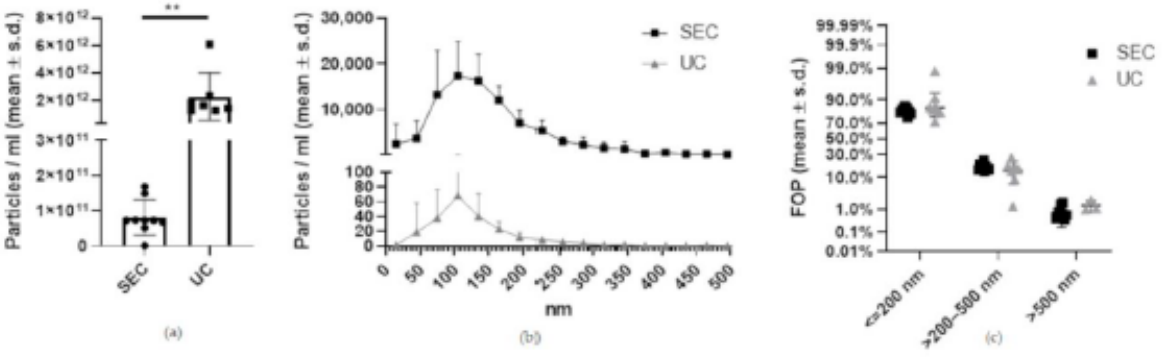

Figure 3. Particle number and size distribution of equine MSC-EVs based on NTA measurements. (**a**) Significantly more particles per ml were found in the UC isolates (** $p = 0.0021$). Black dots correspond to the SEC isolated samples and black squares to the UC isolated samples. (**b**) However, both methods resulted in a similar size distribution pattern, with most particles present below 200 nm. (**c**) Statistical analysis of the size distribution of particles identified by NTA analysis showed no significant differences of particles isolated using the UC or SEC.

2.4. Fluorescence-Triggered Flow Cytometry Shows a Significantly Higher Yield of CMG and CD81-Positive Particles by UC Compared to SEC

Fluorescence-triggered flow cytometry (FT-FC) confirmed the presence of EVs in isolates obtained by both UC and SEC (Figure 4a). UC isolated significantly ($p < 0.0001$) more particles labelled by the lipid membrane dye cell mask green (CMG) (188,752 ± 71,241 (mean ± s.d.) particles/mL) and EV-specific CD81 positive particles (49,616 ± 22,588) than SEC (CMG: 35,811 ± 6729, CD81: 8470 ± 1751 particles/mL) (Figure 4b,c). The yield obtained with UC was thus 5.3-fold higher than SEC for CMG positive particles and 5.85-fold higher for CD81 positive particles. Particle counts based on CMG and CD81 labelling correlated strongly ($r = 0.9959$, $p < 0.0001$), with 25.9% of CMG-labelled particles staining positive for CD81.

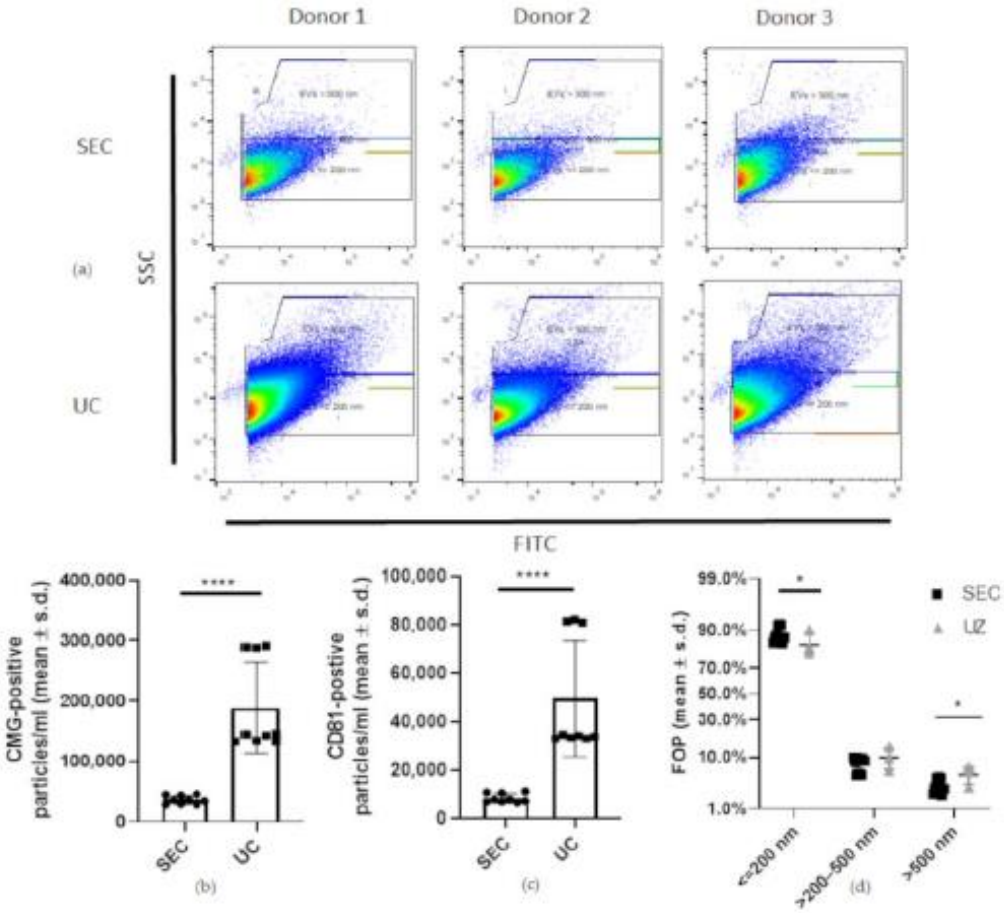

Figure 4. Flow-cytometry-based characterisation of equine MSC-EVs. (**a**) Representative image of fluorescence-triggered flow cytometry analysis of EV isolates enriched by either SEC (**top row**) or UC (**bottom row**). Data were collected by measuring the CD81 signal and CMG (CellMask Green) signal separately (n = 3 technical replicates). On the *y*-axis is the side scattering (SSC) and on the *x*-axis is FITC. (**b**) Significantly (**** $p < 0.0001$) more particles per millilitre stained positive for CMG in the UC isolates (188,752 ± 71,241 particles/mL) compared to the SEC isolates (35,811 ± 6729 particles/mL) (**c**). Significantly (**** $p < 0.0001$) more particles per millilitre stained positive for CD81 in the UC isolates (49,616 ± 22,588) compared to SEC (8470 ± 1751) (**d**). The size distribution of particles ≤200 nm (* $p = 0.0446$) and >500 nm (* $p = 0.0105$) identified by the FT-FC analysis was statistically significantly different between the two isolation methods.

The differences in size distribution between the two isolation methods were subtle but statistically significant for CMG-positive particles ≤200 nm ($p = 0.0446$) and >500 nm ($p = 0.0105$) but not for >200–500 nm ($p = 0.1413$) with SEC isolates yielding more particles in the desired size range (≤200 nm) and fewer larger particles (Figure 4d). Specifically, in the SEC isolates, the FOP of the CMG positive particles ≤200 nm was 88% ± 2.8%, the FOP >200–500 nm was 7.8% ± 1.9% and the FOP >500 nm was 3.1% ± 1.0%. In the UC isolates, the FOP of the CMG positive particles ≤200 nm was 83.8% ± 4.6%, the FOP >200–500 nm was 9.9% ± 3.3% and the FOP >500 nm 5.1% ± 1.6%.

Based on these measurements, 318 mL of SN is required to produce 1×10^6 CMG positive particles ≤200 nm using SEC and 63.8 mL of SN using the UC methods.

FT-FC (CMG-positive) and the NTA measurements of total particle numbers ($r = 0.4987$, $p = 0.0493$) and size distribution relative to FOP ($r = 0.9835$, $p < 0.0001$) significantly correlated. However, FT-FC (CD81-positive) and the NTA measurements of total particle numbers ($r = 0.439$, $p = 0.0889$) did not correlate.

2.5. Western Blot Shows Positive Signals for Two Tetraspanins to Which Cross-Species Reactive Antibodies Are Available

Whole-cell lysates and the EV populations enriched by UC were analysed using a Western blot to check for the presence of tetraspanins using human anti-CD9 and anti-CD63 antibodies. Indeed, the equine MSCs and isolated EVs showed positive signals for these two tetraspanins, which are markers of membrane proteins commonly found across all cell and EV types (Figure 5).

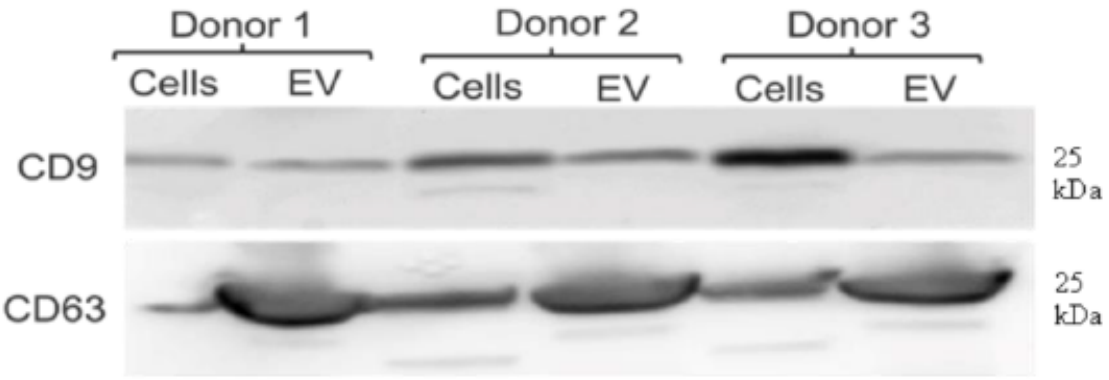

Figure 5. Western blot of equine MSC cell isolates and UC isolated EVs: All isolates from all donors were positive for CD9 and CD63 in the whole-cell lysates and their respective EV isolates.

2.6. Transelectron Microscopy (TEM) Shows Particle Morphology

TEM demonstrated particles sized 35 nm–350 nm surrounded by a lipid bilayer with a variable electron density cargo content, thus confirming the presence of EVs (Figure 6). In the UC isolates, larger vesicles and agglomerates were evident, while in the SEC isolates, vesicles were more homogenously sized, consistent with the size distribution measured by FT-FC (Figure 6). In addition, the potential variation of cargo in the EVs was shown by different electron densities evidenced by different grey scales in the TEM pictures (Figure 6).

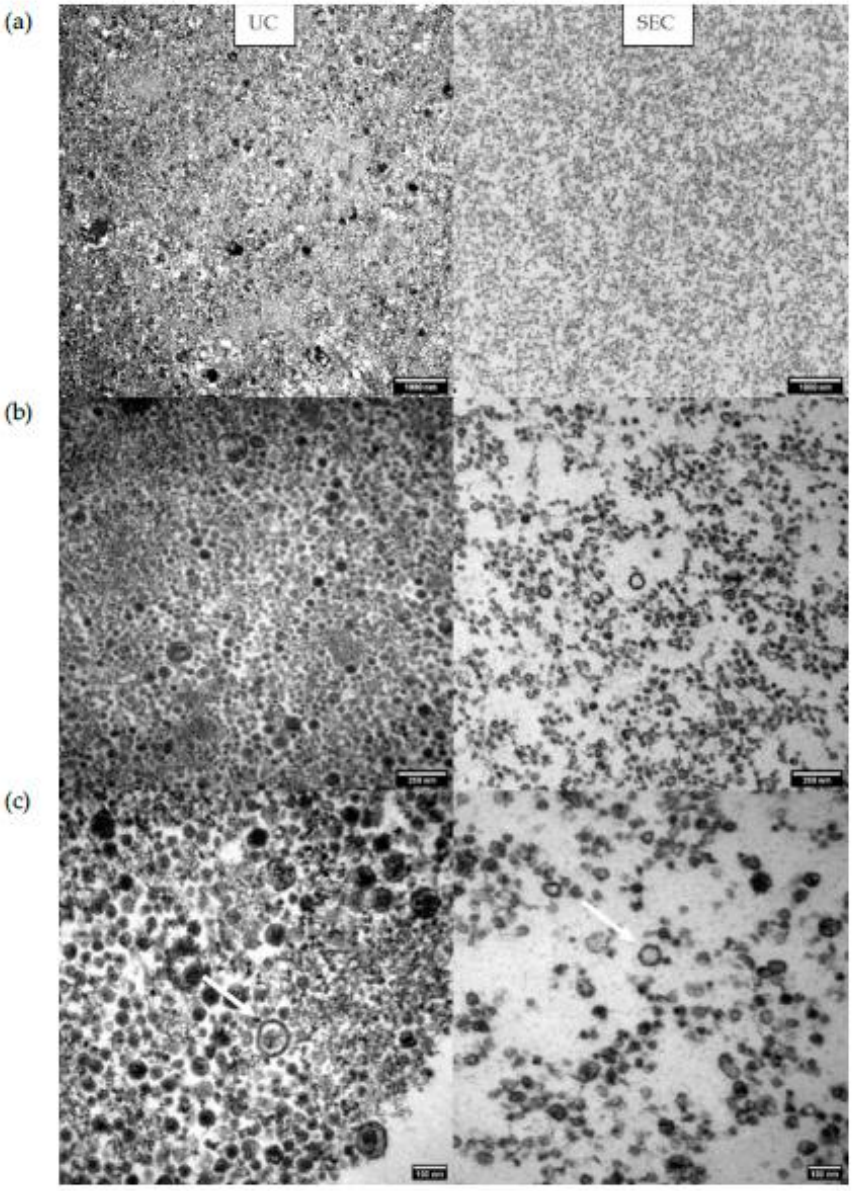

Figure 6. Transelectron Microscopy (TEM) images of the UC EV isolates in the left panels and the SEC EV isolates in the right panels taken at decreasing (top to bottom) magnifications: (**a**) 12,000× magnification gives an overview of the different sizes of the particles with a 1000 nm scale bar; (**b**) 50,000× magnification shows the different electron densities by different grey scales; (**c**) 85,000× magnification shows clearly the EVs identifiable by their lipid bilayer (arrows). In the UC isolates, the size distribution of the EVs is heterogeneous, ranging from large particle agglomerates to small EVs. In contrast, in the SEC isolates, particles are more uniformly sized without agglomerates.

3. Discussion

To facilitate the use of EVs as therapeutics in veterinary medicine, gold standards for EV isolation, characterisation and quality control are urgently required.

EV samples have complex inherent biophysical and biochemical properties such as size, mass density, shape, charge or antigen exposure [57]. Depending on the EV source such as blood, plasma or cell culture supernatant, and intended application, such as a single EV analysis, functional assays or therapeutic administration, several factors need to be considered before choosing an appropriate isolation method or a combination of methods to adapt to the specific needs of EV research [53,54,58]. As the composition of the enriched EVs will differ depending on the isolation protocol used, standardized assays evaluating the yield and size distribution are mandatory before proceeding to ensure reproducibility and facilitate the interpretation of the therapeutic efficacy and scientific community-wide data comparison. In this study, we suggested MISEV criteria for the isolation and characterisation of equine MSC-derived EVs.

EVs were successfully and reproducibly isolated from equine bone-marrow-derived MSCs using both UC and SEC, facilitating a broad comparison of UC and SEC. The MSCs were cultured in serum-free medium for 48 h to exclude possible interferences with serum during the isolation process, as EVs present in the FCS or other serum types used for cell culture can significantly affect the perceived yield of EVs and exert downstream effects, including both therapeutic as well as (xenogeneic) inflammatory effects [59].

UC produced more particles of the desired size range (≤200 nm) per millilitre of supernatant than SEC due to its higher isolation efficacy. The size cutoffs for FT-FC were chosen based on a gating with fluorescence-labelled silica beads of defined sizes, which most closely approximated the dimensions of the different EV subtypes (small ≤200 nm, intermediate 200–500 nm and large >500 nm) [60]. The beads served as a size reference for the distinction of the EV subtypes to separate exosomes (the particles of interest for this study) from the other subtypes because exosomes (30–150 nm) have a defined mode of biogenesis and are highly interesting for regenerative applications, because they have been shown to play essential roles in intercellular communication [61,62]. EVs above that size are less homogenous in origin, e.g., particles above 500 nm are either apoptotic bodies, conglomerates of proteins or other contaminants which are not desired and are characteristic of poor EV isolates [51]. More particles stained positive for CMG than CD81 because this dye incorporated into the lipid bilayer, which was present in all EVs, rather than detecting a tetraspanin like CD81, which was enriched on EVs and not obligatorily present on all EVs [63,64].

The advantages of the UC method include a higher yield and a broad particle size isolation range. However, EVs isolated through UC reportedly have diminished functional capacity compared to EVs isolated using SEC, potentially due to prolonged exposure to high centrifugal forces [38,41]. Furthermore, UC requires more delicate sample handling, complex equipment and hence more experience to obtain a good EV yield than with SEC. In addition, variable UC protocols and parameters involved in the process of EV isolation, such as rotor type, UC-tube quality, centrifugation speed, acceleration, and deceleration, which can be individually adjusted to improve the purity and yield of the isolates, may lead to difficulties with respect to reproducibility and variation between laboratories. Other disadvantages of this method include the potential contamination with exosomal aggregates, which reduces purity and may affect the accuracy of EV quantification and the price of the equipment [48,65–67].

The main advantages of SEC are the simpler technique and the higher purity of the obtained EVs with minor artefacts such as EV aggregates, which facilitate clinical applicability [49,50].

To translate EV-based therapeutics to clinical practice, their quality, safety, and efficacy must be demonstrated, as required for any medicinal product. EV purity is of critical importance for evaluating safety, dosage, potency and efficacy. Specifically, EV purity is crucial to ensure that any observed biological effects are due to EV cargoes and not copurified contaminants, and that EV preparations are free of contaminating proteins and nucleic acids that could have a negative impact upon clinical administration. Copurified protein aggregates can also artificially increase yield measurements and confound EV quantification. A reliable quantification of EVs is essential to ensure batch-to-batch reliabil-

ity and reproducibility between applications, identify effective dose ranges for different therapeutic EV preparations and develop dependable dosing strategies.

The two main EV enumeration procedures currently in use are particle number and size distribution, as assessed by NTA and protein concentration. However, it is well established that the protein concentration does not correlate with particle number readout [49,51,53,68]. A recent metareview looking at dosing regimens found that more than 50% of all studies quantified EVs in total amount of protein and 18% utilised NTA, whereas 21% of the studies did not quantify EVs in any way [47]. As the heterogeneity of EVs and presence of lipoproteins and protein aggregates confound current EV quantification methods, future strategies to standardize EV dosing may also focus on qualitative aspects such as the quantity of known effector molecules or EV potency units based on standardised in vitro potency assays [49]. Therefore, in this study, we characterised equine EVs based on the MISEV criteria using a Western blot, FT-FC, NTA measurements and TEM to address the limited availability of cross-reacting markers for horses. The isolated particles stained positive for CD9 and CD63 as demonstrated by a Western blot and for CD81 using FT-FC [57,69,70]. FT-FC, NTA and TEM confirmed the EV-appropriate size range (between 30 and 150 nm) and TEM the presence of the characteristic lipid bilayers surrounding EVs [71,72].

The absence of validated antibodies is a considerable obstacle in working with equine cells. Although the horse and the human genome are highly conserved, the binding of human antibodies to equine targets is in most cases not effective [59,60]. BLASTED protein sequences of standard EV markers showed a homology of 84% for CD63, 92% for CD9, 98% for TSG101 and 97% for CD81 between horses and humans. We tested available antibodies from different manufacturers in various concentrations, but only CD63 and CD9 gave signals at the expected molecular weight on Western blots. Until antibodies specific to equine EV-related proteins become available, we recommend using a combination of methods, including techniques that do not require antibodies, such as NTA and TEM. TEM can discriminate single EVs from similar-sized non-EV particles and is therefore widely used to monitor the quality and purity of EV-containing samples, e.g., for therapeutic application or downstream analysis [53,73–76].

In addition to a panel of markers, there is a need for more detailed reporting of methodologies and results to facilitate data comparison. For example, the different EV characterisation methods, a dynamic light scattering (NTA) or an antibody (FT-FC)-based technique yield vastly variable particle concentration measurements, as demonstrated by a particles per millilitre count of $8.08 \times 10^{10} \pm 4.73 \times 10^{10}$ (SEC) and $2.24 \times 10^{12} \pm 1.6 \times 10^{12}$ (UC) particles measured with NTA versus 35,811 ± 6729 (SEC) and 188,752 ± 71,241 (UC) CMG-positive particles or 8470 ± 1751 (SEC) and 49,616 ± 22,588 (UC) CD81-positive particles measured with FT-FC. NTA measures the size of particles and their concentration based on the physical principle of Brownian motion. In contrast to FT-FC, where lipid dyes or antibodies are used to specifically label EVs, NTA cannot discriminate between contaminations in the form of particles that might derive from external sources such as washing buffers. In addition, the measurements of the concentration and the size distribution are closely linked to the detection limit of the characterisation method, which leads to differences between the measured concentrations [38,41]. Hence, it is paramount to report which platform was used and how measurements were calibrated and normalised.

While the technical aspects of EV isolation and quantification likely encompass the majority of the limitations in EV purity and yield estimation, biological factors, such as EV-producing cell type, cell culture, confluence and stimulation determine EV cargo and hence therapeutic efficacy and may also influence EV yield [77,78]. As the regenerative and immunomodulatory capacity of MSCs decreases with increasing donor age, the use of allogeneic MSCs to produce EVs represents an attractive cell-free off-the-shelf treatment option, which allows the selection of optimal donor cells, scalable, standardised manufacturing and treatment optimisation for the target disease [79,80]. However, extensive culture expansion drives MSCs toward replicative senescence and a consequent decline in quality

with diminished immunosuppressive and regenerative capacity and proinflammatory features [81,82]. Indeed long-term in vitro culture (high passage) was recently shown to have a greater effect on MSCs (increased β-Galactosidase level) than the natural ageing process of their donor [82]. Ageing and senescence impact MSC characteristics in several ways and also affect the release of bioactive factors and EVs [80,83]. Interestingly, the secretion of EVs by MSCs increases with donor age and late passage cultures, potentially to dispose of undesirable molecules or as distress signal [83,84]. Furthermore, EVs released by senescent cells contain an altered cargo that may contribute to senescence propagation and chronic inflammation [80,83,85]. Therefore, studies focusing on identifying the optimal EV-producing cells (e.g., MSCs) and culture conditions for therapeutic applications and developing standardised EV manufacturing processes also for the selection, isolation and culture of the EV-producing cells are urgently needed to ensure a consistent EV quality, facilitate the identification and production of effective dose ranges and advance the clinical translation of EV based therapies. In addition, further studies assessing the cargo quality and quantity of EVs isolated using different methods are needed to compare the therapeutic potential of the various EV preparations and establish standardised EV manufacturing processes.

In conclusion, our work highlights the problems resulting from the lack of standardised EV isolation and characterisation methods and establishes MISEV-based criteria for the definition of equine MSCs-derived EVs to address the limited availability of cross-reacting markers for horses using multimodal characterisation techniques, including the expression of CD9, CD63 (Western blot) and CD81 (FT-FC), an EV-appropriate size range (between 30 and 150 nm, FT-FC, NTA and TEM) and the presence of the characteristic lipid bilayers surrounding EVs (TEM).

4. Materials and Methods

All experiments were conducted using three biological replicates (MSC derived from 3 horses, $n = 3$) and technical triplicates.

4.1. Bone Marrow Collection and MSC Isolation

Bone marrow was harvested from horses (donor 1: 11-year-old Tinker mare; donor 2: 6-year-old Pura Raza Espanola gelding; donor 3: 23-year-old Austrian Warmblood mare) euthanised for reasons unrelated to this study. Based on the "Good Scientific Practice, Ethics in Science and Research regulation" implemented at the University of Veterinary Medicine Vienna, the Institutional Ethics Committee of the University of Veterinary Medicine Vienna and the Austrian Federal Ministry of Educations Science and Research, in vitro cell culture studies do not require approval if the cells were isolated from tissue which was obtained either solely for diagnostic or therapeutic purposes or in the course of other institutionally and nationally approved experiments.

Immediately postmortem, bone marrow was harvested from the sternum under sterile conditions using a Yamshidi bone marrow aspiration needle (TIN3015, CareFusion, San Diego, CA, USA) and a syringe prefilled with heparin 5000 IE/mL (Gilvasan, Vienna, Austria).

The aspirated bone marrow was mixed with 1× PBS with Mg/Ca (PBS +/+, Gibco, Waltham, MA, USA, 14190144) (1:1) and filtered through a 100 µM cell strainer (Greiner Bio-One, Kremsmünster, Austria, 542000). The mononuclear cell fraction was isolated by density gradient centrifugation using Ficoll Paque Premium (GE Healthcare, Chicago, IL, USA, 11743219) as previously published [85,86]. In brief, the collected bone marrow–PBS +/+ mix was layered onto the Ficoll and centrifuged at room temperature for 30 min at 300 g (Hettich, Westphalia, Germany, Rotanta 460R) without brake. The buffy coat was collected. After washing, the obtained mononuclear cells were seeded in DMEM with 1 g/L glucose, L-glutamine, 110 mg/L sodium pyruvate (Gibco, 31885023) supplemented with 10% FCS (Sigma Aldrich, St. Louis, MO, USA, F7524), 1% Pen/Strep (Sigma, St. Louis, MO, USA, P433-100 mL) and 1% amphotericin B (Biochrom, Cambridge, UK, A 2612-50 mL) and cultured in an incubator with 20% O_2 and 5% CO_2. In the following days, nonadherent cells

were removed by washing and medium change. After three weeks, MSCs were harvested and frozen until further use.

4.2. Trilineage Differentiation

Differentiation experiments were carried out in technical triplicates and maintained in culture for three weeks. The media were exchanged every three days. The controls were cultured in DMEM supplemented with 10% FCS, 1% Pen/Strep and 1% amphotericin B. For adipogenic and osteogenic differentiation, 4000 MSCs were seeded per well of a 12-well plate in DMEM supplemented with 10% FCS, 1% Pen/Strep and 1% amphotericin B for 48 h. After washing with PBS +/+, adipogenesis (ThermoFisher, Waltham, MA, USA, A1007001) or osteogenesis (ThermoFisher, A1007201) differentiation media were added. For chondrogenic differentiation, 350,000 MSCs were pelleted per 15 mL Falcon tube and resuspended in chondrogenesis differentiation media (ThermoFisher, A1007101).

4.3. Staining Protocols

4.3.1. Oil Red Staining

Six parts of Oil red O (Sigma, O0625-25G) were diluted with four parts aqua dest, mixed overnight at room temperature and filtered. Cells were fixed with 60% isopropanol (Riedel de Haen, Seelze, Germany, 24137) for 5 min and afterwards incubated with the working solution of Oil red O for 10 min. Finally, the differentiated cells were washed with 60% isopropanol and aqua dest, counterstained with haematoxylin (Merck, Kenilworth, NJ, USA, 108562) and washed with aqua dest.

4.3.2. Alcian Blue Staining

Paraffin-embedded samples of chondrocyte pellets were cut using a microtome (CUT2511A, MicroTec, Brixen, Italy). Paraffin blocks were precooled at −15 °C and cut to 3 µm sections. The slices were transferred into cold water using two wet brushes and further transferred to 40 °C warm water with nonadhesive standard microscope slides (Carl Roth, Karlsruhe, Germany). They flattened out and were collected with the super frost adhesive microscope glass slides (Thermo Scientific). The slides were labelled and were left to dry at room temperature overnight. Slides were heated for 20 min in the incubator at 60 °C and submerged in Xylol twice for 10 min at room temperature. Afterwards, the slides were incubated for 5–10 min in 100% isopropanol and decreasing ethanol concentrations (96%, 70%, and 50%) for 5–10 min each. Slides were then washed in aqua dest. and stained in haematoxylin for 3 min. Finally, the slides were washed with aqua dest. and stained with eosin for 30 s. After soaking in ethanol and dehydrating in xylene, slides were mounted with Aquatex mounting medium (Merck Millipore, Burlington, MA, USA) and dried overnight. Slides were analysed with the FL Auto Imaging System (Invitrogen (Waltham, MA, USA), EVOS (Hong Kong, China), Thermo Scientific).

4.3.3. Von Kossa Stain

Cells were fixed with 5% formol (Sigma) incubated with 5% silver nitrate (Roth, 9370.9) for 20 min under UV light and washed with aqua dest. Afterwards, they were fixed with 5% sodium thiosulfate, washed with aqua dest. and stained with real red (Waldeck, 221833) for 10 min and washed again.

4.4. EV Isolation

MSCs were thawed and expanded in chemically defined complete medium (DMEM) supplemented with 10% FCS (Sigma Aldrich, F7524), 1% Pen/Strep and 1% amphotericin B until 80–90% confluency, passaged with trypsin (Gibco, 25300-096) and seeded at a defined density of 4×10^6 cells per T175 flask (Sarstedt, Nümbrecht, Germany, 833912002). All cells used were at passage 2, cell morphology was assessed daily, and viability was measured using Trypan blue dye exclusion in conjunction with an automated cell counter (ThermoFisher Countess 3). After 24 h, cells were washed twice with 10 mL filtered

(0.22 µm filter (Sarstedt, 831822)) PBS +/+ and then cultured in 22 mL serum-free DMEM (plus 1% Pen/Strep, 1% amphotericin). After 48 h and doubling of the cell number, which was estimated from preliminary studies with a population doubling level (PDL) of 3 (PDL = 2 + 3.322 (log 8 × 10^6–log 4 × 10^6)), the conditioned medium was collected and transferred into 50 mL Falcon tubes (Sarstedt, 64547254) and precentrifuged at 3000× *g* for 20 min at 4 °C to remove undesired cell debris. The obtained supernatant (SN) was carefully collected without disturbing the cell debris pellet and immediately processed.

4.4.1. Sequential Ultracentrifugation

For ultracentrifugation, 10 mL of precentrifuged SN was transferred into ultracentrifuge tubes (Beranek, 5047) and spun in an ultracentrifuge (L-100K, Beckman coulter, Brea, CA, USA) using a 55.2 Ti fixed-angle rotor at 100,000× *g* (35,000 rpm) for 1.5 h at 4 °C. The invisible pellet was recovered by scraping the walls of the tube where the pellet was suspected to be and simultaneously aspirating with a 5 mL pipette. Together with 1 mL SN, the pellet was transferred into 1.5 mL ultracentrifuge tubes (Beckman coulter, 357448). The second ultracentrifugation was performed in a tabletop ultracentrifuge (Optima Max, Beckman coulter) using a TLA 45 fixed-angle rotor at 100,000× *g* (45,000 rpm) for 1.5 h at 4 °C. Finally, the SN was aspirated and discarded. The EVs were resuspended and either processed for experimental use immediately or stored at −80 °C. The solution for the resuspension of the pellet was chosen according to the requirements for the follow-up experiments. (HEPES (Invitrogen, 14291DJ) for staining or storage, RIPA buffer (Sigma, R0278-50 mL) for Western blot, medium or filtered PBS for treatment experiments).

4.4.2. Size Exclusion Chromatography (SEC)

According to the manufacturer's protocol, EVs were isolated using qEV10/35 nm (IZON, qEV10 35 nm) columns and the Automated Fraction Collector (IZON). All reagents (IZON columns and filtered PBS) were stored at 4 °C and warmed to room temperature before starting the separation. A size exclusion column was mounted into the Automated Fraction Collector (AFC) with the reservoir attached on top, programmed to collect the desired fractions and flushed with 120 mL filtered PBS +/+. All PBS residues were removed with a pipette, and 10 mL of precentrifuged SN was loaded into the reservoir. The AFC has an integrated scale that automatically collects the void volume (20 mL) and the single fractions (5 mL per fraction). SN was loaded into the frit, and the reservoir was filled with filtered PBS +/+. Fraction 1 was discarded, and fractions 2 and 3, containing the desired EVs, were either directly processed or stored at −20 °C. The column was flushed with 120 mL sodium azide (Sigma, RTC000068-1L) and stored for further use at 4 °C.

4.5. Nanotracking Analysis

According to the manufacturer's protocol, the samples were diluted in filtered PBS +/+ (1:1000) and loaded into the device. Samples were measured in scatter mode with a 488 nm laser. Minimum brightness was set to 30, the minimum area to 10, maximum area to 1000, maximum brightness to 255, shutter to 400 and temperature to 25 °C. Isolates were measured in technical and biological triplicates.

4.6. Flow Cytometry

4.6.1. MSCs

For the flow cytometry, cells were trypsinised at passage 2, and 1 × 10^5 cells per sample were washed with PBS +/+ supplemented with 2% FSC (Sigma Aldrich, F7524). The following monoclonal antibodies and respective isotype controls were used for the flow cytometry: PE-CD29 (Clone TS2/16, Mouse IgG, 1:50, Biolegend, San Diego, CA, USA), FITC-CD31 (Clone CO.3E1D4, IgG2a, 1:50, Biorad, Hercules, CA, USA), FITC-CD44 (Clone 25.32, IgG, 1:50, Biorad), Purified CD90 (Clone DH24A, IgM, 1:50, Monoclonal Antibody Center), FITC-PanB cells (Clone CVS36, IgG1, 1:50, Biorad). A total of 1 × 10^4 events were measured per sample.

4.6.2. EVs (Fluorescence-Triggered Flow Cytometry (FT-FC))

Size distribution was evaluated by measuring the CD81 signal and the CellMask Green plasma membrane (CMG) signal separately. EVs were either isolated using UC or SEC as described above. The CMG staining and the gating strategy were performed as described before [60]. The SSC-based size gates were set according to the 100, 200 and 500 nm FITC-labelled silica beads and were merged to a small (≤200 nm), intermediate (>200–<500 nm) and large EV (≥500 nm) size range gate.

4.7. Western Blot

4.7.1. Protein Extraction

Cells were cultured in 10% DMEM until they were 70% confluent. A lysis buffer consisting of RIPA buffer (50 mL) and 2% protease inhibitor cocktail (Roche, Basel, Switzerland, 04693124001) was added to the plates, and the cells were scraped off the plate using cell scrapers (Greiner, 541070). After spinning with 17,200 *g* at 4 °C for 20 min, SN was transferred to an Eppendorf tube and stored at −20 °C. The EV pellet was resuspended in 75 µL of HEPES, vortexed at high speed and stored at −80 °C or directly processed for Western blotting. To determine the protein concentration, a BCA protein assay kit (Thermo Fisher 23227) and the Qubit protein kit (Invitrogen, Q33211) were used according to the manufacturer's protocol.

4.7.2. Western Blotting

A 10× electrophoresis buffer (running buffer) was prepared by mixing 30.3 g/L Tris (Roth, 0188.3), 142.6 g/L glycine (Roth, 0079.3), 1% SDS (Roth, 0601.1) and filling up the volume to 1 L with ddH2O. For working conditions, the stock solution was diluted 1:10 with ddH2O. Harlow buffer (transfer buffer) consists of 80 mL 10× electrophoresis buffer, 200 mL methanol (Roth, 0082.3), filled up to 1 L with ddH2O and stored at 4 °C. Then, 10× TBS was produced by adding 87.66 g/L NaCl (Roth, 0601.1) to 60.57 g/L Tris and filling up to 1 L with ddH2O before adjusting the pH to 7.4 with 6 M HCl (Merck, 1101641000). TBS/T was prepared by diluting 10× TBS 1:10 in ddH2O and adding 1 mL/L of Tween 20 (Roth, 27.2).

A total of 25 µg from the UC isolates of each sample was mixed with Laemmli 2× concentrate (Sigma S3401-1VL) nonreducing (without beta-mercaptoethanol for CD9 and CD63) and filled up to a certain amount with ddH2O, which depends on the pocket size of the precast gel (BioRad, 4561093) (15 comb: 10 µL and 10 comb: 20 µL). After denaturing for 10 min at 70 °C, the samples were loaded on the gel with 5 µL protein marker (Thermo Fisher, 26619). The power supply was set to constant 90 V for 10 min and was afterwards increased to constant 120 V for 70 min. To transfer the protein on a PVDF membrane (BioRad, 1620177), wet blotting using two Whatman papers (BioRad, 1703932) facing the cathode and the PVDF membrane (which was soaked in methanol before use) in between the gel and two Whatman papers facing the anode was performed. All the materials, including the sponges placed at the two ends of the sandwich, were soaked in Harlow buffer, and the blotting procedure was carried out in a tank containing an ice block at constant 350 mA for 1 h. After the blotting process, it was essential to mark the side of the membrane facing the gel. The membrane was washed 3× in TBS/T and blocked for 1 h with 5% nonfatty milk (Maresi) TBS/T buffer. Before incubating the membrane overnight with the first antibody (CD9 antihuman, (BioVision, Milpitas, CA, USA, 6938) or CD63 antihuman (SBI, EXOAB-CD63A-1)) on a shaker at 4 °C, and the membrane was again washed 3× in TBS/T. Finally, the membrane was washed 3× in TBS/T and incubated for 1 h with HRP-linked heavy and light chain antibodies. A Super Signal West Femto (Thermo Scientific, 34094) protein detection kit was used for the detection. The membrane was developed in an imaging system (BioRad, ChemiDoc).

4.7.3. Membrane Stripping

The buffer for the stripping procedure consisted of 15 g glycine (VWR, Radnor, PA, USA), 1 g SDS (Sigma), 10 mL Tween 20 (Sigma) and filled up to a total volume of 1 L with dH2O prior to adjusting the pH to 2.2. The membrane was incubated twice for 5–10 min with the stripping buffer, washed twice for 10 min in PBS and washed twice for 5 min with TBS/T. Afterwards, the membrane was ready for the blocking step.

4.8. Transelectron Microscopy

EVs were isolated from the same flask. After SEC, the isolated EVs were pelleted using a tabletop ultracentrifuge and embedded in paraffin. The block was cut (70 nm), contrasted with Uranyl acetate and lead citrate and examined with an electron light microscope (EM 900, Zeiss, Jena, Germany) using a slow-scan CCD 2K- wide-angle dual-speed camera (TRS).

4.9. Statistical Analysis

The statistical analysis was performed using Graph Pad Prism v.6.01 (GraphPad Software, San Diego, CA, USA). For the comparison of two normally distributed samples, the Student's *t*-test was conducted. The number of used donors (n), the p-values and the respective statistical significance are indicated in each figure. The data are plotted as mean ± standard deviation.

Author Contributions: Conceptualisation, R.S., I.G., J.G. and F.J.; methodology, R.S., I.G. and S.G.; FACS analysis, J.O.; Western Blot, H.B.; validation, I.G., J.G. and F.J.; formal analysis, R.S., I.G. and F.J.; investigation, R.S. and I.G.; resources, J.G. and F.J.; data curation, R.S.; writing—original draft preparation, R.S.; writing—review and editing, I.G., J.G. and F.J.; visualisation, R.S.; supervision, I.G., J.G. and F.J.; project administration, I.G.; funding acquisition I.G., J.G. and F.J. All authors have read and agreed to the published version of the manuscript.

Funding: This research was funded by Stiftung Pro Pferd (grant number PR2020-02).

Institutional Review Board Statement: Ethical review and approval were waived for this study. The Ethics Committee of University of Veterinary Medicine Vienna and the Austrian Federal Ministry of Educations Science and Research confirmed that in vitro cell culture studies do not require approval if the cells were isolated from tissue which was obtained either solely for diagnostic or therapeutic purposes or in the course of other institutionally and nationally approved experiments. Tissue collection was performed according to the "Good Scientific Practice and Ethics in Science and Research" regulation implemented at the University of Veterinary Medicine, Vienna. All samples were obtained from animals euthanised for reasons unrelated to this study.

Informed Consent Statement: The animal owner's consent to collect and analyse the samples and to publish resulting data was obtained according to standard procedures approved by the Ethics and Animal Welfare Committee of the University of Veterinary Medicine, Vienna.

Data Availability Statement: The data presented in this study are available on request from the corresponding author.

Acknowledgments: We acknowledge Waltraud Tschulenk for taking the transelectron microscopy pictures. Open Access Funding by the University of Veterinary Medicine Vienna.

Conflicts of Interest: J.G. is cofounder and shareholder of Evercyte GmbH and TAmiRNA GmbH. All other authors declare no conflict of interest.

References

1. Gugjoo, M.B.; Amarpal; Makhdoomi, D.M.; Sharma, G.T. Equine Mesenchymal Stem Cells: Properties, Sources, Characterization, and Potential Therapeutic Applications. *J. Equine Veter- Sci.* **2018**, *72*, 16–27. [CrossRef] [PubMed]
2. Secunda, R.; Vennila, R.; Mohanashankar, A.M.; Rajasundari, M.; Jeswanth, S.; Surendran, R. Isolation, expansion and characterisation of mesenchymal stem cells from human bone marrow, adipose tissue, umbilical cord blood and matrix: A comparative study. *Cytotechnology* **2014**, *67*, 793–807. [CrossRef] [PubMed]

3. Broeckx, S.Y.; Martens, A.M.; Bertone, A.L.; Van Brantegem, L.; Duchateau, L.; Van Hecke, L.; Dumoulin, M.; Oosterlinck, M.; Chiers, K.; Hussein, H.; et al. The use of equine chondrogenic-induced mesenchymal stem cells as a treatment for osteoarthritis: A randomised, double-blinded, placebo-controlled proof-of-concept study. *Equine Vet. J.* **2019**, *51*, 787–794. [CrossRef] [PubMed]
4. Carrade, D.D.; Affolter, V.K.; Outerbridge, C.A.; Watson, J.L.; Galuppo, L.D.; Buerchler, S.; Kumar, V.; Walker, N.J.; Borjesson, D.L. Intradermal injections of equine allogeneic umbilical cord-derived mesenchymal stem cells are well tolerated and do not elicit immediate or delayed hypersensitivity reactions. *Cytotherapy* **2011**, *13*, 1180–1192. [CrossRef]
5. Koch, T.G.; Heerkens, T.; Thomsen, P.D.; Betts, D.H. Isolation of mesenchymal stem cells from equine umbilical cord blood. *BMC Biotechnol.* **2007**, *7*, 26. [CrossRef]
6. Murata, D.; Miyakoshi, D.; Hatazoe, T.; Miura, N.; Tokunaga, S.; Fujiki, M.; Nakayama, K.; Misumi, K. Multipotency of equine mesenchymal stem cells derived from synovial fluid. *Veter- J.* **2014**, *202*, 53–61. [CrossRef]
7. Ishikawa, S.; Horinouchi, C.; Mizoguchi, R.; Senokuchi, A.; Kamikakimoto, R.; Murata, D.; Hatazoe, T.; Tozaki, T.; Misumi, K.; Hobo, S. Isolation of equine peripheral blood stem cells from a Japanese native horse. *J. Equine Sci.* **2017**, *28*, 153–158. [CrossRef]
8. Platonova, S.; Korovina, D.; Viktorova, E.; Savchenkova, I. Equine Tendinopathy Therapy Using Mesenchymal Stem Cells. *KnE Life Sci.* **2021**, 533–541. [CrossRef]
9. Costa-Almeida, R.; Calejo, I.; Gomes, M.E. Mesenchymal Stem Cells Empowering Tendon Regenerative Therapies. *Int. J. Mol. Sci.* **2019**, *20*, 3002. [CrossRef]
10. Mancuso, P.; Raman, S.; Glynn, A.; Barry, F.; Murphy, J.M. Mesenchymal Stem Cell Therapy for Osteoarthritis: The Critical Role of the Cell Secretome. *Front. Bioeng. Biotechnol.* **2019**, *7*, 9. [CrossRef]
11. Song, Y.; Zhang, J.; Xu, H.; Lin, Z.; Chang, H.; Liu, W.; Kong, L. Mesenchymal stem cells in knee osteoarthritis treatment: A systematic review and meta-analysis. *J. Orthop. Transl.* **2020**, *24*, 121–130. [CrossRef] [PubMed]
12. Van Loon, V.J.; Scheffer, C.J.; Genn, H.J.; Hoogendoorn, A.C.; Greve, J.W. Clinical follow-up of horses treated with allogeneic equine mesenchymal stem cells derived from umbilical cord blood for different tendon and ligament disorders. *Veter- Q.* **2014**, *34*, 92–97. [CrossRef] [PubMed]
13. Beerts, C.; Suls, M.; Broeckx, S.Y.; Seys, B.; Vandenberghe, A.; Declercq, J.; Duchateau, L.; Vidal, M.A.; Spaas, J.H. Tenogenically Induced Allogeneic Peripheral Blood Mesenchymal Stem Cells in Allogeneic Platelet-Rich Plasma: 2-Year Follow-up after Tendon or Ligament Treatment in Horses. *Front. Veter- Sci.* **2017**, *4*, 158. [CrossRef] [PubMed]
14. Vidal, M.A.; Robinson, S.O.; Lopez, M.J.; Paulsen, D.B.; Borkhsenious, O.; Johnson, J.R.; Moore, R.M.; Gimble, J.M. Comparison of Chondrogenic Potential in Equine Mesenchymal Stromal Cells Derived from Adipose Tissue and Bone Marrow. *Vet. Surg.* **2008**, *37*, 713–724. [CrossRef] [PubMed]
15. Ferris, D.J.; Frisbie, D.D.; Kisiday, J.D.; McIlwraith, C.W.; Hague, B.A.; Major, M.D.; Schneider, R.K.; Zubrod, C.J.; Kawcak, C.E.; Goodrich, L.R. Clinical Outcome After Intra-Articular Administration of Bone Marrow Derived Mesenchymal Stem Cells in 33 Horses with Stifle Injury. *Vet. Surg.* **2014**, *43*, 255–265. [CrossRef]
16. Timmers, L.; Lim, S.K.; Hoefer, I.E.; Arslan, F.; Lai, R.C.; van Oorschot, A.A.; Goumans, M.J.; Strijder, C.; Sze, S.K.; Choo, A.; et al. Human mesenchymal stem cell-conditioned medium improves cardiac function following myocardial infarction. *Stem Cell Res.* **2011**, *6*, 206–214. [CrossRef]
17. Caplan, A.I.; Dennis, J.E. Mesenchymal stem cells as trophic mediators. *J. Cell. Biochem.* **2006**, *98*, 1076–1084. [CrossRef]
18. Skalnikova, H.K. Proteomic techniques for characterisation of mesenchymal stem cell secretome. *Biochimie* **2013**, *95*, 2196–2211. [CrossRef]
19. Lai, R.C.; Tan, S.S.; Teh, B.J.; Sze, S.K.; Arslan, F.; De Kleijn, D.P.; Choo, A.; Lim, S.K. Proteolytic Potential of the MSC Exosome Proteome: Implications for an Exosome-Mediated Delivery of Therapeutic Proteasome. *Int. J. Proteom.* **2012**, *2012*, 1–14. [CrossRef]
20. Ribitsch, I.; Oreff, G.; Jenner, F. Regenerative Medicine for Equine Musculoskeletal Diseases. *Animals* **2021**, *11*, 234. [CrossRef]
21. Ekoniusz, S.; Bandrzejewska, A.; Muraca, M.; Srivastava, A.; Janowski, M.; Lukomska, B. Extracellular Vesicles in Physiology, Pathology, and Therapy of the Immune and Central Nervous System, with Focus on Extracellular Vesicles Derived from Mesenchymal Stem Cells as Therapeutic Tools. *Front. Cell. Neurosci.* **2016**, *10*, 109. [CrossRef]
22. Monleón, I.; Martinez-Lorenzo, M.J.; Monteagudo, L.; Lasierra, P.; Taulés, M.; Iturralde, M.; Piñeiro, A.; Larrad, L.; Alava, M.A.; Naval, J.; et al. Differential Secretion of Fas Ligand- or APO2 Ligand/TNF-Related Apoptosis-Inducing Ligand-Carrying Microvesicles During Activation-Induced Death of Human T Cells. *J. Immunol.* **2001**, *167*, 6736–6744. [CrossRef] [PubMed]
23. Phinney, D.G.; Pittenger, M.F. Concise Review: MSC-Derived Exosomes for Cell-Free Therapy. *Stem Cells* **2017**, *35*, 851–858. [CrossRef] [PubMed]
24. Yeo, R.W.Y.; Lai, R.C.; Zhang, B.; Tan, S.S.; Yin, Y.; Teh, B.J.; Lim, S.K. Mesenchymal stem cell: An efficient mass producer of exosomes for drug delivery. *Adv. Drug Deliv. Rev.* **2013**, *65*, 336–341. [CrossRef]
25. Kordelas, L.; Rebmann, V.; Ludwig, A.-K.; Radtke, S.; Ruesing, J.; Doeppner, T.R.; Epple, M.; Horn, P.A.; Beelen, D.W.; Giebel, B. MSC-derived exosomes: A novel tool to treat therapy-refractory graft-versus-host disease. *Leukemia* **2014**, *28*, 970–973. [CrossRef]
26. Möller, A.; Lobb, R.J. The evolving translational potential of small extracellular vesicles in cancer. *Nat. Cancer* **2020**, *20*, 697–709. [CrossRef]
27. DesRochers, L.M.; Bordeleau, F.; Reinhart-King, C.A.; Cerione, R.A.; Antonyak, M.A. Microvesicles provide a mechanism for intercellular communication by embryonic stem cells during embryo implantation. *Nat. Commun.* **2016**, *7*, 11958. [CrossRef]
28. Kamerkar, S.; LeBleu, V.S.; Sugimoto, H.; Yang, S.; Ruivo, C.; Melo, S.; Lee, J.J.; Kalluri, R. Exosomes facilitate therapeutic targeting of oncogenic KRAS in pancreatic cancer. *Nat.* **2017**, *546*, 498–503. [CrossRef]

29. Agrahari, V.; Burnouf, P.-A.; Burnouf, T.; Agrahari, V. Nanoformulation properties, characterization, and behavior in complex biological matrices: Challenges and opportunities for brain-targeted drug delivery applications and enhanced translational potential. *Adv. Drug Deliv. Rev.* **2019**, *148*, 146–180. [CrossRef]
30. Raposo, G.; Stahl, P.D. Extracellular vesicles: A new communication paradigm? *Nat. Rev. Mol. Cell Biol.* **2019**, *20*, 509–510. [CrossRef]
31. MacDonald, E.S.; Barrett, J.G. The Potential of Mesenchymal Stem Cells to Treat Systemic Inflammation in Horses. *Front. Veter- Sci.* **2020**, *6*, 507. [CrossRef] [PubMed]
32. Lin, K.-C.; Yip, H.-K.; Shao, P.-L.; Wu, S.-C.; Chen, K.-H.; Chen, Y.-T.; Yang, C.-C.; Sun, C.-K.; Kao, G.-S.; Chen, S.-Y.; et al. Combination of adipose-derived mesenchymal stem cells (ADMSC) and ADMSC-derived exosomes for protecting kidney from acute ischemia–reperfusion injury. *Int. J. Cardiol.* **2016**, *216*, 173–185. [CrossRef] [PubMed]
33. Grillari, J.; Mäkitie, R.E.; Kocijan, R.; Haschka, J.; Vázquez, D.C.; Semmelrock, E.; Hackl, M. Circulating miRNAs in bone health and disease. *Bone* **2020**, *145*, 115787. [CrossRef] [PubMed]
34. Xu, X.; Lai, Y.; Hua, Z.-C. Apoptosis and apoptotic body: Disease message and therapeutic target potentials. *Biosci. Rep.* **2019**, *39*. [CrossRef] [PubMed]
35. Kalluri, R.; LeBleu, V.S. The biology, function, and biomedical applications of exosomes. *Science* **2020**, *367*, eaau6977. [CrossRef]
36. Margolis, L.; Sadovsky, Y. The biology of extracellular vesicles: The known unknowns. *PLoS Biol.* **2019**, *17*, e3000363. [CrossRef]
37. Iraci, N.; Leonardi, T.; Gessler, F.; Vega, B.; Pluchino, S. Focus on Extracellular Vesicles: Physiological Role and Signalling Properties of Extracellular Membrane Vesicles. *Int. J. Mol. Sci.* **2016**, *17*, 171. [CrossRef]
38. Mol, E.A.; Goumans, M.-J.; Doevendans, P.A.; Sluijter, J.P.G.; Vader, P. Higher functionality of extracellular vesicles isolated using size-exclusion chromatography compared to ultracentrifugation. *Nanomedicine* **2017**, *13*, 2061–2065. [CrossRef]
39. Lobb, R.J.; Becker, M.; Wen, S.W.; Wong, C.S.F.; Wiegmans, A.P.; Leimgruber, A.; Möller, A. Optimized exosome isolation protocol for cell culture supernatant and human plasma. *J. Extracell. Vesicles* **2015**, *4*, 27031. [CrossRef]
40. Nieuwland, R.; Falcón-Pérez, J.M.; Théry, C.; Witwer, K.W. Rigor and standardization of extracellular vesicle research: Paving the road towards robustness. *J. Extracell. Vesicles* **2020**, *10*. [CrossRef]
41. Kennedy, T.L.; Russell, A.J.; Riley, P. Experimental limitations of extracellular vesicle-based therapies for the treatment of myocardial infarction. *Trends Cardiovasc. Med.* **2020**. [CrossRef] [PubMed]
42. Voga, M.; Adamic, N.; Vengust, M.; Majdic, G. Stem Cells in Veterinary Medicine—Current State and Treatment Options. *Front. Veter- Sci.* **2020**, *7*, 278. [CrossRef] [PubMed]
43. Kooijmans, S.A.; de Jong, O.G.; Schiffelers, R.M. Exploring interactions between extracellular vesicles and cells for innovative drug delivery system design. *Adv. Drug Deliv. Rev.* **2021**, *173*, 252–278. [CrossRef] [PubMed]
44. Silva, A.K.; Morille, M.; Piffoux, M.; Arumugam, S.; Mauduit, P.; Larghero, J.; Bianchi, A.; Aubertin, K.; Blanc-Brude, O.; Noël, D.; et al. Development of extracellular vesicle-based medicinal products: A position paper of the group "Extracellular Vesicle translatiOn to clinicaL perspectiVEs—EVOLVE France". *Adv. Drug Deliv. Rev.* **2021**, *179*, 114001. [CrossRef] [PubMed]
45. Xu, R.; Greening, D.W.; Zhu, H.-J.; Takahashi, N.; Simpson, R.J. Extracellular vesicle isolation and characterization: Toward clinical application. *J. Clin. Investig.* **2016**, *126*, 1152–1162. [CrossRef] [PubMed]
46. Klyachko, N.L.; Arzt, C.J.; Li, S.M.; Gololobova, O.A.; Batrakova, E.V. Extracellular Vesicle-based Therapeutics: Preclinical and Clinical Investigations. *Pharmaceutics* **2020**, *12*, 1171. [CrossRef] [PubMed]
47. Gudbergsson, J.M.; Johnsen, K.B.; Skov, M.N.; Duroux, M. Systematic review of factors influencing extracellular vesicle yield from cell cultures. *Cytotechnology* **2015**, *68*, 579–592. [CrossRef]
48. Gurunathan, S.; Kang, M.-H.; Jeyaraj, M.; Qasim, M.; Kim, J.-H. Review of the Isolation, Characterization, Biological Function, and Multifarious Therapeutic Approaches of Exosomes. *Cells* **2019**, *8*, 307. [CrossRef]
49. Gupta, D.; Zickler, A.M.; El Andaloussi, S. Dosing extracellular vesicles. *Adv. Drug Deliv. Rev.* **2021**, *178*, 113961. [CrossRef]
50. Salmond, N.; Williams, K.C. Isolation and characterization of extracellular vesicles for clinical applications in cancer—Time for standardization? *Nanoscale Adv.* **2021**, *3*, 1830–1852. [CrossRef]
51. Théry, C.; Witwer, K.W.; Aikawa, E.; Alcaraz, M.J.; Anderson, J.D.; Andriantsitohaina, R.; Antoniou, A.; Arab, T.; Archer, F.; Atkin-Smith, G.K.; et al. Minimal information for studies of extracellular vesicles 2018 (MISEV2018): A position statement of the International Society for Extracellular Vesicles and update of the MISEV2014 guidelines. *J. Extracell. Vesicles* **2018**, *7*, 1535750. [CrossRef] [PubMed]
52. Royo, F.; Théry, C.; Falcón-Pérez, J.M.; Nieuwland, R.; Witwer, K.W. Methods for Separation and Characterization of Extracellular Vesicles: Results of a Worldwide Survey Performed by the ISEV Rigor and Standardization Subcommittee. *Cells* **2020**, *9*, 1955. [CrossRef] [PubMed]
53. Lötvall, J.; Hill, A.F.; Hochberg, F.; Buzás, E.I.; Di Vizio, D.; Gardiner, C.; Gho, Y.S.; Kurochkin, I.V.; Mathivanan, S.; Quesenberry, P.; et al. Minimal experimental requirements for definition of extracellular vesicles and their functions: A position statement from the International Society for Extracellular Vesicles. *J. Extracell. Vesicles* **2014**, *3*, 26913. [CrossRef] [PubMed]
54. Pascucci, L.; Alessandri, G.; Dall'Aglio, C.; Mercati, F.; Coliolo, P.; Bazzucchi, C.; Dante, S.; Petrini, S.; Curina, G.; Ceccarelli, P. Membrane vesicles mediate pro-angiogenic activity of equine adipose-derived mesenchymal stromal cells. *Veter- J.* **2014**, *202*, 361–366. [CrossRef] [PubMed]

55. Livshits, M.A.; Khomyakova, E.; Evtushenko, E.; Lazarev, V.N.; Kulemin, N.; Semina, S.E.; Generozov, E.; Govorun, V.M. Isolation of exosomes by differential centrifugation: Theoretical analysis of a commonly used protocol. *Sci. Rep.* **2015**, *5*, 17319. [CrossRef] [PubMed]
56. Li, P.; Kaslan, M.; Lee, S.H.; Yao, J.; Gao, Z. Progress in Exosome Isolation Techniques. *Theranostics* **2017**, *7*, 789–804. [CrossRef]
57. Busatto, S.; Zendrini, A.; Radeghieri, A.; Paolini, L.; Romano, M.; Presta, M.; Bergese, P. The nanostructured secretome. *Biomater. Sci.* **2019**, *8*, 39–63. [CrossRef]
58. Lange-Consiglio, A.; Perrini, C.; Tasquier, R.; Deregibus, M.C.; Camussi, G.; Pascucci, L.; Marini, M.G.; Corradetti, B.; Bizzaro, D.; De Vita, B.; et al. Equine Amniotic Microvesicles and Their Anti-Inflammatory Potential in a Tenocyte Model In Vitro. *Stem Cells Dev.* **2016**, *25*, 610–621. [CrossRef]
59. Khasawneh, R.R.; Al Sharie, A.H.; Rub, E.A.-E.; Serhan, A.O.; Obeidat, H.N. Addressing the impact of different fetal bovine serum percentages on mesenchymal stem cells biological performance. *Mol. Biol. Rep.* **2019**, *46*, 4437–4441. [CrossRef]
60. Oesterreicher, J.; Pultar, M.; Schneider, J.; Mühleder, S.; Zipperle, J.; Grillari, J.; Holnthoner, W. Fluorescence-Based Nanoparticle Tracking Analysis and Flow Cytometry for Characterization of Endothelial Extracellular Vesicle Release. *Int. J. Mol. Sci.* **2020**, *21*, 9278. [CrossRef]
61. Cvjetkovic, A.; Lötvall, J.; Lässer, C. The influence of rotor type and centrifugation time on the yield and purity of extracellular vesicles. *J. Extracell. Vesicles* **2014**, *3*. [CrossRef] [PubMed]
62. Böing, A.N.; van der Pol, E.; Grootemaat, A.E.; Coumans, F.A.W.; Sturk, A.; Nieuwland, R. Single-step isolation of extracellular vesicles by size-exclusion chromatography. *J. Extracell. Vesicles* **2014**, *3*. [CrossRef] [PubMed]
63. Monguió-Tortajada, M.; Gálvez-Montón, C.; Bayes-Genis, A.; Roura, S.; Borràs, F.E. Extracellular vesicle isolation methods: Rising impact of size-exclusion chromatography. *Cell. Mol. Life Sci.* **2019**, *76*, 2369–2382. [CrossRef] [PubMed]
64. Lane, R.; Korbie, D.; Trau, M.; Hill, M.M. Optimizing Size Exclusion Chromatography for Extracellular Vesicle Enrichment and Proteomic Analysis from Clinically Relevant Samples. *Proteomics* **2019**, *19*, e1800156. [CrossRef] [PubMed]
65. Sidhom, K.; Obi, P.; Saleem, A. A Review of Exosomal Isolation Methods: Is Size Exclusion Chromatography the Best Option? *Int. J. Mol. Sci.* **2020**, *21*, 6466. [CrossRef] [PubMed]
66. An, M.; Wu, J.; Zhu, J.; Lubman, D.M. Comparison of an Optimized Ultracentrifugation Method versus Size-Exclusion Chromatography for Isolation of Exosomes from Human Serum. *J. Proteome Res.* **2018**, *17*, 3599–3605. [CrossRef]
67. Brennan, K.; Martin, K.; Fitzgerald, S.P.; O'Sullivan, J.; Wu, Y.; Blanco, A.; Richardson, C.; Mc Gee, M.M. A comparison of methods for the isolation and separation of extracellular vesicles from protein and lipid particles in human serum. *Sci. Rep.* **2020**, *10*, 1039. [CrossRef]
68. Kowal, J.; Arras, G.; Colombo, M.; Jouve, M.; Morath, J.P.; Primdal-Bengtson, B.; Dingli, F.; Loew, D.; Tkach, M.; Théry, C. Proteomic comparison defines novel markers to characterize heterogeneous populations of extracellular vesicle subtypes. *Proc. Natl. Acad. Sci. USA* **2016**, *113*, E968–E977. [CrossRef]
69. Perrini, C.; Strillacci, M.G.; Bagnato, A.; Esposti, P.; Marini, M.G.; Corradetti, B.; Bizzaro, D.; Idda, A.; Ledda, S.; Capra, E.; et al. Microvesicles secreted from equine amniotic-derived cells and their potential role in reducing inflammation in endometrial cells in an in-vitro model. *Stem Cell Res. Ther.* **2016**, *7*, 1–15. [CrossRef]
70. Coumans, F.A.W.; Brisson, A.R.; Buzas, E.I.; Dignat-George, F.; Drees, E.E.E.; El-Andaloussi, S.; Emanueli, C.; Gasecka, A.; Hendrix, A.; Hill, A.F.; et al. Methodological Guidelines to Study Extracellular Vesicles. *Circ. Res.* **2017**, *120*, 1632–1648. [CrossRef]
71. Taylor, D.D.; Shah, S. Methods of isolating extracellular vesicles impact down-stream analyses of their cargoes. *Methods* **2015**, *87*, 3–10. [CrossRef] [PubMed]
72. Stam, J.; Bartel, S.; Bischoff, R.; Wolters, J.C. Isolation of extracellular vesicles with combined enrichment methods. *J. Chromatogr. B* **2021**, *1169*, 122604. [CrossRef] [PubMed]
73. Moghadasi, S.; Elveny, M.; Rahman, H.S.; Suksatan, W.; Jalil, A.T.; Abdelbasset, W.K.; Yumashev, A.V.; Shariatzadeh, S.; Motavalli, R.; Behzad, F.; et al. A paradigm shift in cell-free approach: The emerging role of MSCs-derived exosomes in regenerative medicine. *J. Transl. Med.* **2021**, *19*, 1–21. [CrossRef] [PubMed]
74. Kalluri, R. The biology and function of exosomes in cancer. *J. Clin. Investig.* **2016**, *126*, 1208–1215. [CrossRef]
75. Mizenko, R.R.; Brostoff, T.; Rojalin, T.; Koster, H.J.; Swindell, H.S.; Leiserowitz, G.S.; Wang, A.; Carney, R.P. Tetraspanins are unevenly distributed across single extracellular vesicles and bias sensitivity to multiplexed cancer biomarkers. *J. Nanobiotechnol.* **2021**, *19*, 1–17. [CrossRef]
76. Jankovičová, J.; Sečová, P.; Michalková, K.; Antalíková, J. Tetraspanins, More than Markers of Extracellular Vesicles in Reproduction. *Int. J. Mol. Sci.* **2020**, *21*, 7568. [CrossRef]
77. Linares, R.; Tan, S.; Gounou, C.; Arraud, N.; Brisson, A.R. High-speed centrifugation induces aggregation of extracellular vesicles. *J. Extracell. Vesicles* **2015**, *4*, 29509. [CrossRef]
78. Szatanek, R.; Baran, J.; Siedlar, M.; Baj-Krzyworzeka, M. Isolation of extracellular vesicles: Determining the correct approach (Review). *Int. J. Mol. Med.* **2015**, *36*, 11–17. [CrossRef]
79. Kretlow, J.D.; Jin, Y.-Q.; Liu, W.; Zhang, W.J.; Hong, T.-H.; Zhou, G.; Baggett, L.S.; Mikos, A.G.; Cao, Y. Donor age and cell passage affects differentiation potential of murine bone marrow-derived stem cells. *BMC Cell Biol.* **2008**, *9*, 60. [CrossRef]
80. Boulestreau, J.; Maumus, M.; Rozier, P.; Jorgensen, C.; Noël, D. Mesenchymal Stem Cell Derived Extracellular Vesicles in Aging. *Front. Cell Dev. Biol.* **2020**, *8*, 107. [CrossRef]

81. Zhang, Y.; Ravikumar, M.; Ling, L.; Nurcombe, V.; Cool, S.M. Age-Related Changes in the Inflammatory Status of Human Mesenchymal Stem Cells: Implications for Cell Therapy. *Stem Cell Rep.* **2021**, *16*, 694–707. [CrossRef] [PubMed]
82. Siennicka, K.; Zołocińska, A.; Dębski, T.; Pojda, Z. Comparison of the Donor Age-Dependent and In Vitro Culture-Dependent Mesenchymal Stem Cell Aging in Rat Model. *Stem Cells Int.* **2021**, *2021*, 1–16. [CrossRef] [PubMed]
83. Urbanelli, L.; Buratta, S.; Sagini, K.; Tancini, B.; Emiliani, C. Extracellular Vesicles as New Players in Cellular Senescence. *Int. J. Mol. Sci.* **2016**, *17*, 1408. [CrossRef] [PubMed]
84. Lunyak, V.V.; Amaro-Ortiz, A.; Gaur, M. Mesenchymal Stem Cells Secretory Responses: Senescence Messaging Secretome and Immunomodulation Perspective. *Front. Genet.* **2017**, *8*, 220. [CrossRef] [PubMed]
85. Cammack, R.; Atwood, T.; Campbell, P.; Parish, H.; Smith, A.; Vella, F.; Stirling, J. *Oxford Dictionary of Biochemistry and Molecular Biology*; Oxford University Press: Oxford, UK, 2008.
86. Ribitsch, I.; Chang-Rodriguez, S.; Egerbacher, M.; Gabner, S.; Gueltekin, S.; Huber, J.; Schuster, T.; Jenner, F. Sheep Placenta Cotyledons: A Noninvasive Source of Ovine Mesenchymal Stem Cells. *Tissue Eng. Part C Methods* **2017**, *23*, 298–310. [CrossRef] [PubMed]

International Journal of
Molecular Sciences

MDPI

Article

Mesenchymal Stem Cell Conditioned Medium Modulates Inflammation in Tenocytes: Complete Conditioned Medium Has Superior Therapeutic Efficacy than Its Extracellular Vesicle Fraction

Robert Soukup [1], Iris Gerner [1,2], Thomas Mohr [3,4,5], Sinan Gueltekin [1], Johannes Grillari [2,6,7,*] and Florien Jenner [1,2,*]

1 VETERM, Equine Surgery Unit, Department for Companion Animals and Horses, Vetmeduni, 1210 Vienna, Austria; iris.gerner@vetmeduni.ac.at (I.G.)
2 Austrian Cluster for Tissue Regeneration, 1200 Vienna, Austria
3 Science Consult DI Thomas Mohr KG, 2353 Guntramsdorf, Austria
4 Center for Cancer Research, Comprehensive Cancer Center, Medical University of Vienna, 1090 Vienna, Austria
5 Department of Analytical Chemistry, University of Vienna, 1090 Vienna, Austria
6 Ludwig Boltzmann Institute for Traumatology, The Research Center in Cooperation with AUVA, 1200 Vienna, Austria
7 Institute of Molecular Biotechnology, University of Natural Resources and Life Sciences, 1090 Vienna, Austria
* Correspondence: johannes.grillari@trauma.lbg.ac.at (J.G.); florien.jenner@vetmeduni.ac.at (F.J.)

Abstract: Tendinopathy, a prevalent overuse injury, lacks effective treatment options, leading to a significant impact on quality of life and socioeconomic burden. Mesenchymal stem/stromal cells (MSCs) and their secretome, including conditioned medium (CM) and extracellular vesicles (EVs), have shown promise in tissue regeneration and immunomodulation. However, it remains unclear which components of the secretome contribute to their therapeutic effects. This study aimed to compare the efficacy of CM, EVs, and the soluble protein fraction (PF) in treating inflamed tenocytes. CM exhibited the highest protein and particle concentrations, followed by PF and EVs. Inflammation significantly altered gene expression in tenocytes, with CM showing the most distinct separation from the inflamed control group. Treatment with CM resulted in the most significant differential gene expression, with both upregulated and downregulated genes related to inflammation and tissue regeneration. EV treatment also demonstrated a therapeutic effect, albeit to a lesser extent. These findings suggest that CM holds superior therapeutic efficacy compared with its EV fraction alone, emphasizing the importance of the complete secretome in tendon injury treatment.

Keywords: equine mesenchymal stem cells (MSC); MSC secretome; MSC extracellular vesicles (EVs); MSC protein fraction; cell-free therapy; tenocytes regeneration

Citation: Soukup, R.; Gerner, I.; Mohr, T.; Gueltekin, S.; Grillari, J.; Jenner, F. Mesenchymal Stem Cell Conditioned Medium Modulates Inflammation in Tenocytes: Complete Conditioned Medium Has Superior Therapeutic Efficacy than Its Extracellular Vesicle Fraction. *Int. J. Mol. Sci.* **2023**, *24*, 10857. https://doi.org/10.3390/ijms241310857

Academic Editors: Wasim S. Khan and Young Woo Eom

Received: 17 May 2023
Revised: 9 June 2023
Accepted: 23 June 2023
Published: 29 June 2023

1. Introduction

Tendinopathy, a disabling overuse injury, is prevalent among athletes and sedentary subjects, afflicting 25% of the adult population and accounting for 30–50% of all sports injuries [1,2]. No current treatment restores the functional properties of injured tendons, resulting in a significant impact on quality of life and high socioeconomic pressure, with the annual health expenditure on human tendon injuries exceeding €145 billion.

The repair response of tendons following injury is inefficient, resulting in a fibrovascular scar that never attains the gross, histological, or mechanical characteristics of normal tendon and thus predisposes to recurring injury and tendinopathy [1–8]. Tendon injury induces a local inflammatory response, characterized by an influx of inflammatory cells that release chemotactic and proinflammatory cytokines and growth factors, promote the recruitment and proliferation of macrophages and resident tendon fibroblasts, and initiate

the healing process [3–12]. The inflammatory milieu can modify tenocyte physiology by increasing metabolic activity and inducing an activated, proinflammatory phenotype with inflammation memory and the capacity for endogenous production of inflammatory cytokines such as TNF-α and IL-1β [12]. There is growing evidence that inflammation (the first phase of the injury response), specifically its lack of resolution, has a crucial role in disease progression, especially when shifting to a chronic state [3–12].

Tendon treatment with mesenchymal stem/stromal cells (MSCs) has been employed in equine orthopaedics since 2003 and has yielded promising results, reducing reinjury rates in the equine superficial digital flexor tendon, the functional equivalent to the human Achilles tendon, from 56% to 18% [13–20]. Yet, translational progress into human clinical practice so far has been disappointing, partially due to the regulatory and manufacturing challenges inherent to all cell therapies and safety concerns such as potential tumorigenicity [21]. In addition, inflammatory conditions can compromise MSC's differentiation capacity and therapeutic potential, as MSCs react context-sensitively to their respective pathophysiological microenvironments [22]. However, MSCs show poor engraftment and cell survival following transplantation and exert their therapeutic effect predominantly by secreting bioactive factors (collectively termed "secretome"), including soluble factors and extracellular vesicles (EVs) with their cargo of proteins, lipids, metabolites, and nucleic acids [23–25]. The secretome mirrors the ability of the parental cells to condition and program the surrounding microenvironment, influencing a variety of endogenous responses, in particular in injured tissues. Indeed, both the whole secretome (or conditioned medium, CM) and its EV fraction have shown equivalent therapeutic effects on their producer cells in a wide variety of diseases, including spinal cord injury, cardiomyopathy, osteoarthritis, and tendinitis, thus paving the way for the development of cell-free therapies [23,24,26–33].

MSC-CM and EVs have shown immunomodulatory effects by modulating macrophage polarization toward a pro-resolving M2 phenotype, reducing the expression of pro-inflammatory cytokines such as TNFα, interleukin (IL)-1β and IL-6 and increasing the secretion of anti-inflammatory factors including IL-10 and IL-4 [34–36]. In addition, MSC-CM and EVs contribute directly to tissue regeneration by enhancing tissue-specific extracellular matrix (ECM) component production and downregulating catabolic matrix metalloproteinases (MMPs) [35,36].

The regenerative potential of MSC-CM and EVs in tendon and ligament repair was shown in vitro and in vivo in various species. including mice, rats, rabbits, sheep, horses, and humans [34,37–48]. MSC-derived CM (MSC-CM) promoted rat tenocyte proliferation via activation of extracellular signal-regulated kinase1/2 (ERK1/2) signal molecules compared with the untreated control group [49]. Similarly, MSC-CM promoted tendon-bone healing of the rat rotator cuff by inhibiting M1 and supporting M2 macrophage polarization [34]. Furthermore, in horses, MSC-CM demonstrated an immunomodulatory effect by inhibiting the proliferation of peripheral blood mononuclear cells (PBMCs) in vivo and induced neovascularization, which was not observed before treatment and declined during the progression of the healing process, characterized by a decrease in vessel size and quantity [50]. MSC-EVs demonstrated their immunomodulatory capacity in a variety of tendon injury models in vivo by reducing macrophage NF-κB activity and the IL-1β and IFN-γ response, decreasing M1 and supporting M2 macrophage polarization, and increasing the production of anti-inflammatory cytokines such as IL-4 and IL-10 [37,43,45,47]. In addition, MSC-EVs administered into tendon and enthesis defects resulted in enhanced proliferation of tendon stem/progenitor cells (TSPCs), better restoration of the tendon and enthesis architecture, an improved histological score, greater expression of genes related to collagen and tendon matrix formation, including collagen (Col) type I, mohawk (MKX), scleraxis (SCX)tenomodulin (TNMD) and tissue inhibitor of metalloproteinase-3 (TIMP-3), and decreased matrix metalloproteinases (MMP)-3 expression [37,38,40,44,46].

While the therapeutic potential of MSC-CM and its EV fraction for regenerative medicine in general and the treatment of tendon injuries in particular is well established, it is still unclear whether components of the CM act synergistically or redundantly and

whether the entire CM, isolated EVs, or only selected soluble factors are required to achieve a therapeutic effect [51,52]. Attempts to use single paracrine factors, such as beta fibroblast growth factor (bFGF), hepatocyte growth factor (HGF), and vascular endothelial growth factor (VEGF), to treat cardiovascular diseases so far have shown unsatisfactory outcomes, demonstrating that these factors alone are not sufficient to induce regeneration [52]. A study comparing the therapeutic efficacy of complete MSC-CM and MSC-EVs alone on skeletal muscle regeneration in vitro and in vivo demonstrated that the two fractions promote different aspects of regeneration after muscle injury and act synergistically to promote muscle regeneration [53]. In detail, CM but not the EV fraction inhibited cellular senescence, but only EVs impacted nuclear translocation of NF-κB and decreased lysosomal activity in glioma cells. Similar results were obtained in a wound closure model, suggesting that the complete CM has superior regenerative capacity than its purified subfractions [54].

Therefore, this study compares the therapeutic effect of CM, its EV fraction, and its soluble protein fraction (PF, CM without EVs) on inflamed tenocytes to test the hypothesis that the conditioned medium has greater therapeutic efficacy than its EV fraction alone. The study is carried out in equine cells, as horses suffer from naturally occurring tendinopathy analogous to humans and are well-established animal models, also recommended by the U.S. Food and Drug Administration (FDA) and the European Medicines Agency (EMA) [55–57].

2. Results

2.1. Equine Bone Marrow-Derived MSCs and EVs Show Characteristic Markers

The cells isolated from the bone marrow of the three donor horses were plastic adherent and expressed typical MSC markers such as CD90 (73.1% ± 5.3 positive cells), CD44 (77.2% ± 3.1 positive cells), and CD29 (72% ± 3.7 positive cells) (Figure 1a) [58]. They exhibited the ability to differentiate into adipocytes (Figure 1b), chondrocytes (Figure 1c), and osteoblasts (Figure 1d), demonstrating their trilineage differentiation potential [58]. We characterized the EVs according to the MISEV2018 guidelines using nanotracking analysis, fluorescence-triggered flow cytometry (lipid membrane dye cell mask green (CMG) and CD81), Western Blot (positive for the two tetraspanins, CD9 and CD63), and transelectron microscopy as we previously described [58].

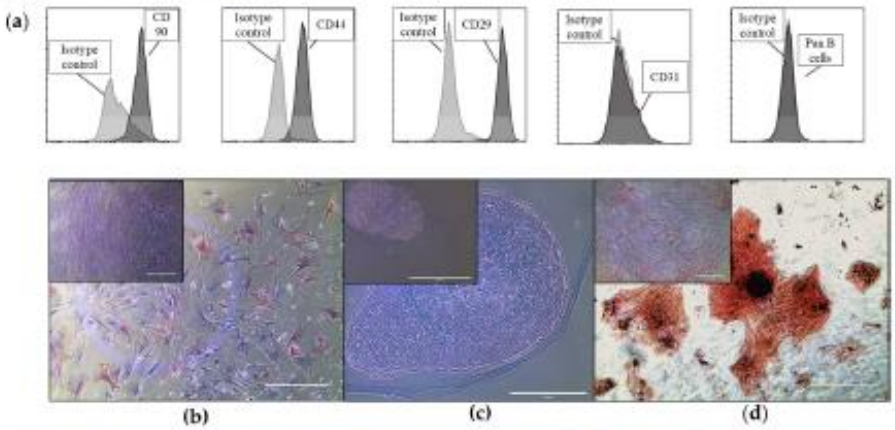

Figure 1. Shows representative images of the characterization of equine bone-marrow-derived cells with trilineage differentiation capacity and canonical surface marker expression of MSCs. (**a**) Cells were stained with specific cell surface antigens (dark grey plots) or Ig isotype controls (light grey plots) and analyzed by flow cytometry. Cells stained positive for CD90, CD44, and CD29 and negative for CD31 and Pan B, as well as IgG isotype controls. Displayed on the *x*-axis is either PE or FITC conjugated to one of the previously mentioned antibodies. (**b–d**) Images show bone-marrow-derived cells differentiating into the adipogenic (**b**), chondrogenic (**c**), and osteogenic (**d**) lineages, stained with Oil red O, Alcian blue, and von Kossa stain, respectively. The corresponding controls (cells grown in an expansion medium) are shown in the insert in the top left corner of each micrograph. Scale bars: 400 µm.

2.2. CM Fraction Has the Highest Protein- and Particle Concentration

After CM production for 48 h, the measured protein concentration was highest in the CM fraction, with a mean of 130 ± 6.2 µg/mL (Table 1). The protein concentration in the CM fraction was 4.3 times higher than in the EV fraction (30.4 ± 0.5 µg/mL) ($p = 0.0019$) and 1.8 times higher than in the PF fraction (73.2 ± 0.9 µg/mL) ($p = 0.0066$). The PF fraction contained 2.4 times more protein than the EV fraction ($p = 0.0005$) (Figure 2a and Table 1).

Table 1. Measured protein- and particle-concentration per fraction: The CM fraction contained the highest protein content (µg/mL) followed by the PF. The lowest protein concentration was found in the EV fraction. The highest overall particle concentration (particles/mL) was found in the CM which is also true for the particle numbers >195 nm. However, more particles were enriched in the EV fraction ≤195 nm. No measurable particles were present in the PF.

	CM	EV	PF
Protein (µg/mL)	130 ± 6.18	30.4 ± 0.5	73.2 ± 0.9
Particle number (total NTA) (particles/mL)	$1.53 \times 10^{11} \pm 2.01 \times 10^{10}$	$1.03 \times 10^{11} \pm 2.04 \times 10^{10}$	Not detected
Particle number ≤ 195 nm (NTA) (particles/mL)	$5.36 \times 10^{10} \pm 7.67 \times 10^{9}$	$5.61 \times 10^{10} \pm 1.06 \times 10^{10}$	Not detected
Particle number > 195 nm (NTA) (particles/mL)	$1.09 \times 10^{11} \pm 2.51 \times 10^{10}$	$4.67 \times 10^{10} \pm 9.81 \times 10^{9}$	Not detected

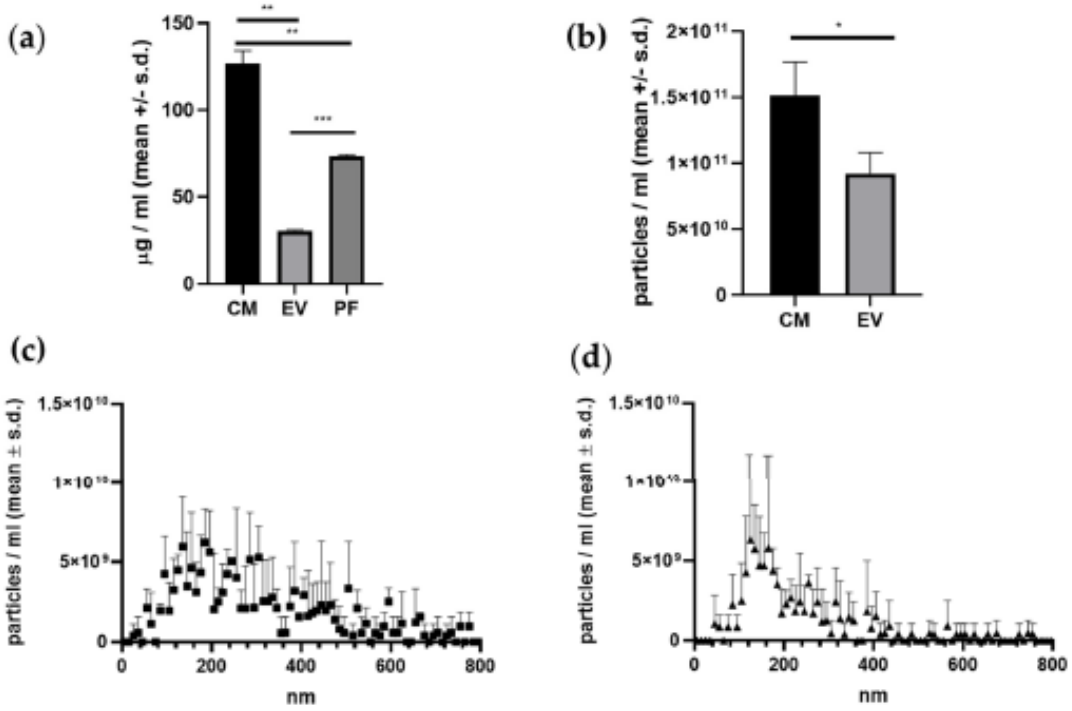

Figure 2. MSCs from 3 equine donors were cultured and the cell-free supernatant was collected and centrifuged to obtain CM, EVs and PF. (**a**) shows that the protein concentration was significantly higher in the CM fraction than in the EV and PF fractions (** = $p = 0.0019$ and *** = $p = 0.0066$, respectively). Moreover, the protein concentration was higher in the PF fraction than in the EV fraction (*** = $p = 0.0005$). (**b**) shows that the particle concentration was significantly higher in the CM fraction than in the EV fraction (* = $p = 0.0179$). (**c**,**d**) illustrate the size distribution of the EVs and CM, respectively. The EV fraction contained more particles ≤195 nm, resulting in a more homogeneous size distribution compared with the CM fraction.

Particle concentration was also higher in the CM fraction compared with the EV fraction, with $1.53 \times 10^{11} \pm 2.01 \times 10^{10}$ particles/mL in the CM fraction and $1.03 \times 10^{11} \pm 2.04 \times 10^{10}$ particles/mL in the EV fraction (Figure 2b). No particles were detected in the PF fraction. The size distribution of the particles was more homogeneous in the EV fraction, with $5.61 \times 10^{10} \pm 1.06 \times 10^{10}$ particles/mL particles $\leq$ 195 nm and $4.67 \times 10^{10} \pm 9.81 \times 10^{9}$ particles/mL particles > 195 nm. In the CM fraction, $5.36 \times 10^{10} \pm 7.67 \times 10^{9}$ particles/mL were $\leq$195 nm while $1.09 \times 10^{11} \pm 2.51 \times 10^{10}$ particles/mL were >195 nm (Figure 2c,d and Table 1).

There was no significant variation in protein content, particle concentration, or size distribution among the donors.

2.3. Inflammation Induces a Significant Change in Tenocytes' Gene Expression

The induction of inflammation was induced by serum starvation plus chemical stimulation with 10 ng/mL TNFα and 10 ng/mL ILb1 for 24 h. This resulted in the differential expression of 1496 genes, representing 12.5% of all identified genes (11,925 genes) as compared with the healthy control (Tables 2 and 3, Figure 3). 346 (23%) were upregulated in the inflamed control compared with the healthy control, and 1150 (78%) were downregulated. The upregulated genes were found to be strongly associated with inflammation, including Colony Stimulating Factor 3 (CSF3), C-C Motif Chemokine Ligand 11 (CCL11), CCL2, CCL20, CCL5, C-X-C Motif Chemokine Ligand 1 (CXCL1), CXCL6, CXCL8, Interleukin 36 Gamma (IL36G), IL6, NF-kappa-B inhibitor alpha (NFKBIA), and Prostaglandin D2 Synthase (PTGDS). Pathway analysis yielded 112 pathways that were downregulated upon inflammation and 98 that were upregulated (Table 3).

All inflamed groups, treated and untreated alike, clustered distantly from the healthy control group in principal component analysis (Figure 3).

Table 2. Top 10 down-regulated genes of the three treatment groups (conditioned medium (CM), extracellular vesivles (EV) and soluble protein fraction (PF)) and the healthy control (CRTL) compared with the inflamed CTRL: Only genes with an adjusted *p*-value of $p < 0.1$ and FC > 1.5 are considered significant.

Top 10 Downregulated Genes in the Treatment/Healthy CTRL vs. Inflamed CTRL (Sorted by Ascending Adjusted *p*-Value)											
CM			**EV**			**PF**			**Healthy CTRL**		
Gene	**FC**	**Adj. *p*-Value**	**Gene**	**FC**	**Adj. *p*-Value**	**Gene**	**FC**	**Adj. *p*-Value**	**Gene**	**FC**	**Adj. *p*-Value**
ADGRD1	−23.750	9.5536×10^{-7}	FUZ	−36.203	3.0566×10^{-16}	NOXA1	−40.887	6.1398×10^{-20}	PSME2	2.11877	2.5995×10^{-40}
SAA	−31.261	5.7985×10^{-6}	NTN1	−30.152	0.00027148	TRIM6	−34.742	3.7594×10^{-17}	KYAT3	1.86235	2.2722×10^{-35}
HIVEP3	−15.446	1.0763×10^{-5}	GPM6B	−29.649	0.00027148	H1-9	−30.859	4.3641×10^{-8}	RAB20	3.90099	2.2722×10^{-35}
COL14A1	−28.138	9.163×10^{-5}	podocalyxin like	−28.229	0.01057581	TCP11	−33.531	1.2429×10^{-5}	DBNL	2.24989	9.5604×10^{-34}
ZIC2	−12.980	0.00011	LRRC23	−27.298	0.01865918	MRPL54	−31.808	2.4525×10^{-5}	SNAP29	1.72103	5.1924×10^{-32}
VSIR	−17.357	0.00038	C6orf47	−21.264	0.03612666	ZNF382	−17.616	5.3998×10^{-5}	CCL2	4.07345	3.5555×10^{-30}
FBXO32	−16.372	0.00056	CMYA5	−18.940	1.5926×10^{-7}	FAM216B	−16.926	0.00018	CCL11	3.49896	6.2286×10^{-30}
PLA2G2A	−26.155	0.00062	ZKSCAN8	−17.918	0.00027148	NTN1	−29.748	0.00031	PI3	3.77388	2.2449×10^{-29}
SCARA5	−43.596	0.00067	CSPG4	−17.519	1.3391×10^{-5}	CCDC40	−26.832	0.00257	CCL5	5.21572	4.8974×10^{-29}
SPNS3	−31.756	0.00205	GSK-3	−17.2511	0.00031	IL17RA	−17.499	0.00443	SIDT2	3.70467	3.1246×10^{-27}

Table 3. Top 10 up-regulated genes of the three treatment groups (conditioned medium (CM), extracellular vesivles (EV) and soluble protein fraction (PF)) and the healthy control (CRTL) compared with the Inflamed CTRL: Only genes with an adjusted *p*-value of $p < 0.1$ and FC > 1.5 are considered significant.

Top 10 Upregulated Genes in the Treatment/Healthy CTRL vs. Inflamed CTRL (Sorted by Ascending Adjusted *p*-Value)											
CM			EV			PF			Healthy CTRL		
Gene	FC	Adj. *p*-Value	Gene	FC	Adj. *p*-Value	Gene	FC	Adj. *p*-Value	Gene	FC	Adj. *p*-Value
PIRT	186.866	9.78×10^{-10}	ZNF582	443.953	7.7528×10^{-46}	ZNF582	432.963	9.88×10^{-43}	ZNF582	−45.537	8.3178×10^{-50}
ELMO1	181.622	3.61×10^{-10}	PIRT	197.946	6.2092×10^{-12}	PIRT	186.640	3.19×10^{-10}	ENSECAG00000016730	−28.492	5.4407×10^{-42}
ZNF501	239.838	3.61×10^{-7}	ELMO1	173.926	1.6926×10^{-6}	CCND1	198.841	3.53×10^{-7}	CCDC88A	−27.159	1.195×10^{-32}
ENSECAG00000023978	184.840	1.75×10^{-6}	ZNF501	226.906	1.9717×10^{-6}	metallothionein-1A	451.660	3.53×10^{-7}	CELF2	−28.702	6.2556×10^{-29}
TPGS2	173.051	4.13×10^{-6}	ENSECAG00000023978	174.590	1.4739×10^{-5}	TPGS2	178.046	8.18×10^{-7}	FSTL1	−32.601	1.8517×10^{-25}
ENSECAG00000013505	182.588	7.55×10^{-6}	ZNF182	286.245	1.6141×10^{-5}	ELMO1	167.381	4.86×10^{-6}	PTMA	−26.727	1.2088×10^{-21}
STAC	215.231	3.03×10^{-5}	ENSECAG00000013505	160.195	0.00035	ZNF182	292.836	7.23×10^{-6}	CALCA	−47.284	2.7129×10^{-21}
CCND1	163.745	0.00012	DCX	205.337	0.00060	ZNF501	214.091	1.24×10^{-5}	C7H11orf58	−29.221	4.2637×10^{-20}
RAD51D	210.350	0.00038	ASB5	161.541	0.00447	MT1B	163.702	0.00018	ANXA5	−41.201	2.5081×10^{-19}
ASB5	176.871	0.00038	GRID1	273.429	0.01865	ACBD7	319.023	0.00020	APC	−17.720	1.6149×10^{-17}

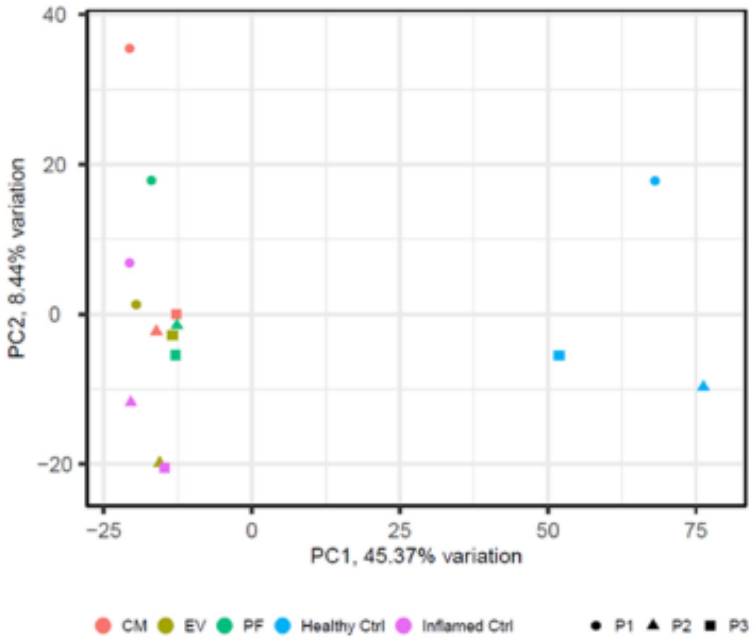

Figure 3. Principal Component Analysis (PCA) plot displaying the differential gene expression data from patient cells. Three patients (P1, P2, and P3) are represented by different symbols, while the treatments and controls are distinguished by different colors. The healthy control (light blue) is separated from the other samples. Cells treated with CM (red dots), inflamed control (purple dots), EV-treated cells (green dots), and PF-treated cells (light green dots) cluster close to each other.

2.4. Conditioned Medium Achieves a Higher Effect on Differential Gene Expression of Inflamed Tenocytes Than EVs or PF Alone

The tenocytes exhibited a significant differential gene expression as a result of inflammation (Figure 4a). CM had the strongest treatment effect on inflamed tenocytes, resulting in statistically significant differential expression of 120 genes, of which 42 genes (35%) were down-regulated (Table 2) and 78 genes (65%) were up-regulated compared with the inflamed control with no treatment (Figure 4b and Table 3). Treatment with PF had the second strongest effect on gene expression, resulting in the statistically significant differential expression of 57 genes, of which 17 genes (30%) were down-regulated (Table 2) and 40 genes (70%) were up-regulated compared with the inflamed control (Figure 4d and Table 3). Treatment with EV resulted in the statistically significant differential expression of 33 genes, of which 16 genes (48.5%) were down-regulated (Table 2) and 17 genes (51.5%) were up-regulated compared with the inflamed control (Figure 4c and Table 3).

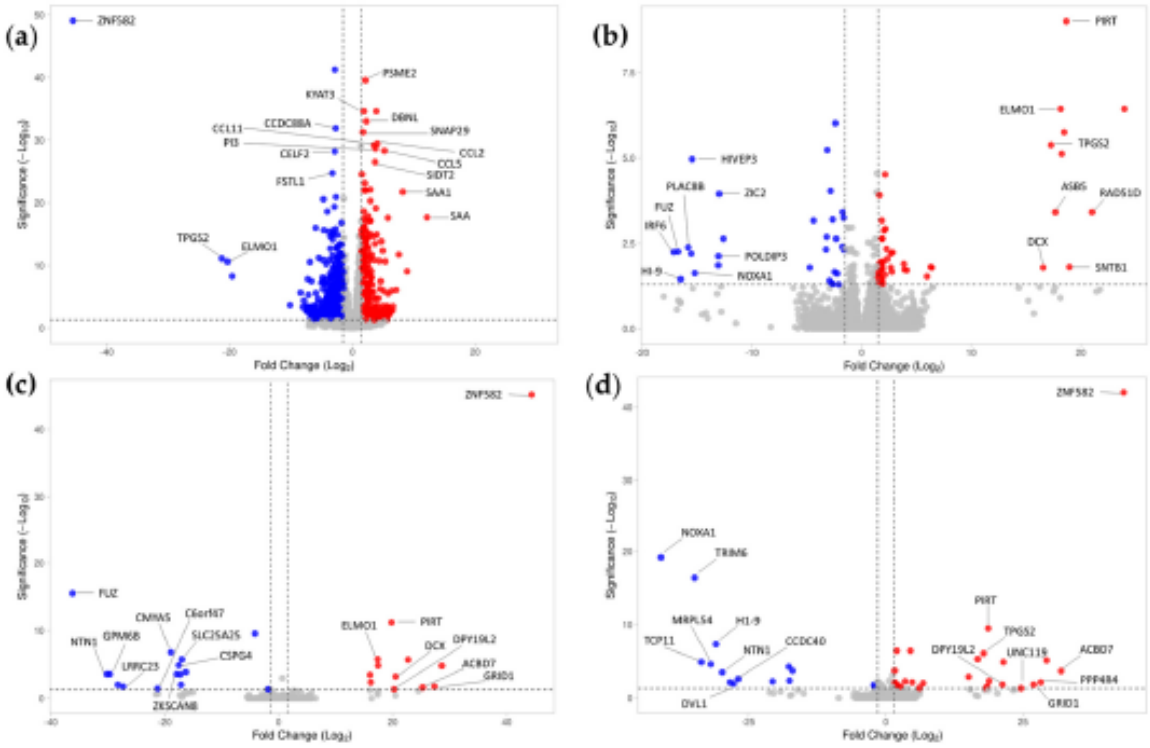

Figure 4. Volcano plot of differentially expressed (DE) genes in the patient cells: The plot highlights the top 20 DE genes, which have been appropriately labeled for identification. (**a**) Control Inflamed vs. Control Healthy (**b**) CM vs. Control Inflamed, (**c**) EV vs. Control Inflamed and (**d**) PF vs. Control Inflamed are displayed in absolute numbers. The volcano plots show the log2 fold change on the *x*-axis and the log10 adjusted *p*-value on the *y*-axis. Significantly upregulated genes are shown in red, significantly downregulated genes in blue, and non-significant genes in grey. Only genes with an adjusted *p*-value of $p < 0.1$ and FC > 1.5 are considered significant.

CM treatment downregulated 42 genes compared with the untreated inflamed group (Figures 4b and 5a and Table 2). Of these 24 genes (57%) that were unique to CM treatment, 13 genes (31%) were shared with healthy control, three (7%) with PF, one (2%) with EV, and one (2%) with PF and healthy control. The genes that were downregulated following treatment with CM included genes linked to inflammation (CCL20, Serum amyloid A (SAA), SSA1, and Tumor necrosis factor-inducible gene 6 protein (TNFAIP6)) and extracellular matrix organization (Collagen type XIV alpha 1 chain (COL14A1) and Matrix metalloproteinase 13 (MMP13)). In addition, CM treatment upregulated 78 genes compared with the

untreated inflamed control, of which 18 (23%) were unique to CM treatment, nine (12%) were shared with PF treatment and healthy control, six (8%) with EV and PF treatment, five (6%) with PF treatment, two (3%) with EV treatment, and two (3%) with EV, PF, and healthy control. The genes that were upregulated upon CM treatment included genes associated with cell cycle and mitosis (various cyclins, kinesin family members, and ATPase family members), DNA damage response and repair (DNA damage-induced apoptosis suppressor (DDIA), Fanconi Anemia Complementation Group D2 (FANCD2), High Mobility Group AT-hook 2 (HMGA2), Platelet-activating factor acetylhydrolase 2 (PAFAH2), V-rel avian reticuloendotheliosis viral oncogene homolog A (RELA)), and metabolism and transport (Glutamine-fructose-6-phosphate transaminase 2 (GFPT2), Methionine Aminopeptidase 1 (METAP1), and Synaptic Vesicle Glycoprotein 2C (SV2C)) (Figure 4b and Table 3).

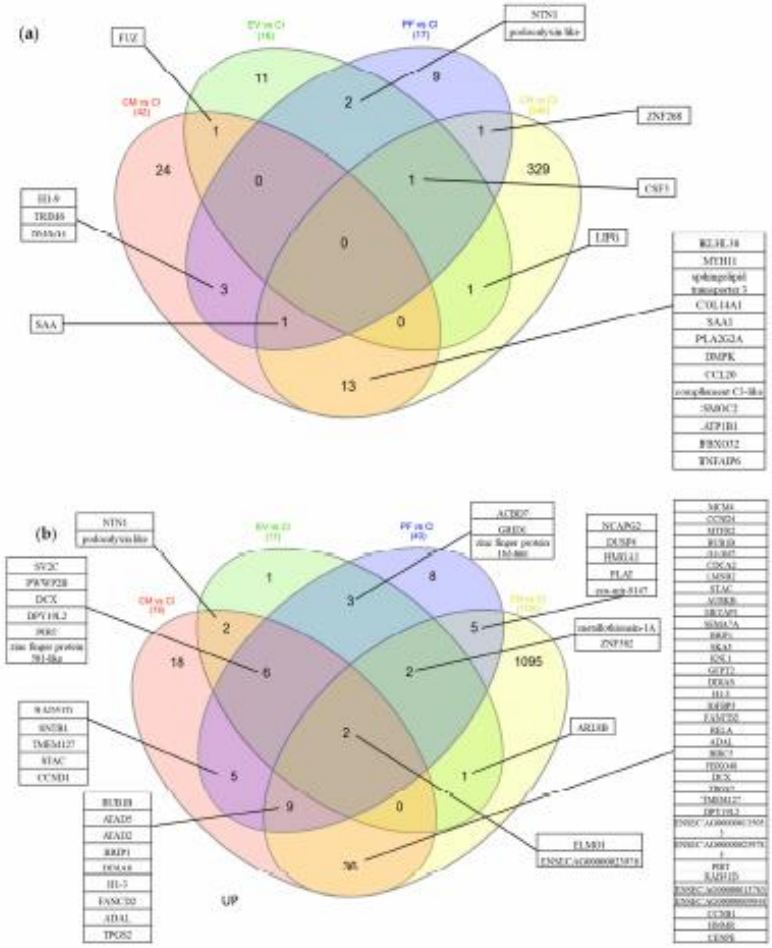

Figure 5. Venn diagram of DE genes in the patient cells: (**a**) Venn diagram of genes which are downregulated upon treatment and in the healthy control compared with inflamed control. (**b**) Venn diagram of genes which are upregulated upon treatment and in the healthy control compared with inflamed control. Only genes with an adjusted *p*-value of $p < 0.1$ and FC > 1.5 are considered significant. In panel (**a**), the Venn diagram shows the number of downregulated genes in the treated cells and healthy control compared with the inflamed control. The number of genes unique to each treatment is displayed in the respective circle, while the overlapping regions represent the number of shared genes between the treatments. Panel (**b**) shows the Venn diagram of upregulated genes in the same comparison. Only genes with an adjusted *p*-value of $p < 0.1$ and FC > 1.5 are considered significant.

EV treatment downregulated 16 genes compared with the untreated inflamed group (Figures 4c and 5a and Table 2). Of these 11 genes (69%) that were unique to EV treatment, two (12.5%) genes were shared with PF, one (6.25%) with CM, one (6.25%) with healthy control, and one (6.25%) with PF and healthy control. Among the genes downregulated upon EV treatment were the cytokine CSF3 and glycogen synthase kinase 3 alpha. Furthermore, we observed that EV treatment upregulated 17 genes, of which one (6%) gene was unique to EV treatment, six (35%) were shared with CM and PF, three (18%) genes were shared with PF, two (12%) with CM, two (12%) with PF treatment and healthy control, two (12%) with CM, EV fraction, and healthy control, and one (6%) only with healthy control. The genes that were upregulated upon EV treatment were associated with cytoskeleton organization (ADP Ribosylation Factor Like GTPase 8B (ARL8B) and Doublecortin (DCX)), extracellular matrix organization (Inter-alpha-trypsin inhibitor heavy chain 1 (ITIH1)), and epigenetic modification (Ankyrin Repeat and SOCS Box Containing 5 (ASB5) and Acyl-CoA binding domain containing 7 (ACBD7)) (Figures 4c and 5b and Table 3).

Treatment with PF led to the downregulation of 17 genes compared with the inflamed control (Figures 4d and 5a and Table 2). Of these nine (53%) were unique to PF treatment, three (18%) were shared with CM, two (12%) were shared with EV, one (6%) with EV fraction and healthy control, one (6%) with CM fraction and healthy control, and one (6%) was shared with healthy control. Among the genes downregulated upon PF treatment were genes associated with inflammation (CSF3, IL17RA, and SAA), protein degradation (Tripartite Motif-Containing 6 (TRIM6)), and oxidative stress (NADPH oxidase activator 1 (NOXA1)). Treatment with PF upregulated 40 genes compared with the inflamed control, of which eight (20%) were unique to PF treatment, five (4%) were shared with healthy control, three (7.5%) were shared with EV, two (5%), two (5%) were shared with CM fraction and healthy control, six (15%) were shared with CM, five (12.5%) were shared with CM, and nine (22.5%) were shared with CM fraction and healthy control. The genes that were upregulated upon PF treatment were associated with DNA damage response and repair (BRCA1-Interacting Protein 1 (BRIP1), Fanconi Anemia Complementation Group D2 (FANCD2) and RAD51 Paralog D (RAD51D)), cell cycle regulation (BUB1 Mitotic Checkpoint Serine/Threonine Kinase B (BUB1B), Cyclin D1 (CCND1), Non-SMC Condensin II Complex Subunit G2 (NCAPG2) and Protein Phosphatase 4 Regulatory Subunit 4 (PPP4R4)), cytoskeleton organization (DCX, Dpy-19 Like 2 (DPY19L2), Engulfment and Cell Motility 1 (ELMO1) and Unc-119 Lipid Binding Chaperone (UNC119)), membrane trafficking and fusion (Syntrophin Beta 1 (SNTB1) and Synaptic Vesicle Glycoprotein 2C (SV2C)), and transcriptional regulation (Glutamate Receptor Ionotropic Delta 1 (GRID1), High Mobility Group AT-hook 1 (HMGA1) and Zinc Finger Protein 582 (ZNF582)) compared with the inflamed control (Figures 4d and 5b and Table 3).

2.5. Pathways

CM treatment resulted in the downregulation of 21 pathways (Figure 6a and Table 4). Of these, 8 pathways (38%) were unique to the CM treatment, while 12 (57%) were shared with the healthy control group and 1 (5%) with both the EV treatment and the healthy control group. Furthermore, 28 pathways were found to be upregulated only by CM treatment, with 17 (61%) of these pathways being unique to CM treatment and the remaining 11 (39%) being shared with the healthy control group (Figure 6b and Table 5).

In contrast, EV treatment upregulated no pathway and downregulated 3, of which 2 pathways (67%) were shared between EV treatment and the healthy control group and 1 (33%) with both the CM treatment and the healthy control group (Figure 6a and Table 4).

PF treatment did not significantly regulate any known pathway.

Table 4. Down-regulated KEGG pathways in the treatment groups conditioned medium (CM) and extracellular vesicles (EV) compared with the inflamed CTRL. Protein fraction (PF) treatment did not significantly regulate any known pathway. Only pathways with adjusted *p*-value < 0.1 are considered significant.

Downregulated Pathways					
CM			EV		
Pathway	FC	Adj. *p*-Value	Pathway	FC	Adj. *p*-Value
Secretion of hydrochloric acid in parietal cells	−1.1589254	0.09355804	Glycerolipids_and_glycerophospholipids	−0.6118861	0.06337278
Nephrogenesis	−1.0681281	0.01124854	Myd88 distinct input/output pathway	−0.5034747	0.06337278
Fatty acid omegaoxidation	−1.0049143	0.07476631	Autosomal recessive osteopetrosis pathways	−0.5445	0.06826365
Complement activation	−0.7625858	0.07859295			
Interleukin1 induced activation of nfkb	−0.674886	0.03094377			
Tryptophan metabolism	−0.6162714	0.04539786			
Mammalian disorder of sexual development	−0.6081617	0.03202702			
Biomarkers for urea cycle disorders	−0.5883797	0.05081052			
Cysteine and methionine catabolism	−0.5820551	0.04634927			
Oxidative stress response	−0.5797825	0.09005984			
Eicosanoid synthesis	−0.5773651	0.03997058			
Overview of nanoparticle effects	−0.5647847	0.03762172			
Beta alanine metabolism	−0.5222863	0.09005984			
Matrix metalloproteinases	−0.4351830	0.07476631			
S1P receptor signal transduction	−0.4120393	0.05402778			
Autosomal recessive osteopetrosis pathways	−0.4056264	0.07915106			
Valine leucine and isoleucine degradation	−0.3839604	0.08790938			
Sarscov2 innate immunity evasion and cellspecific immune response	−0.3664584	0.04539786			
Selenium micronutrient network	−0.3640307	0.05698454			
Onecarbon metabolism and related pathways	0.31911033	0.08974443			
Leukocyte transendothelial migration	−0.2761994	0.07915106			

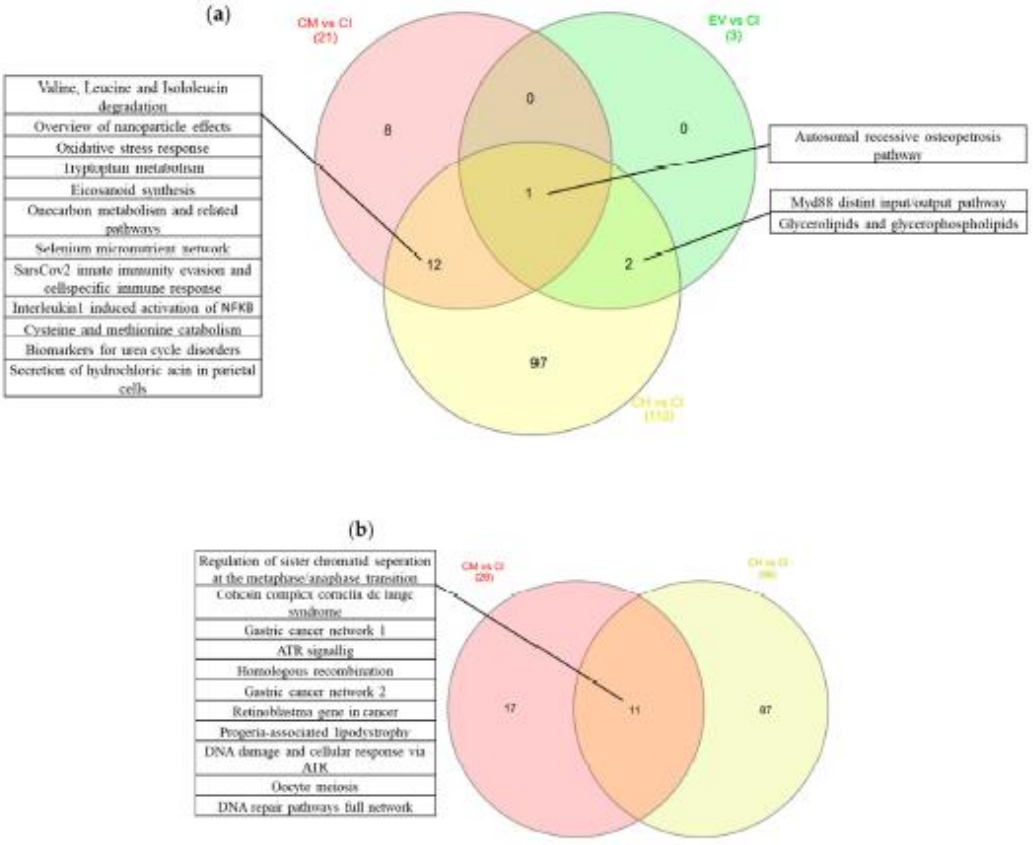

Figure 6. Venn diagram of pathways: (**a**) Venn diagram of pathways which are downregulated upon treatment and in the healthy control compared with inflamed control. (**b**) Venn diagram of pathways which are upregulated upon treatment and in the healthy control compared with inflamed control. Only genes with an adjusted *p*-value of $p < 0.1$ and FC > 1.5 are considered significant.

Table 5. Up-regulated KEGG pathways in the treatment group conditioned medium (CM) compared with the inflamed CTRL. Treatment with extracellular vesicles (EV) and protein fraction (PF) did not significantly regulate any known pathway. Only pathways with adjusted *p*-value < 0.1 are considered significant.

Upregulated Pathways		
CM		
Pathway	**FC**	**Adj. *p*-Value**
Nucleotide excision repair in xeroderma pigmentosum	0.3494815	0.07130188
Pyrimidine metabolism	0.37184491	0.08655644
Dna repair pathways full network	0.40690974	0.04539786
Oocyte meiosis	0.40797081	0.03997058
Nucleotide excision repair (WP)	0.42922411	0.03776133
Nucleotide excision repair (KEGG)	0.42922411	0.03776133
Progeriaassociated lipodystrophy	0.4650666	0.04539786

Table 5. *Cont.*

Upregulated Pathways		
CM		
Pathway	**FC**	**Adj. *p*-Value**
Pyrimidine metabolism	0.47735464	0.03202702
Cell cycle (WP)	0.49283852	0.05915343
Cell cycle (KEGG)	0.4933381	0.05577275
Gastric cancer network 1	0.49568256	0.09520106
DNA irdamage and cellular response via ATR	0.50092208	0.04101562
Base excision repair	0.55896011	0.09005984
Cohesin complex cornelia de lange syndrome	0.58300193	0.01124854
Mammary gland development pathway puberty stage 2 of 4	0.58799809	0.04539786
Base excision repair	0.59293411	0.09955858
Gastric cancer network 2	0.67347864	0.04101562
ATR signaling	0.68398751	0.07272085
Homologous recombination	0.70623154	0.04539786
Retinoblastoma gene in cancer	0.71687919	0.03776133
Nucleotide metabolism	0.76157908	0.04101562
Serine metabolism	0.76326554	0.01124854
Mismatch repair	0.81963998	0.03202702
Regulation of sister chromatid separation at the metaphaseanaphase transition	0.86498193	0.03856315
DNA replication	0.904723	0.03094377
DNA mismatch repair	0.92494463	0.03202702
Acquired partial lipodystrophy barraquersimons syndrome	0.93639734	0.03202702
DNA replication	0.96512563	0.03202702

3. Discussion

Complete CM had the strongest treatment effect on inflamed tenocytes in our study. While all three treatments yielded significant differences compared with the untreated inflamed control, the EV fraction and the PF were not able to influence the gene expression level to the same extent as the CM fraction.

In line with our findings, the synergistic effects of the secretome's EV and soluble protein components and the corresponding therapeutic superiority of complete CM compared with its subfractions, were shown in a variety of other cells and assays [53,54,59–61]. A comparison of the effects of CM and EV on adipose-derived MSCs (aMSCs) on muscle regeneration revealed that both CM and EV protect against cellular senescence but demonstrate higher proliferation and differentiation with CM, while only EVs reduced inflammation [53]. In an in vitro OA model comparing the therapeutic efficacy of human ASCs derived CM and EVs, both CM and EV reduced hypertrophic collagen 10, but only CM significantly decreased MMP activity and prostaglandin 2 (PGE2) expression [61]. Similarly, a study evaluating the effects of whole CM and its EV and PF fractions on inflamed nucleus pulposus and annulus fibrosus cells in vitro demonstrated a superior immunomodulatory and MMP inhibitory effect of whole CM compared with its subfractions [60]. A comparison of the effects of the peripheral blood mononuclear cell-derived secretome and its subfractions also found that the complete secretome induced better neo-

angiogenesis than its apportioned constituents, namely the EV, lipid, and protein fractions individually [54].

In contrast, divergent findings were made by investigating the CM of human adipose-derived MSCs, where EVs alone, similar to the whole CM, were capable of promoting cell proliferation and migration in skeletal muscle cells. Furthermore, small extracellular EVs outperformed conditioned media of adipose tissue in migration and regeneration potential, although this study standardized EVs and CM on equivalent protein concentrations and did not consider unpacked proteins [61]. Another explanation for EVs outperforming CM on migration in this particular study is that the ability to recruit host cells for migration occurs more efficiently through EVs than through other paracrine factors that are present in the CM [62,63].

On the other hand, in a comparison of the therapeutic efficacy of amniotic MSCs derived whole CM, its PF, and EV fractions on immune cell proliferation and differentiation, whole CM and its PF fraction decreased peripheral blood mononuclear cell proliferation, reduced inflammatory polarization of T-cells, enhanced regulatory T-cell and M2 macrophage polarization, and reduced activation of B-cells, while EVs showed no immunomodulatory effect [59].

The divergent results of the various studies comparing of the therapeutic effects of complete CM and its EV fraction may be explained by the differences in the CM/EV donor cells, the media and substrates used for cell culture, cell confluence, preconditioning, the isolation and concentration procedures, the dosage and the treated cells [58,64–68].

Properties of CM/EV isolates are highly dependent on the donor cell type since different cell sources secrete various type of signals beneficial for alternating types of downstream applications [69,70]. In addition, isolation methods, especially for EVs, have an impact on the type and the properties of the enriched EVs [71,72]. Cell culture parameters such as seeding density or passaging frequency can further influence the regenerative potential [73,74].

In addition to the stem cell source, differences in secretome composition are significant when comparing fetal or adult donors [75,76]. Furthermore, pre-conditioning of the donor cells either with various compounds or by modification of the culture conditions leads to altered secretome profiles [77–80]. Another big obstacle when comparing CM and its subfraction is the standardization strategy for studies, the optimal dosage of the treatment, and the number of doses. CM is typically standardized based on the protein concentration, whereas the most common way to determine the therapeutic dose of an EV treatment is by quantifying the number of particles using NTA in an isolate. By using this method, the study focuses on all EVs, regardless of cargo. Future experiments are needed to assess the dose-dependent effects of all three fractions individually, with the aim of identifying the minimum effective dosage and confirming the superior therapeutic efficacy of complete CM compared with its fractions. An alternative approach is to focus on one type of cargo by quantifying a specific component such as nucleic acids, proteins, or lipids in the EVs or using Raman spectroscopy to ascertain the reproducibility of the CM/EV product composition for quality control [81].

Factors that are potentially beneficial for regeneration are distributed both within EVs and in the soluble fraction of the CM [82–84]. Furthermore, the presence of ribosomal proteins and the corresponding factors for translation in EVs would have a direct impact on the recipient cells by expressing proteins de novo [85]. Recently, proteomic analysis demonstrated diverging protein composition between the CM and the EVs, indicating that the vesicle-bound and soluble proteins differ, which confirms the necessity to analyze different parts of the secretome independently to get better insights into the course of events that take place upon administration of the CM and its subfractions before possible clinical use and also to have a clear understanding of protein expressions in healthy organisms and how they are altered by certain diseases with cell-free therapies in numerous clinical applications [43–45]. A better understanding of these processes would provide more information for potential tailored therapeutic options for the secretome.

This study, together with others, provides promising results in vitro. However, prior to translation into the clinic, several questions still have to be addressed, such as the route of administration of the agent, which is characterized by the absorption profile, the distribution throughout the body, the metabolism rate, and the elimination of the clearance [86]. In particular, clearance of EVs is a big problem since it has been shown that EVs, regardless of the route of administration, are quickly cleared from blood circulation and discharged from the body [87,88]. All these properties likely affect the therapeutic potential of the treatment. Upcoming studies are urgently needed that aim to resolve the issues mentioned above and pave the way for reproducible and optimized studies with cell-free treatment approaches.

This study is not without shortcomings. While we did standardize the EV or protein concentration within each treatment, it was not possible to standardize the EV or protein concentration between treatments as enriching one would affect the composition of the other and would ultimately cause loss of material. This issue is demonstrated by the fact that the protein concentration from the EV fraction and the PF combined does not equal the protein concentration of the CM (Figure 3a). In addition to that, the EV concentration in the EV fraction is lower than in the CM (Figure 3b). These observations can be explained by the filtering properties of the size exclusion chromatography (SEC) columns, which may lead to the loss of some EVs and proteins during the filtering process [89].

In conclusion, the differential gene expression data revealed that none of the three treatments was able to restore the healthy status of the patient cells following inflammation (Figure 3). However, treatment with the complete CM resulted in the highest number of differentially expressed genes relative to the inflamed control, suggesting a superior therapeutic effect compared with EV or PF treatment alone and a possible synergistic effect of the different secretome fractions.

4. Materials and Methods

4.1. Bone Marrow Collection and MSC Isolation

Bone marrow was harvested from three horses (donor 1: 11-year-old Tinker mare; donor 2: 6-year-old Pura Raza Espanola gelding; donor 3: 23-year-old Austrian Warmblood mare) euthanized for reasons unrelated to this study and without chronic diseases. Based on the "Good Scientific Practice, Ethics in Science and Research regulation" implemented at the University of Veterinary Medicine Vienna, the Institutional Ethics Committee of the University of Veterinary Medicine Vienna, and the Austrian Federal Ministry of Educations, Science, and Research, in vitro cell culture studies do not require approval if the cells were isolated from tissue that was obtained either solely for diagnostic or therapeutic purposes or in the course of other institutionally and nationally approved experiments.

Immediately post-mortem, bone marrow was harvested from the sternum under sterile conditions, as we previously described [58,90].

The aspirated bone marrow was mixed with 1× PBS with Mg/Ca (Life Technologies, UK, shipped from NL, PBS+/+, Gibco, 1404009) (1:1) and filtered through a 100 µM cell strainer (Greiner Bio-One GmbH, Germany, shipped from Germany, 542000). The mononuclear cell fraction was isolated by density gradient centrifugation using Ficoll Paque Premium (Cytiva, Sweden, shipped from France, 11743219) as previously published [58,90–92]. In brief, the collected bone marrow—PBS +/+ mix was layered onto the Ficoll and centrifuged at room temperature for 30 min at 300× *g* (Hettich, Germany, shipped from Germany, Rotanta 460R) without brake. The buffy coat was collected and washed once with PBS +/+ by centrifuging with 300× *g* for 5 min. The obtained mononuclear cells were seeded in DMEM (Gibco, 31885023) supplemented with 10% FCS (Sigma Aldrich US, shipped from Germany, F7524), 1% Pen/Strep (Sigma, P433-100 mL), and 1% Amphotericin B (Biochrom Germany, shipped from Germany, A 2612-50 mL) and cultured in an incubator with 20% O_2 and 5% CO_2. The medium was changed every 2-3 days. Isolated MSCs were characterized according to the criteria defined by the International Society for Cellular Therapies: plastic adherence, expression of surface markers CD90, CD44, and CD29, lack of

expression of CD31, Pan B and IgG, and adipogenic, chondrogenic, and osteogenic trilineage differentiation potential. After reaching 80–90% confluency, MSCs were harvested and frozen until further use.

4.2. Isolation of the Conditioned Medium (Fractions), Characterization, and Quantification

MSCs were thawed and expanded in chemically defined complete medium (DMEM) supplemented with 10% FCS (Capricon Scientific, Germany, shipped from Germany, FBS-12A), 1% Pen/Strep, and 1% amphotericin B until 80–90% confluency, passaged with trypsin (Gibco, 25300096), and seeded at a defined density of 4×10^6 cells per T175 flask (Sarstedt, Nümbrecht, Germany, 833912002). All cells used were at passage 2, cell morphology was assessed daily, and viability was measured using Trypan blue dye exclusion in conjunction with an automated cell counter (ThermoFisher Countess 3). To ensure that regenerative effects originate exclusively from the MSCs secretome and not from culture supplements and to avoid the confounding factor of the inherent batch-to-batch variability of serum [93–95]. MSCs were washed twice with 10 mL filtered (0.22 µm filter (Sarstedt, Nümbrecht, Germany, shipped from Germany, 831822)) PBS +/+ after 24 h and then cultured under serum-free conditions without antibiotics (DMEM with 1 g/L Glucose, L-Glutamine, 110 mg/L Sodium Pyruvate w/o Pen/Strep, FCS, and Amphotericin B)). After 48 h, a total volume of 60 mL of the conditioned medium (CM) was collected, transferred into 50 mL Falcon tubes (Sarstedt, 64547254), and pre-centrifuged at 3000× *g* for 20 min at 4 °C to remove undesired cell debris. After the centrifugation, the CM was used without further concentration steps at its original concentration. The CM was divided into thirds; one third was used as full CM, and the other two-thirds were immediately loaded onto qEV10/35 nm (IZON, qEV10 35 nm) columns, which have an optimal recovery range of 35 nm to 350 nm according to the manufacturer's protocol. The eluted EVs from fractions 2 and 3 were pooled and served as the extracellular vesicle (EV) fraction. Fractions number 10 and 11 contain a high rate of proteins and were used as the protein fraction (PF). Fractions 1, 4–9, 12, and higher were discarded. CM, EVs, and PF were stored at 4 °C and used within 3 h.

Nanotracking Analysis (NTA) was performed to measure the size distribution and quantity of the isolated particles in scatter mode with a 488 nm laser. The minimum brightness was set to 30, the minimum area to 10, the maximum area to 1000, the maximum brightness to 255, the shutter to 400 and the temperature to 25 °C. Isolates were measured in technical triplicates. Fluorescence-triggered flow cytometry (FT-FC)) was used to characterize the EVs and evaluate their size distribution as described previously [58,96]. Western blot against CD9 and CD63 and transelectron microscopy were carried out as we previously described [58].

Protein concentration was measured with the Qubit Protein Assay Kit (ThermoFisher, Q33211) using the Qubit 4 Fluorometer (Thermo Fisher Scientific, Singapore, shipped from Germany) according to the manufacturer's protocol. In brief, a working solution was prepared by diluting the Qbit reagent 1:200 in Qubit buffer (190 µL) for each sample (10 µL). The samples and the protein standards were mixed with the working solution 1:20 and incubated for 15 min light protected at room temperature. Finally, the samples were read in the device.

For all three treatments, the concentration of protein and EVs was standardized to the lowest measurements for each fraction. The EV fractions were standardized to contain 1×10^9 EVs/mL and an optimal size range between 35 nm and 350 nm based on the used isolation columns. The PF was standardized to contain 72 µg/mL protein without any detectable EVs. We chose to normalize the CM fraction based on the lowest measured protein concentration (118 µg/mL containing 1.365×10^{11} particles/mL $\pm$ 1.43×10^{10}) rather than on the EV concentration because the difference between the protein content of the CM and the PF was larger than the differences in the EV concentration between the CM and the EV fraction (Figure 2a).

4.3. Tenocyte Isolation

Tendon samples were obtained from the mid-metacarpal region of the superficial digital flexor tendon of the same three horses as already described by our group [58,97]. In brief, the paratenon was removed under sterile conditions, and the tendons were sectioned into small pieces (<0.5 × 0.5 × 0.5 cm). Isolation of cells was performed by migration from explants in DMEM supplemented with 10% FCS, 1% Pen/Strep, and 1% Amphotericin B in an incubator with 20% O_2 and 5% CO_2 (explants were removed after 7–10 days). Cells were expanded until 80–90% confluency before passage.

4.4. Inflammation and Treatment Strategy

All in vitro experiments were performed with three biological replicates (three donors) and three technical replicates 400,000 tenocytes were seeded per well on 12-well plates and cultured in DMEM supplemented with 10% FCS, 1% Pen/Strep, and 1% Amphotericin B in an incubator with 20% O_2 and 5% CO_2 for 48 h. After 48 h, tenocytes were rigorously washed twice with filtered PBS +/+ and divided into 5 groups: a healthy control group, an inflamed untreated control group, and three inflamed treated groups with CM, EV, or PF treatment (time 0). As serum starvation induces an inflammatory response, the healthy control group was cultured in DMEM with 1 g/L Glucose, L-Glutamine, 110 mg/L Sodium Pyruvate w/o Pen/Strep, FCS and Amphotericin B with 20% EV-depleted FCS (FCS was depleted using Amicon Ultra 15, (Merck Millipore Ltd, Irland, shipped from Germany, UFC910024) 3000 g for 55 min at 4 °C) to provide the minimum amount of nutrients while simultaneously reducing the compromising effect of too high serum levels on the phenotypic drift in tenocytes, which is hallmarked by the reduction of tendon marker genes such as Scx, Mkx, and collagen subtypes, and thus ensuring the health of the control group [98–102]. Tenocytes of the inflamed groups were cultured in serum-and antibiotic-free medium (DMEM with 1 g/L Glucose, L-Glutamine, 110 mg/L Sodium Pyruvate), and inflammation was induced by serum starvation plus chemical stimulation with 10 ng/mL TNFα (ImmunoTools, Germany, shipped from Germany, 11343013) and 10 ng/mL ILb1 (ImmunoTools, Germany, shipped from Germany, 103010501) for 24 h. After 24 h (time 24 h), half (500 µL) of the inflamed serum– and antibiotic-free medium (1 mL) was removed, and 1 mL of treatment (autologous CM, EVs, or PF) was added. The inflamed controls received 1 mL of fresh inflamed serum and antibiotic-free media, and the healthy controls received 1 mL of fresh medium with 20% EV-depleted FCS. After 24 h (time 48 h), the tenocytes of all treatment and control groups were harvested for mRNA sequencing.

4.5. Flow Cytometry

Cells were trypsinized at passage 2. Subsequently, 1×10^5 cells per sample were washed with PBS supplemented with 2% FCS. The flow cytometry analysis utilized the following monoclonal antibodies and their respective isotype controls: PE-CD29 (Clone TS2/16, Mouse IgG, 1:50, Biolegend, San Diego, CA, USA), FITC-CD31 (Clone CO.3E1D4, IgG2a, 1:50, Biorad, Hercules, CA, USA), FITC-CD44 (Clone 25.32, IgG, 1:50, Biorad), Purified CD90 (Clone DH24A, IgM, 1:50, Monoclonal Antibody Center), FITC-PanB cells (Clone CVS36, IgG1, 1:50, Biorad). A total of 1×10^4 events were measured per sample.

4.6. Trilineage Differentiation

Experimental differentiation procedures were conducted in triplicates (passage 2), and the cultures were maintained for a duration of three weeks. The cultural media were refreshed every three days. The control samples were cultured in DMEM supplemented with 10% FCS, 1% Pen/Strep, and 1% amphotericin B. Adipogenic and osteogenic differentiations were performed by seeding 4000 MSCs per well of a 12-well plate in DMEM supplemented with 10% FCS, 1% Pen/Strep, and 1% amphotericin B for 48 h. Subsequently, the cells were washed with PBS and treated with either adipogenesis ((ThermoFisher, Waltham, MA, USA, A1007001)) or osteogenesis (ThermoFisher, A1007201) differentiation media. For chondrogenic differentiation, 350,000 MSCs were collected in 15 mL Falcon

tubes and pelleted, followed by resuspension in chondrogenesis (ThermoFisher, A1007101) differentiation media.

4.6.1. Oil Red Staining

A solution was prepared by diluting six parts of Oil red O (Sigma, O0625-25G) in four parts of distilled water. The mixture was allowed to mix overnight at room temperature and subsequently filtered. The cells were fixed using 60% isopropanol (Riedel de Haen, Seelze, Germany, 24137) for 5 min, followed by incubation with the prepared Oil red O solution for 10 min. Finally, the differentiated cells were washed with 60% isopropanol and distilled water, counterstained with haematoxylin (Merck, Kenilworth, NJ, USA, 108562), and washed again with distilled water.

4.6.2. Alcian Blue Staining

Paraffin-embedded samples of chondrocyte pellets were sectioned at a thickness of 3 µm using a microtome (CUT2511A, MicroTec, Brixen, Italy). The paraffin blocks were pre-cooled at −15 °C and cut into sections, which were then transferred to cold water using wet brushes and subsequently transferred to warm water at 40 °C with nonadhesive standard microscope slides. The sections were flattened out and collected on super frost adhesive microscope glass slides. The slides were labeled and allowed to dry overnight at room temperature. Following this, the slides were heated at 60 °C for 20 min in an incubator, submerged in xylene twice for 10 min at room temperature, and incubated in 100% isopropanol and decreasing concentrations of ethanol (96%, 70%, and 50%) for 5–10 min each. Subsequently, the slides were washed with distilled water and stained with haematoxylin for 3 min. Finally, the slides were washed with distilled water, stained with eosin for 30 s, dehydrated in ethanol, and mounted using Aquatex mounting medium (Merck Millipore, Burlington, MA, USA). The slides were then dried overnight and analyzed using the FL Auto Imaging System (Invitrogen (Waltham, MA, USA), EVOS (Life Technologies, Bothell, WA, USA, shipped from Germany)).

4.6.3. Von Kossa Stain

The cells were fixed with 5% formaldehyde (Sigma), followed by incubation with 5% silver nitrate (Carl Roth, Austria, shipped from Austria, 9370.9) under UV light for 20 min. Afterward, the cells were washed with distilled water, fixed with 5% sodium thiosulfate, and washed again with distilled water. Subsequently, the cells were stained with nuclear fast red (Waldeck GmbH, Germany, shipped from Germany, 221833) for 10 min and washed once more.

4.7. mRNA-Sequencing of the "Patient Cells" (Tenocytes)

Due to cost considerations, we combined the technical replicates for RNASeq and ran one sample for each biological replicate (donor) per treatment/control group. The overall quality of the next-generation sequencing data was evaluated automatically and manually with fastQC v0.11.8 and multiQC v1.7 [103,104]. Reads from all passing samples were adapter-trimmed and quality-filtered using bbduk from the bbmap package v38.69 and filtered for a minimum length of 17 nt and phred quality of 30. Alignment steps were performed with STAR v2.7 using samtools v1.9 for indexing, whereas reads were mapped against the genomic reference GRCm38.p6 provided by Ensembl (Cambridge, UK) [105–107]. Assignment of features to the mapped reads was completed with htseq-count v0.13 [108]. Differential expression analysis with edgeR v3.30 used the quasi-likelihood negative binomial generalized log-linear model functions provided by the package [109]. The independent filtering method of DESeq2 was adapted for use with edgeR to remove low-abundant genes and thus optimize the false discovery rate (FDR) correction [110]. RT-qPCR validation was not used in this study due to the well-established robust nature of RNAseq methods [111,112].

4.8. Data Analysis

We selected a less stringent p-value cutoff of 0.1 in our analysis to avoid missing potentially relevant genes with subtle but biologically significant expression changes. By employing a more inclusive approach, we enhanced the sensitivity of our analysis, explored novel insights, accounted for biological complexity, addressed sample size limitations, and facilitated integration with other datasets. We ensured statistical rigor while capturing valuable findings beyond a stricter cutoff. RNASeq data were read into the R statistical environment and processed using the DESeq2 package [110]. Statistical analysis of preprocessed NGS data was completed with R v3.6 and the packages pheatmap v1.0.12, pcaMethods v1.78, and genefilter v1.68. Differential expression analysis with edgeR v3.28 used the quasi-likelihood negative binomial generalized log-linear model functions provided by the package [109]. The independent filtering method of DESeq2 was adapted for use with edgeR to remove low-abundance mRNAs and thus optimize the false discovery rate (FDR) correction [110]. To determine differentially expressed genes, a linear mixed model with subject ID as a random effect was chosen. Significant differential expression (DE) was assumed for adjusted p-values < 0.1 and a fold change (FC) > 1.5. Results were put into a biological context using gene set variation analysis with the molecular signature database, Wiki and KEGG pathways as input [113–116]. Significant differences between GSVA scores were determined using LIMMA and the linear mixed model as described above [117].

Principle component analysis (PCA) was used to assess the clustering of samples based on treatment groups. The statistical analysis, a repeated measures ANOVA, was performed using Graph Pad Prism v.6.01 (GraphPad Software, San Diego, CA, USA). The number of used donors (n), the p-values and the respective statistical significance are indicated in each figure. The data are plotted as mean with ± standard error of mean in scatter plots and ±standard deviation in bar graphs.

Venn diagrams and volcano plots were generated using online tools (InteractiveVenn and VolcaNoseR) [118,119].

Author Contributions: Conceptualization, I.G., J.G. and F.J.; methodology, R.S. and S.G.; data analysis, T.M.; validation, I.G., J.G. and F.J.; formal analysis, R.S., I.G. and F.J.; investigation, R.S. and I.G.; resources, J.G. and F.J.; data curation, R.S.; writing—original draft preparation, R.S.; writing—review and editing, I.G., J.G. and F.J.; visualization, R.S.; supervision, I.G., J.G. and F.J.; funding acquisition, J.G. and F.J. All authors have read and agreed to the published version of the manuscript.

Funding: We kindly acknowledge support by the Austrian Science Fund (FWF) and Herzfelder'sche Familienstiftung: P35268-B to J.G.

Institutional Review Board Statement: The presented study is an in vitro study using cells isolated from waste material from horses euthanized for reasons unrelated to this study. Ethical review and approval were waived for this study. The Ethics Committee of University of Veterinary Medicine Vienna and the Austrian Federal Ministry of Educations Science and Research confirmed that in vitro cell culture studies do not require approval if the cells were isolated from tissue which was obtained either solely for diagnostic or therapeutic purposes or in the course of other institutionally and nationally approved experiments. Tissue collection was performed according to the "Good Scientific Practice and Ethics in Science and Research" regulation implemented at the University of Veterinary Medicine, Vienna. All samples were obtained from animals euthanized for reasons unrelated to this study.

Informed Consent Statement: The animal owner's consent to collect and analyze the samples and to publish resulting data was obtained according to standard procedures approved by the Ethics and Animal Welfare Committee of the University of Veterinary Medicine, Vienna.

Data Availability Statement: The data presented in this study are available on request from the corresponding author.

Conflicts of Interest: J.G. is cofounder and shareholder of Evercyte GmbH and TAmiRNA GmbH. T.M. is founder of Science Consult—DI Thomas Mohr KG. All other authors declare no conflict of interest.

References

1. Docheva, D.; Müller, S.A.; Majewski, M.; Evans, C.H. Biologics for tendon repair. *Adv. Drug Deliv. Rev.* **2015**, *84*, 222–239. [CrossRef]
2. Walden, G.; Liao, X.; Donell, S.; Raxworthy, M.J.; Riley, G.P.; Saeed, A. A Clinical, Biological, and Biomaterials Perspective into Tendon Injuries and Regeneration. *Tissue Eng. Part B Rev.* **2016**, *23*, 44–58. [CrossRef]
3. Millar, N.L.; Silbernagel, K.G.; Thorborg, K.; Kirwan, P.D.; Galatz, L.M.; Abrams, G.D.; Murrell, G.A.C.; McInnes, I.B.; Rodeo, S.A. Tendinopathy. *Nat. Rev. Dis. Prim.* **2021**, *7*, 1. [CrossRef] [PubMed]
4. Schulze-Tanzil, G.; Al-Sadi, O.; Wiegand, E.; Ertel, W.; Busch, C.; Kohl, B.; Pufe, T. The role of pro-inflammatory and immunoregulatory cytokines in tendon healing and rupture: New insights. *Scand. J. Med. Sci. Sports* **2011**, *21*, 337–351. [CrossRef]
5. Thomopoulos, S.; Parks, W.C.; Rifkin, D.B.; Derwin, K.A. Mechanisms of tendon injury and repair. *J. Orthop. Res.* **2015**, *33*, 832–839. [CrossRef] [PubMed]
6. Cambré, I.; Gaublomme, D.; Burssens, A.; Jacques, P.; Schryvers, N.; De Muynck, A.; Meuris, L.; Lambrecht, S.; Carter, S.; de Bleser, P.; et al. Mechanical strain determines the site-specific localization of inflammation and tissue damage in arthritis. *Nat. Commun.* **2018**, *9*, 4613. [CrossRef]
7. Maffulli, N.; Ewen, S.W.B.; Waterston, S.W.; Reaper, J.; Barrass, V. Tenocytes from Ruptured and Tendinopathic Achilles Tendons Produce Greater Quantities of Type III Collagen than Tenocytes from Normal Achilles Tendons: An in Vitro Model of Human Tendon Healing. *Am. J. Sports Med.* **2000**, *28*, 499–505. [CrossRef] [PubMed]
8. Nichols, A.E.C.; Best, K.T.; Loiselle, A.E. The cellular basis of fibrotic tendon healing: Challenges and opportunities. *Transl. Res.* **2019**, *209*, 156–168. [CrossRef]
9. Abraham, A.C.; Shah, S.A.; Golman, M.; Song, L.; Li, X.; Kurtaliaj, I.; Akbar, M.; Millar, N.L.; Abu-Amer, Y.; Galatz, L.M.; et al. Targeting the NF-κB signaling pathway in chronic tendon disease. *Sci. Transl. Med.* **2019**, *11*, eaav4319. [CrossRef] [PubMed]
10. Tang, C.; Chen, Y.; Huang, J.; Zhao, K.; Chen, X.; Yin, Z.; Heng, B.C.; Chen, W.; Shen, W. The roles of inflammatory mediators and immunocytes in tendinopathy. *J. Orthop. Transl.* **2018**, *14*, 23–33. [CrossRef]
11. Dakin, S.G.; Newton, J.; Martinez, F.O.; Hedley, R.; Gwilym, S.; Jones, N.; Reid, H.A.B.; Wood, S.; Wells, G.; Appleton, L.; et al. Chronic inflammation is a feature of Achilles tendinopathy and rupture. *Br. J. Sports Med.* **2018**, *52*, 359–367. [CrossRef]
12. Dakin, S.G. Inflammation or damage: Fibroblasts decide. *Sci. Transl. Med.* **2019**, *11*, eaax9562. [CrossRef]
13. Young, R.G.; Butler, D.L.; Weber, W.; Caplan, A.I.; Gordon, S.L.; Fink, D.J. Use of mesenchymal stem cells in a collagen matrix for achilles tendon repair. *J. Orthop. Res.* **1998**, *16*, 406–413. [CrossRef]
14. Smith, R.K.W.; Korda, M.; Blunn, G.W.; Goodship, A.E. Isolation and implantation of autologous equine mesenchymal stem cells from bone marrow into the superficial digital flexor tendon as a potential novel treatment. *Equine Vet. J.* **2003**, *35*, 99–102. [CrossRef]
15. Smith, R.K.W. Mesenchymal stem cell therapy for equine tendinopathy. *Disabil. Rehabil.* **2008**, *30*, 1752–1758. [CrossRef]
16. Smith, R.K.W.; Webbon, P.M. Harnessing the stem cell for the treatment of tendon injuries: Heralding a new dawn? *Br. J. Sports Med.* **2005**, *39*, 582–584. [CrossRef] [PubMed]
17. Smith, R.K.W.; Werling, N.J.; Dakin, S.G.; Alam, R.; Goodship, A.E.; Dudhia, J. Beneficial Effects of Autologous Bone Marrow-Derived Mesenchymal Stem Cells in Naturally Occurring Tendinopathy. *PLoS ONE* **2013**, *8*, e75697. [CrossRef]
18. Dyson, S.J. Medical management of superficial digital flexor tendonitis: A comparative study in 219 horses (1992–2000). *Equine Vet. J.* **2004**, *36*, 415–419. [CrossRef]
19. Godwin, E.E.; Young, N.J.; Dudhia, J.; Beamish, I.C.; Smith, R.K.W. Implantation of bone marrow-derived mesenchymal stem cells demonstrates improved outcome in horses with overstrain injury of the superficial digital flexor tendon. *Equine Vet. J.* **2012**, *44*, 25–32. [CrossRef] [PubMed]
20. Costa-Almeida, R.; Calejo, I.; Gomes, M.E. Mesenchymal Stem Cells Empowering Tendon Regenerative Therapies. *Int. J. Mol. Sci.* **2019**, *20*, 3002. [CrossRef] [PubMed]
21. Horwitz, E.M.; Gordon, P.L.; Koo, W.K.K.; Marx, J.C.; Neel, M.D.; McNall, R.Y.; Muul, L.; Hofmann, T. Isolated allogeneic bone marrow-derived mesenchymal cells engraft and stimulate growth in children with osteogenesis imperfecta: Implications for cell therapy of bone. *Proc. Natl. Acad. Sci. USA* **2002**, *99*, 8932–8937. [CrossRef] [PubMed]
22. Brandt, L.; Schubert, S.; Scheibe, P.; Brehm, W.; Franzen, J.; Gross, C.; Burk, J. Tenogenic Properties of Mesenchymal Progenitor Cells Are Compromised in an Inflammatory Environment. *Int. J. Mol. Sci.* **2018**, *19*, 2549. [CrossRef] [PubMed]
23. Gnecchi, M.; He, H.; Liang, O.D.; Melo, L.G.; Morello, F.; Mu, H.; Noiseux, N.; Zhang, L.; Pratt, R.E.; Ingwall, J.S.; et al. Paracrine action accounts for marked protection of ischemic heart by Akt-modified mesenchymal stem cells. *Nat. Med.* **2005**, *11*, 367–368. [CrossRef]
24. Caplan, A.I.; Correa, D. The MSC: An injury drugstore. *Cell Stem Cell* **2011**, *9*, 11–15. [CrossRef]
25. Baldari, S.; Di Rocco, G.; Piccoli, M.; Pozzobon, M.; Muraca, M.; Toietta, G. Challenges and Strategies for Improving the Regenerative Effects of Mesenchymal Stromal Cell-Based Therapies. *Int. J. Mol. Sci.* **2017**, *18*, 2087. [CrossRef]
26. Timmers, L.; Lim, S.K.; Hoefer, I.E.; Arslan, F.; Lai, R.C.; van Oorschot, A.A.M.; Goumans, M.J.; Strijder, C.; Sze, S.K.; Choo, A.; et al. Human mesenchymal stem cell-conditioned medium improves cardiac function following myocardial infarction. *Stem Cell Res.* **2011**, *6*, 206–214. [CrossRef]

27. Espinosa, G.; Plaza, A.; Schenffeldt, A.; Alarcón, P.; Gajardo, G.; Uberti, B.; Morán, G.; Henriquez, C. Equine bone marrow-derived mesenchymal stromal cells inhibit reactive oxygen species production by neutrophils. *Vet. Immunol. Immunopathol.* **2020**, *221*, 109975. [CrossRef]
28. Bastos, F.Z.; Barussi, F.C.M.; Leite, L.M.B.; Jamur, V.R.; Soares, A.D.A.; Senegaglia, A.C.; Michelotto, P.V., Jr. Quality control and immunomodulatory potential for clinical-grade equine bone marrow-derived mesenchymal stromal cells and conditioned medium. *Res. Vet. Sci.* **2020**, *132*, 407–415. [CrossRef] [PubMed]
29. Khatab, S.; van Osch, G.J.; Kops, N.; Bastiaansen-Jenniskens, Y.M.; Bos, P.; Verhaar, J.A.; Bernsen, M.R.; van Buul, G.M. Mesenchymal stem cell secretome reduces pain and subchondral bone alterations in a mouse osteoarthritis model. *Osteoarthr. Cartil.* **2018**, *26*, S15–S16. [CrossRef]
30. da Silva Meirelles, L.; Fontes, A.M.; Covas, D.T.; Caplan, A.I. Mechanisms involved in the therapeutic properties of mesenchymal stem cells. *Cytokine Growth Factor Rev.* **2009**, *20*, 419–427. [CrossRef]
31. Lener, T.; Gimona, M.; Aigner, L.; Börger, V.; Buzas, E.; Camussi, G.; Chaput, N.; Chatterjee, D.; Court, F.A.; Del Portillo, H.A.; et al. Applying extracellular vesicles based therapeutics in clinical trials—An ISEV position paper. *J. Extracell. Vesicles* **2015**, *4*, 30087. [CrossRef]
32. Ribitsch, I.; Oreff, G.L.; Jenner, F. Regenerative Medicine for Equine Musculoskeletal Diseases. *Animals* **2021**, *11*, 234. [CrossRef] [PubMed]
33. Keyhanmanesh, R.; Rahbarghazi, R.; Aslani, M.R.; Hassanpour, M.; Ahmadi, M. Systemic delivery of mesenchymal stem cells condition media in repeated doses acts as magic bullets in restoring IFN-γ/IL-4 balance in asthmatic rats. *Life Sci.* **2018**, *212*, 30–36. [CrossRef] [PubMed]
34. Chen, W.; Sun, Y.; Gu, X.; Cai, J.; Liu, X.; Zhang, X.; Chen, J.; Hao, Y.; Chen, S. Conditioned medium of human bone marrow-derived stem cells promotes tendon-bone healing of the rotator cuff in a rat model. *Biomaterials* **2021**, *271*, 120714. [CrossRef] [PubMed]
35. Lange-Consiglio, A.; Perrini, C.; Tasquier, R.; Deregibus, M.C.; Camussi, G.; Pascucci, L.; Marini, M.G.; Corradetti, B.; Bizzaro, D.; De Vita, B.; et al. Equine Amniotic Microvesicles and Their Anti-Inflammatory Potential in a Tenocyte Model In Vitro. *Stem Cells Dev.* **2016**, *25*, 610–621. [CrossRef] [PubMed]
36. Perrini, C.; Strillacci, M.G.; Bagnato, A.; Esposti, P.; Marini, M.G.; Corradetti, B.; Bizzaro, D.; Idda, A.; Ledda, S.; Capra, E.; et al. Microvesicles secreted from equine amniotic-derived cells and their potential role in reducing inflammation in endometrial cells in an in-vitro model. *Stem Cell Res. Ther.* **2016**, *7*, 169. [CrossRef]
37. Shi, Z.; Wang, Q.; Jiang, D. Extracellular vesicles from bone marrow-derived multipotent mesenchymal stromal cells regulate inflammation and enhance tendon healing. *J. Transl. Med.* **2019**, *17*, 211. [CrossRef]
38. Wang, Y.; He, G.; Guo, Y.; Tang, H.; Shi, Y.; Bian, X.; Zhu, M.; Kang, X.; Zhou, M.; Lyu, J.; et al. Exosomes from tendon stem cells promote injury tendon healing through balancing synthesis and degradation of the tendon extracellular matrix. *J. Cell. Mol. Med.* **2019**, *23*, 5475–5485. [CrossRef]
39. Wang, C.; Hu, Q.; Song, W.; Yu, W.; He, Y. Adipose Stem Cell–Derived Exosomes Decrease Fatty Infiltration and Enhance Rotator Cuff Healing in a Rabbit Model of Chronic Tears. *Am. J. Sports Med.* **2020**, *48*, 1456–1464. [CrossRef]
40. Jenner, F.; Wagner, A.; Gerner, I.; Ludewig, E.; Trujanovic, R.; Rohde, E.; von Rechenberg, B.; Gimona, M.; Traweger, A. Evaluation of the Potential of Umbilical Cord Mesenchymal Stromal Cell–Derived Small Extracellular Vesicles to Improve Rotator Cuff Healing: A Pilot Ovine Study. *Am. J. Sports Med.* **2023**, *51*, 331–342. [CrossRef]
41. Liu, Y.; Kano, F.; Hashimoto, N.; Xia, L.; Zhou, Q.; Feng, X.; Hibi, H.; Miyazaki, A.; Iwamoto, T.; Matsuka, Y.; et al. Conditioned Medium from the Stem Cells of Human Exfoliated Deciduous Teeth Ameliorates Neuropathic Pain in a Partial Sciatic Nerve Ligation Model. *Front. Pharmacol.* **2022**, *13*, 745020. Available online: https://www.frontiersin.org/articles/10.3389/fphar.2022.745020 (accessed on 11 February 2023). [CrossRef]
42. Sevivas, N.; Teixeira, F.G.; Portugal, R.; Araújo, L.; Carriço, L.F.; Ferreira, N.; Vieira da Silva, M.; Espregueira-Mendes, J.; Anjo, S.; Manadas, B.; et al. Mesenchymal Stem Cell Secretome: A Potential Tool for the Prevention of Muscle Degenerative Changes Associated with Chronic Rotator Cuff Tears. *Am. J. Sports Med.* **2016**, *45*, 179–188. [CrossRef]
43. Shen, H.; Yoneda, S.; Abu-Amer, Y.; Guilak, F.; Gelberman, R.H. Stem cell-derived extracellular vesicles attenuate the early inflammatory response after tendon injury and repair. *J. Orthop. Res.* **2020**, *38*, 117–127. [CrossRef]
44. Yu, H.; Cheng, J.; Shi, W.; Ren, B.; Zhao, F.; Shi, Y.; Yang, P.; Duan, X.; Zhang, J.; Fu, X.; et al. Bone marrow mesenchymal stem cell-derived exosomes promote tendon regeneration by facilitating the proliferation and migration of endogenous tendon stem/progenitor cells. *Acta Biomater.* **2020**, *106*, 328–341. [CrossRef] [PubMed]
45. Shi, Y.; Kang, X.; Wang, Y.; Bian, X.; He, G.; Zhou, M.; Tang, K. Exosomes Derived from Bone Marrow Stromal Cells (BMSCs) Enhance Tendon-Bone Healing by Regulating Macrophage Polarization. *Med. Sci. Monit.* **2020**, *26*, e923328. [CrossRef]
46. Gissi, C.; Radeghieri, A.; Antonetti Lamorgese Passeri, C.; Gallorini, M.; Calciano, L.; Oliva, F.; Veronesi, F.; Zendrini, A.; Cataldi, A.; Bergese, P.; et al. Extracellular vesicles from rat-bone-marrow mesenchymal stromal/stem cells improve tendon repair in rat Achilles tendon injury model in dose-dependent manner: A pilot study. *PLoS ONE* **2020**, *15*, e0229914. [CrossRef] [PubMed]
47. Huang, Y.; He, B.; Wang, L.; Yuan, B.; Shu, H.; Zhang, F.; Sun, L. Bone marrow mesenchymal stem cell-derived exosomes promote rotator cuff tendon-bone healing by promoting angiogenesis and regulating M1 macrophages in rats. *Stem Cell Res. Ther.* **2020**, *11*, 496. [CrossRef] [PubMed]

48. Li, J.; Yao, Z.; Xiong, H.; Cui, H.; Wang, X.; Zheng, W.; Qian, Y.; Fan, C. Extracellular vesicles from hydroxycamptothecin primed umbilical cord stem cells enhance anti-adhesion potential for treatment of tendon injury. *Stem Cell Res. Ther.* **2020**, *11*, 500. [CrossRef]
49. Chen, Q.; Liang, Q.; Zhuang, W.; Zhou, J.; Zhang, B.; Xu, P.; Ju, Y.; Morita, Y.; Luo, Q.; Song, G. Tenocyte proliferation and migration promoted by rat bone marrow mesenchymal stem cell-derived conditioned medium. *Biotechnol. Lett.* **2018**, *40*, 215–224. [CrossRef] [PubMed]
50. Lange-Consiglio, A.; Rossi, D.; Tassan, S.; Perego, R.; Cremonesi, F.; Parolini, O. Conditioned Medium from Horse Amniotic Membrane-Derived Multipotent Progenitor Cells: Immunomodulatory Activity In Vitro and First Clinical Application in Tendon and Ligament Injuries In Vivo. *Stem Cells Dev.* **2013**, *22*, 3015–3024. [CrossRef] [PubMed]
51. Bartekova, M.; Radosinska, J.; Jelemensky, M.; Dhalla, N.S. Role of cytokines and inflammation in heart function during health and disease. *Heart Fail. Rev.* **2018**, *23*, 733–758. [CrossRef] [PubMed]
52. Beohar, N.; Rapp, J.; Pandya, S.; Losordo, D.W. Rebuilding the Damaged Heart: The Potential of Cytokines and Growth Factors in the Treatment of Ischemic Heart Disease. *J. Am. Coll. Cardiol.* **2010**, *56*, 1287–1297. [CrossRef] [PubMed]
53. Mitchell, R.; Mellows, B.; Sheard, J.; Antonioli, M.; Kretz, O.; Chambers, D.; Zeuner, M.-T.; Tomkins, J.E.; Denecke, B.; Musante, L.; et al. Secretome of adipose-derived mesenchymal stem cells promotes skeletal muscle regeneration through synergistic action of extracellular vesicle cargo and soluble proteins. *Stem Cell Res. Ther.* **2019**, *10*, 116. [CrossRef] [PubMed]
54. Wagner, T.; Traxler, D.; Simader, E.; Beer, L.; Narzt, M.-S.; Gruber, F.; Madlener, S.; Laggner, M.; Erb, M.; Vorstandlechner, V.; et al. Different pro-angiogenic potential of γ-irradiated PBMC-derived secretome and its subfractions. *Sci. Rep.* **2018**, *8*, 18016. [CrossRef]
55. Ahrberg, A.B.; Horstmeier, C.; Berner, D.; Brehm, W.; Gittel, C.; Hillmann, A.; Josten, C.; Rossi, G.; Schubert, S.; Winter, K.; et al. Effects of mesenchymal stromal cells versus serum on tendon healing in a controlled experimental trial in an equine model. *BMC Musculoskelet. Disord.* **2018**, *19*, 230. [CrossRef] [PubMed]
56. Preparation of IDEs and INDs for Products Intended to Repair or Replace Knee Cartilage. 2011. Available online: https://www.fda.gov/media/82562/download (accessed on 2 March 2023).
57. Reflection Paper on In-Vitro Cultured Chondrocyte Containing Products for Cartilage Repair of the Knee. Available online: https://www.ema.europa.eu/en/documents/scientific-guideline/reflection-paper-vitro-cultured-chondrocyte-containing-products-cartilage-repair-knee_en.pdf (accessed on 2 March 2023).
58. Soukup, R.; Gerner, I.; Gültekin, S.; Baik, H.; Oesterreicher, J.; Grillari, J.; Jenner, F. Characterisation of Extracellular Vesicles from Equine Mesenchymal Stem Cells. *Int. J. Mol. Sci.* **2022**, *23*, 5858. [CrossRef]
59. Papait, A.; Ragni, E.; Cargnoni, A.; Vertua, E.; Romele, P.; Masserdotti, A.; Perucca Orfei, C.; Signoroni, P.B.; Magatti, M.; Silini, A.R.; et al. Comparison of EV-free fraction, EVs, and total secretome of amniotic mesenchymal stromal cells for their immunomodulatory potential: A translational perspective. *Front. Immunol.* **2022**, *13*, 960909. Available online: https://www.frontiersin.org/articles/10.3389/fimmu.2022.960909 (accessed on 3 March 2023). [CrossRef]
60. González-Cubero, E.; González-Fernández, M.L.; Olivera, E.R.; Villar-Suárez, V. Extracellular vesicle and soluble fractions of adipose tissue-derived mesenchymal stem cells secretome induce inflammatory cytokines modulation in an in vitro model of discogenic pain. *Spine J.* **2022**, *22*, 1222–1234. [CrossRef]
61. Giannasi, C.; Niada, S.; Magagnotti, C.; Ragni, E.; Andolfo, A.; Brini, A.T. Comparison of two ASC-derived therapeutics in an in vitro OA model: Secretome versus extracellular vesicles. *Stem Cell Res. Ther.* **2020**, *11*, 521. [CrossRef]
62. Sung, B.H.; Parent, C.A.; Weaver, A.M. Extracellular vesicles: Critical players during cell migration. *Dev. Cell* **2021**, *56*, 1861–1874. [CrossRef]
63. Kriebel, P.W.; Majumdar, R.; Jenkins, L.M.; Senoo, H.; Wang, W.; Ammu, S.; Chen, S.; Narayan, K.; Iijima, M.; Parent, C.A. Extracellular vesicles direct migration by synthesizing and releasing chemotactic signals. *J. Cell Biol.* **2018**, *217*, 2891–2910. [CrossRef]
64. Voga, M.; Adamic, N.; Vengust, M.; Majdic, G. Stem Cells in Veterinary Medicine-Current State and Treatment Options. *Front. Vet. Sci.* **2020**, *7*, 278. [CrossRef]
65. Margolis, L.; Sadovsky, Y. The biology of extracellular vesicles: The known unknowns. *PLoS Biol.* **2019**, *17*, e3000363. [CrossRef] [PubMed]
66. Xu, X.; Lai, Y.; Hua, Z.C. Apoptosis and apoptotic body: Disease message and therapeutic target potentials. *Biosci. Rep.* **2019**, *39*, BSR20180992. [CrossRef] [PubMed]
67. Théry, C.; Witwer, K.W.; Aikawa, E.; Alcaraz, M.J.; Anderson, J.D.; Andriantsitohaina, R.; Antoniou, A.; Arab, T.; Archer, F.; Atkin-Smith, G.K.; et al. Minimal information for studies of extracellular vesicles 2018 (MISEV2018): A position statement of the International Society for Extracellular Vesicles and update of the MISEV2014 guidelines. *J. Extracell. Vesicles* **2018**, *7*, 1535750. [CrossRef] [PubMed]
68. Iraci, N.; Leonardi, T.; Gessler, F.; Vega, B.; Pluchino, S. Focus on Extracellular Vesicles: Physiological Role and Signalling Properties of Extracellular Membrane Vesicles. *Int. J. Mol. Sci.* **2016**, *17*, 171. [CrossRef]
69. Niada, S.; Giannasi, C.; Magagnotti, C.; Andolfo, A.; Brini, A.T. Proteomic analysis of extracellular vesicles and conditioned medium from human adipose-derived stem/stromal cells and dermal fibroblasts. *J. Proteom.* **2021**, *232*, 104069. [CrossRef]
70. Niada, S.; Giannasi, C.; Gualerzi, A.; Banfi, G.; Brini, A.T. Differential Proteomic Analysis Predicts Appropriate Applications for the Secretome of Adipose-Derived Mesenchymal Stem/Stromal Cells and Dermal Fibroblasts. *Stem Cells Int.* **2018**, *2018*, 7309031. [CrossRef]

71. Monguió-Tortajada, M.; Gálvez-Montón, C.; Bayes-Genis, A.; Roura, S.; Borràs, F.E. Extracellular vesicle isolation methods: Rising impact of size-exclusion chromatography. *Cell. Mol. Life Sci.* **2019**, *76*, 2369–2382. [CrossRef]
72. Van Deun, J.; Mestdagh, P.; Sormunen, R.; Cocquyt, V.; Vermaelen, K.; Vandesompele, J.; Bracke, M.; De Wever, O.; Hendrix, A. The impact of disparate isolation methods for extracellular vesicles on downstream RNA profiling. *J. Extracell. Vesicles* **2014**, *3*, 24858. [CrossRef] [PubMed]
73. Patel, D.B.; Gray, K.M.; Santharam, Y.; Lamichhane, T.N.; Stroka, K.M.; Jay, S.M. Impact of cell culture parameters on production and vascularization bioactivity of mesenchymal stem cell-derived extracellular vesicles. *Bioeng. Transl. Med.* **2017**, *2*, 170–179. [CrossRef] [PubMed]
74. Miclau, K.; Hambright, W.S.; Huard, J.; Stoddart, M.J.; Bahney, C.S. Cellular expansion of MSCs: Shifting the regenerative potential. *Aging Cell* **2023**, *22*, e13759. [CrossRef]
75. Gualerzi, A.; Niada, S.; Giannasi, C.; Picciolini, S.; Morasso, C.; Vanna, R.; Rossella, V.; Masserini, M.; Bedoni, M.; Ciceri, F.; et al. Raman spectroscopy uncovers biochemical tissue-related features of extracellular vesicles from mesenchymal stromal cells. *Sci. Rep.* **2017**, *7*, 9820. [CrossRef]
76. Shin, S.; Lee, J.; Kwon, Y.; Park, K.S.; Jeong, J.H.; Choi, S.J.; Bang, S.I.; Chang, J.W.; Lee, C. Comparative proteomic analysis of the mesenchymal stem cells secretome from adipose, bone marrow, placenta and wharton's jelly. *Int. J. Mol. Sci.* **2021**, *22*, 845. [CrossRef]
77. Uberti, B.; Plaza, A.; Henriquez, C. Pre-conditioning Strategies for Mesenchymal Stromal/Stem Cells in Inflammatory Conditions of Livestock Species. *Front. Vet. Sci.* **2022**, *9*, 806069. Available online: https://www.frontiersin.org/articles/10.3389/fvets.2022.806069 (accessed on 8 March 2023). [CrossRef] [PubMed]
78. Zhao, L.; Hu, C.; Han, F.; Cai, F.; Wang, J.; Chen, J. Preconditioning is an effective strategy for improving the efficiency of mesenchymal stem cells in kidney transplantation. *Stem Cell Res. Ther.* **2020**, *11*, 197. [CrossRef]
79. Han, K.-H.; Kim, A.-K.; Kim, M.-H.; Kim, D.-H.; Go, H.-N.; Kim, D.-I. Enhancement of angiogenic effects by hypoxia-preconditioned human umbilical cord-derived mesenchymal stem cells in a mouse model of hindlimb ischemia. *Cell Biol. Int.* **2016**, *40*, 27–35. [CrossRef] [PubMed]
80. Matta, A.; Nader, V.; Lebrin, M.; Gross, F.; Prats, A.C.; Cussac, D.; Galinier, M.; Roncalli, J. Pre-Conditioning Methods and Novel Approaches with Mesenchymal Stem Cells Therapy in Cardiovascular Disease. *Cells* **2022**, *11*, 1620. [CrossRef]
81. Carlomagno, C.; Giannasi, C.; Niada, S.; Bedoni, M.; Gualerzi, A.; Brini, A.T. Raman Fingerprint of Extracellular Vesicles and Conditioned Media for the Reproducibility Assessment of Cell-Free Therapeutics. *Front. Bioeng. Biotechnol.* **2021**, *9*, 640617. Available online: https://www.frontiersin.org/articles/10.3389/fbioe.2021.640617 (accessed on 8 March 2023). [CrossRef]
82. He, C.; Dai, M.; Zhou, X.; Long, J.; Tian, W.; Yu, M. Comparison of two cell-free therapeutics derived from adipose tissue: Small extracellular vesicles versus conditioned medium. *Stem Cell Res. Ther.* **2022**, *13*, 86. [CrossRef]
83. Crum, R.J.; Capella-Monsonis, H.; Badylak, S.F.; Hussey, G.S. Extracellular Vesicles for Regenerative Medicine Applications. *Appl. Sci.* **2022**, *12*, 7472. [CrossRef]
84. Helissey, C.; Guitard, N.; Théry, H.; Goulinet, S.; Mauduit, P.; Girleanu, M.; Favier, A.L.; Drouet, M.; Parnot, C.; Chargari, C.; et al. Two New Potential Therapeutic Approaches in Radiation Cystitis Derived from Mesenchymal Stem Cells: Extracellular Vesicles and Conditioned Medium. *Biology* **2022**, *11*, 980. [CrossRef] [PubMed]
85. Zhu, Y.; Chen, X.; Pan, Q.; Wang, Y.; Su, S.; Jiang, C.; Li, Y.; Xu, N.; Wu, L.; Lou, X.; et al. A Comprehensive Proteomics Analysis Reveals a Secretory Path- and Status-Dependent Signature of Exosomes Released from Tumor-Associated Macrophages. *J. Proteome Res.* **2015**, *14*, 4319–4331. [CrossRef] [PubMed]
86. Eddershaw, P.J.; Beresford, A.P.; Bayliss, M.K. ADME/PK as part of a rational approach to drug discovery. *Drug Discov. Today* **2000**, *5*, 409–414. [CrossRef] [PubMed]
87. Charoenviriyakul, C.; Takahashi, Y.; Morishita, M.; Matsumoto, A.; Nishikawa, M.; Takakura, Y. Cell type-specific and common characteristics of exosomes derived from mouse cell lines: Yield, physicochemical properties, and pharmacokinetics. *Eur. J. Pharm. Sci.* **2017**, *96*, 316–322. [CrossRef] [PubMed]
88. Smyth, T.; Kullberg, M.; Malik, N.; Smith-Jones, P.; Graner, M.W.; Anchordoquy, T.J. Biodistribution and delivery efficiency of unmodified tumor-derived exosomes. *J. Control. Release* **2015**, *199*, 145–155. [CrossRef]
89. Park, S.-R.; Kim, J.-W.; Jun, H.-S.; Roh, J.Y.; Lee, H.-Y.; Hong, I.-S. Stem Cell Secretome and Its Effect on Cellular Mechanisms Relevant to Wound Healing. *Mol. Ther.* **2018**, *26*, 606–617. [CrossRef]
90. Delling, U.; Lindner, K.; Ribitsch, I.; Jülke, H.; Brehm, W. Comparison of bone marrow aspiration at the sternum and the tuber coxae in middle-aged horses. *Can. J. Vet. Res.* **2012**, *76*, 52–56.
91. Ribitsch, I.; Chang-Rodriguez, S.; Egerbacher, M.; Gabner, S.; Gueltekin, S.; Huber, J.; Schuster, T.; Jenner, F. Sheep Placenta Cotyledons: A Noninvasive Source of Ovine Mesenchymal Stem Cells. *Tissue Eng. Part C Methods* **2017**, *23*, 298–310. [CrossRef]
92. Cammack, R.; Atwood, T.; Campbell, P.; Parish, H.; Smith, A.; Vella, F.; Stirling, J. *Oxford Dictionary of Biochemistry and Molecular Biology*; Oxford University Press: Oxford, UK, 2008; ISBN 9780191727641.
93. Karnieli, O.; Friedner, O.M.; Allickson, J.G.; Zhang, N.; Jung, S.; Fiorentini, D.; Abraham, E.; Eaker, S.S.; Yong, T.K.; Chan, A.; et al. A consensus introduction to serum replacements and serum-free media for cellular therapies. *Cytotherapy* **2017**, *19*, 155–169. [CrossRef]

94. European Commission. Note for guidance on minimising the risk of transmitting animal spongiform encephalopathy agents via human and veterinary medicinal products (EMA/410/01 rev.3). *Off. J. Eur. Union* **2011**, *C*, 73/01. Available online: https://eur-lex.europa.eu/legal-content/EN/TXT/?uri=CELEX:52011XC0305(04) (accessed on 10 March 2023).
95. Mendicino, M.; Bailey, A.M.; Wonnacott, K.; Puri, R.K.; Bauer, S.R. MSC-Based Product Characterization for Clinical Trials: An FDA Perspective. *Cell Stem Cell* **2014**, *14*, 141–145. [CrossRef]
96. Oesterreicher, J.; Pultar, M.; Schneider, J.; Mühleder, S.; Zipperle, J.; Grillari, J.; Holnthoner, W. Fluorescence-Based Nanoparticle Tracking Analysis and Flow Cytometry for Characterization of Endothelial Extracellular Vesicle Release. *Int. J. Mol. Sci.* **2020**, *21*, 9278. [CrossRef]
97. Oreff, G.L.; Fenu, M.; Vogl, C.; Ribitsch, I.; Jenner, F. Species variations in tenocytes' response to inflammation require careful selection of animal models for tendon research. *Sci. Rep.* **2021**, *11*, 12451. [CrossRef] [PubMed]
98. Kugo, H.; Sukketsiri, W.; Iwamoto, K.; Suihara, S.; Moriyama, T.; Zaima, N. Low glucose and serum levels cause an increased inflammatory factor in 3T3-L1 cell through Akt, MAPKs and NF-κB activation. *Adipocyte* **2021**, *10*, 232–241. [CrossRef]
99. Kogel, V.; Trinh, S.; Gasterich, N.; Beyer, C.; Seitz, J. Long-Term Glucose Starvation Induces Inflammatory Responses and Phenotype Switch in Primary Cortical Rat Astrocytes. *J. Mol. Neurosci.* **2021**, *71*, 2368–2382. [CrossRef] [PubMed]
100. van Vijven, M.; Wunderli, S.L.; Ito, K.; Snedeker, J.G.; Foolen, J. Serum deprivation limits loss and promotes recovery of tenogenic phenotype in tendon cell culture systems. *J. Orthop. Res.* **2021**, *39*, 1561–1571. [CrossRef]
101. Mueller, A.J.; Tew, S.R.; Vasieva, O.; Clegg, P.D.; Canty-Laird, E.G. A systems biology approach to defining regulatory mechanisms for cartilage and tendon cell phenotypes. *Sci. Rep.* **2016**, *6*, 33956. [CrossRef]
102. Brink, H.E.; Miller, G.J.; Beredjiklian, P.K.; Nicoll, S.B. Serum-dependent effects on adult and fetal tendon fibroblast migration and collagen expression. *Wound Repair Regen.* **2006**, *14*, 179–186. [CrossRef]
103. Anders, S. Babraham Bioinformatics—FastQC A Quality Control tool for High Throughput Sequence Data. *Soil.* 2010. Available online: https://www.bioinformatics.babraham.ac.uk/projects/fastqc/ (accessed on 10 March 2023).
104. Ewels, P.; Magnusson, M.; Lundin, S.; Käller, M. MultiQC: Summarize analysis results for multiple tools and samples in a single report. *Bioinformatics* **2016**, *32*, 3047–3048. [CrossRef] [PubMed]
105. Dobin, A.; Davis, C.A.; Schlesinger, F.; Drenkow, J.; Zaleski, C.; Jha, S.; Batut, P.; Chaisson, M.; Gingeras, T.R. STAR: Ultrafast universal RNA-seq aligner. *Bioinformatics* **2013**, *29*, 15–21. [CrossRef]
106. Li, H.; Handsaker, B.; Wysoker, A.; Fennell, T.; Ruan, J.; Homer, N.; Marth, G.; Abecasis, G.; Durbin, R. Subgroup, 1000 Genome Project Data Processing the Sequence Alignment/Map format and SAMtools. *Bioinformatics* **2009**, *25*, 2078–2079. [CrossRef]
107. Zerbino, D.R.; Achuthan, P.; Akanni, W.; Amode, M.R.; Barrell, D.; Bhai, J.; Billis, K.; Cummins, C.; Gall, A.; Girón, C.G.; et al. Ensembl 2018. *Nucleic Acids Res.* **2018**, *46*, D754–D761. [CrossRef]
108. Anders, S.; Pyl, P.T.; Huber, W. HTSeq—A Python framework to work with high-throughput sequencing data. *Bioinformatics* **2015**, *31*, 166–169. [CrossRef]
109. Robinson, M.D.; McCarthy, D.J.; Smyth, G.K. edgeR: A Bioconductor package for differential expression analysis of digital gene expression data. *Bioinformatics* **2010**, *26*, 139–140. [CrossRef] [PubMed]
110. Love, M.I.; Huber, W.; Anders, S. Moderated estimation of fold change and dispersion for RNA-seq data with DESeq2. *Genome Biol.* **2014**, *15*, 550. [CrossRef]
111. Coenye, T. Do results obtained with RNA-sequencing require independent verification? *Biofilm* **2021**, *3*, 100043. [CrossRef]
112. Feng, L.; Liu, H.; Liu, Y.; Lu, Z.; Guo, G.; Guo, S.; Zheng, H.; Gao, Y.; Cheng, S.; Wang, J.; et al. Power of Deep Sequencing and Agilent Microarray for Gene Expression Profiling Study. *Mol. Biotechnol.* **2010**, *45*, 101–110. [CrossRef] [PubMed]
113. Hänzelmann, S.; Castelo, R.; Guinney, J. GSVA: Gene set variation analysis for microarray and RNA-Seq data. *BMC Bioinformatics* **2013**, *14*, 7. [CrossRef] [PubMed]
114. Liberzon, A.; Birger, C.; Thorvaldsdóttir, H.; Ghandi, M.; Mesirov, J.P.; Tamayo, P. The Molecular Signatures Database Hallmark Gene Set Collection. *Cell Syst.* **2015**, *1*, 417–425. [CrossRef]
115. Martens, M.; Ammar, A.; Riutta, A.; Waagmeester, A.; Slenter, D.N.; Hanspers, K.; Miller, R.A.; Digles, D.; Lopes, E.N.; Ehrhart, F.; et al. WikiPathways: Connecting communities. *Nucleic Acids Res.* **2021**, *49*, D613–D621. [CrossRef]
116. Kanehisa, M.; Furumichi, M.; Sato, Y.; Ishiguro-Watanabe, M.; Tanabe, M. KEGG: Integrating viruses and cellular organisms. *Nucleic Acids Res.* **2021**, *49*, D545–D551. [CrossRef] [PubMed]
117. Ritchie, M.E.; Phipson, B.; Wu, D.; Hu, Y.; Law, C.W.; Shi, W.; Smyth, G.K. limma powers differential expression analyses for RNA-sequencing and microarray studies. *Nucleic Acids Res.* **2015**, *43*, e47. [CrossRef]
118. Heberle, H.; Meirelles, G.V.; da Silva, F.R.; Telles, G.P.; Minghim, R. InteractiVenn: A web-based tool for the analysis of sets through Venn diagrams. *BMC Bioinform.* **2015**, *16*, 169. [CrossRef] [PubMed]
119. Goedhart, J.; Luijsterburg, M.S. VolcaNoseR is a web app for creating, exploring, labeling and sharing volcano plots. *Sci. Rep.* **2020**, *10*, 20560. [CrossRef] [PubMed]

9 Discussion and Conclusion

MSC-derived secretomes have been shown to have therapeutic potential in a variety of disease models, such as sepsis, and to support the repair of the liver, lungs, skin and the heart while also possessing neuroprotective and neurotrophic abilities [296–301].

Various species including mice, rats, rabbits, horses, and humans have demonstrated the regenerative potential of MSC-CM and EVs in tendon and ligament repair, as evidenced in vitro and *in vivo* [161,261–265,272–277,302]. In rat models, MSC-CM promoted tenocyte proliferation by activating ERK1/2 signal molecules, compared to untreated control groups [162]. In addition, in rat rotator cuff models, MSC-CM inhibited M1 and supported M2 macrophage polarization, promoting tendon-bone healing [161]. Furthermore, in horses, MSC-CM inhibited PBMC proliferation *in vivo* and induced neovascularization, which declined during the healing process as vessel size and quantity decreased [163].

MSC-EVs demonstrated their immunomodulatory capacity in various *in vivo* tendon injury models, reducing macrophage NF-κB activity, as well as the IL-1β and IFN-γ response, while increasing the production of anti-inflammatory cytokines such as IL-4 and IL-10 [261–263,265]. Additionally, the administration of MSC-EVs into tendon defects enhanced the proliferation of TSPCs, improved the restoration of tendon architecture, histological score, and expression of genes related to collagen and tendon matrix formation. These genes included collagen (Col) type I, mohawk (MKX), scleraxis (SCX), tenomodulin (TNMD), and tissue inhibitor of metalloproteinase-3 (TIMP-3), while also decreasing MMP-3 expression [261,274,275,277,302].

The absence of replicating cells puts secretome-based therapies into a potentially preferred position over cell therapies with respect to patient safety concerns and facilitates product standardization and storage. Cell secretomes and their sub-fractions can be evaluated for dosage, potency, and efficacy analogous to conventional pharmaceuticals agents which may facilitate their use in clinical practice. However, the exciting and new field of secretome therapies, or therapies using subfractions of secretomes like e.g. EVs, is only at the very beginning of the road towards clinical applicability.

In the presented work, we highlighted and addressed problems arising from the lack of standardized EV isolation, purification, characterization and quantification protocols. However, EVs isolated through UC reportedly have diminished functional capacity compared to EVs

isolated using SEC, potentially due to prolonged exposure to high centrifugal forces [303,304]. UC and SEC was compared based on the minimal criteria (MISEV criteria) for EV isolation and characterization postulated by the ISEV using western blot, fluorescence-triggered flow cytometry (FT-FC), NTA measurements and TEM to address the limited availability of cross-reacting markers for horses. Both methods led to successful EV isolation from equine MCS supernatants. The obtained particles expressed markers characteristic for EVs and showed a comparable size distribution pattern. However, UC yielded more particles per ml of MSC supernatant than SEC. Although a considerable difference in EV yields was found, it is not clear if the difference is truly method based or if it resulted from sample handling. Besides the obvious method difference, the impact of temperature differences on short-term storage of conditioned media is significant. SEC columns are stored at 4 °C and equilibrated at room temperature prior to use. The applied supernatant should have room temperature as well to achieve optimal isolation of EVs (according to the manufacturer). UC is performed in a 4 °C cooled centrifuge. Studies have shown that storing conditioned media at low temperatures, such as 4 °C, can preserve the stability and activity of the biomolecules for up to 48 hours. However, higher temperatures, such as room temperature or above, can lead to the rapid degradation of these biomolecules, resulting in decreased efficacy of the conditioned media. Additionally, temperature fluctuations during storage can also have a negative impact on the stability and activity of the biomolecules.

Another important finding was a discrepancy in particle counts using different measurement approaches. NTA detected significantly more particles than FT-FC which can be explained by the principle of the measurement. NTA measures the size of particles and their concentration based on the physical principle of Brownian motion. In contrast to FT-FC, where lipid dyes or antibodies are used to specifically label EVs, NTA cannot discriminate between EVs and contaminants in the form of particles that might derive from external sources such as washing buffers. However, NTA devices are also available with lasers, which allow detection of labeled EVs like FT-FC. In addition, the measurements of the concentration and the size distribution are closely linked to the detection limit of the characterization method which leads to differences between the measured concentrations [305,306].

The differences in EV isolation, characterization and dosage make it difficult to compare published work on EVs in general and specifically their therapeutic efficacy which hampers progress in the field. The therapeutic potential of EVs depends on their cargo, which differs based on the origin and activation status of the producer cell, and their surface- and

transmembrane molecules that govern target specificity and EV-uptake by recipient cells [164,303,304,307–316]. The resulting heterogeneity of EVs in both content and functionality, at the same time necessitates and impedes standardized, well-defined EV manufacturing processes. However, a defined therapeutic efficacy and reliable dosing are prerequisites for the application in routine clinical settings. In addition, EV purity is crucial to ensure that any observed effects are truly based on the applied EV and not co-purified contaminants like salts or soluble proteins and nucleic acids. Co-purified protein aggregates may lead to false positive counts and confound EV quantification. This may explain why protein concentrations do not correlate with particle numbers [312,314,315,317]. A recent meta-review looking at dosing regimens, found that more than 50 % of all studies quantified EVs in total amount of protein and 18 % utilized NTA, whereas 21 % of the studies did not quantify EVs at all [314]. Standardized purification and analytical methods will facilitate to determine the true potential of EVs, to discover of functional heterogeneity and to develop reliable EV-based regenerative therapies.

In addition, it is crucial to increase the understanding of the physicochemical properties and functions of EVs based on donor cell conditions and isolation methods.

Identification of optimal secretome donor cells and their preconditioning status are the fine-tuning steps on the way to future treatments. Furthermore, age or passage number of the donor cells are of fundamental importance. Extensive culture expansion drives MSCs toward replicative senescence and a consequent decline in quality with diminished immunosuppressive and regenerative capacity and pro-inflammatory features [318,319]. Indeed long-term in vitro culture (high passage) was recently shown to have a greater effect on MSCs (increased β-Galactosidase level) than the natural ageing process of their donor. Interestingly, the secretion of EVs by MSCs increases with donor age and late passage cultures maybe in order to dispose undesirable molecules or as distress signal [318,320]. Furthermore, EVs released by senescent cells contain an altered cargo that may contribute to senescence propagation and chronic inflammation [318,320,321]. The use of allogeneic MSCs to produce EVs offers an attractive cell-free, off-the shelf treatment option which allows for the selection of optimal donor cells as well as scalable and standardized manufacturing to target a specific disease.

Most of the standardization and characterization approached discussed above are based on quantitative parameters. Others focus one type of cargo by quantifying a specific component such as nucleic acids, proteins or lipids in the EVs [16]. Future studies should also focus on qualitative aspects such as the quantity of known effector molecules or EV potency units based

on standardized in vitro potency assay [315] A recent report claims to facilitate the reproducibility of EV isolations as well as CM by using Raman spectroscopy to identify both the soluble factors and the EV components that may provide a regenerative effect [322].

The second paper investigated the effects of the secretome and its subfractions, the EV fraction and the protein fraction (PF), of bmMSCs on chemically inflamed tenocytes. Our study found that complete CM had the most potent treatment effect on inflamed tenocytes. Although all three treatments showed significant differences compared to the untreated inflamed control, the EV fraction and the PF) did not exert the same level of influence on gene expression as the CM fraction.

Similar findings have been reported in previous studies, demonstrating the synergistic effects of the secretome's EVs and soluble proteins, highlighting the therapeutic superiority of complete CM over its subfractions in various cell types and assays [323–327]. For example, when comparing the effects of CM and EVs from adipose-derived MSCs (aMSCs) on muscle regeneration, both CM and EVs protected against cellular senescence, but CM showed higher proliferation and differentiation, while only EVs reduced inflammation [325]. Similarly, in an in vitro model of osteoarthritis, CM and EVs derived from human ADSCs reduced hypertrophic collagen 10, but only CM significantly decreased MMP activity and prostaglandin 2 (PGE2) expression [326]. Moreover, in a study evaluating the effects of CM, EVs, and PF fractions on inflamed nucleus pulposus and annulus fibrosus cells, whole CM demonstrated superior immunomodulatory and MMP inhibitory effects compared to its subfractions [324]. Comparing the effects of PBMCs-derived secretome and its subfractions also revealed that the complete secretome induced better neo-angiogenesis than its individual components [327].

However, divergent results have been observed in studies investigating CM and EVs from human aMSCs. In some cases, EVs alone, like whole CM, promoted cell proliferation and migration in skeletal muscle cells. Additionally, small extracellular EVs outperformed conditioned media of adipose tissue in terms of migration and regeneration potential, although these studies standardized EVs and CM based on equivalent protein concentrations and did not consider unpacked proteins [326]. Another explanation for EVs outperforming CM in migration is the more efficient recruitment of host cells through EVs compared to other paracrine factors present in CM [328,329].

On the other hand, when comparing the therapeutic efficacy of amniotic MSCs-derived CM, PF, and EV fractions on immune cell proliferation and differentiation, whole CM and its PF

fraction decreased PBMC proliferation, reduced inflammatory polarization of T-cells, enhanced regulatory T-cell and M2 macrophage polarization, and reduced B-cell activation, while EVs showed no immunomodulatory effect [323].

The divergent results observed in these studies comparing complete CM and its EV fraction can be attributed to differences in the donor cells, culture media, substrates, cell confluence, preconditioning, isolation and concentration procedures, dosage, and the treated cells. The properties of CM and EV isolates highly depend on the donor cell type, as different cell sources secrete various signals suitable for different downstream applications [282,330]. Isolation methods, especially for EVs, also influence the type and properties of the enriched EVs [331,332]. Furthermore, cell culture parameters such as seeding density and passaging frequency can further affect the regenerative potential [333,334]. Additionally, differences in secretome composition can be significant when comparing fetal and adult donors, and pre-conditioning of donor cells can alter secretome profiles [335,336].

Standardization strategies, optimal dosage, and the number of doses also pose challenges when comparing CM and its subfractions. CM is typically standardized based on protein concentration, while EV treatments are often quantified based on the number of particles using NTA. Cargo-specific quantification of nucleic acids, proteins, or lipids in EVs or using Raman spectroscopy can provide a more focused approach for quality control [322].

Both EVs and the soluble fraction of CM contain factors potentially beneficial for regeneration, and the presence of ribosomal proteins and translation factors in EVs directly impacts recipient cells by enabling *de novo* protein expression [337]. Proteomic analysis has revealed diverging protein compositions between CM and EVs, emphasizing the need to analyze different parts of the secretome independently to gain better insights into the therapeutic mechanisms. Understanding these processes would inform tailored therapeutic options for the secretome [262,265,274].

Although promising in vitro results have been obtained from this study and others, several questions remain unanswered before translation into clinical applications. Factors such as the route of administration, absorption profile, distribution throughout the body, metabolism rate, and clearance of EVs need to be addressed, as clearance of EVs poses a significant challenge [338–340]. Future studies should aim to resolve these issues and establish reproducible and optimized protocols for cell-free treatment approaches.

It is important to note some limitations of our study. While we standardized the EV or protein concentration within each treatment, it was not possible to standardize the concentrations between treatments due to the potential loss of material during enrichment, causing differences in protein concentration and EV yield. The filtration process during SEC may lead to the loss of EVs and proteins [151]. Additionally, the differentially expressed gene data revealed that none of the three treatments fully restored the healthy status of the inflamed cells. However, treatment with complete CM resulted in the highest number of differentially expressed genes compared to the inflamed control, suggesting a superior therapeutic effect and a possible synergistic effect of the different secretome fractions.

It is imperative to highlight our decision to employ SEC rather than UC for the isolation of EVs. This preference is rooted in the reported reduction in functional capacity observed in EVs isolated through UC compared to those isolated using SEC. This disparity is attributed to the potential deleterious effects of prolonged exposure to high centrifugal forces in UC. Additionally, the utilization of UC demands more intricate sample handling, involves complex equipment, and necessitates a higher level of expertise to achieve optimal EV yield when compared to SEC. Notably, diverse UC protocols and parameters, including rotor type, UC-tube quality, centrifugation speed, acceleration, and deceleration, present customization opportunities that, while enhancing purity and yield, concurrently introduce challenges related to reproducibility and inter-laboratory variation. Furthermore, drawbacks associated with UC encompass the likelihood of contamination with exosomal aggregates, thereby diminishing purity and potentially compromising the accuracy of EV quantification. Additionally, the cost of equipment is a pertinent consideration in the evaluation of UC. In contrast, SEC offers distinct advantages, notably its simplified technique and the attainment of higher EV purity with minimal artifacts such as EV aggregates. These attributes enhance the clinical applicability of SEC in EV isolation.

There are still a lot of challenges with cell-free therapies in numerous clinical applications. In addition to the technological aspects of EV isolation and quantification which our recent paper focuses on, also biological factors, such as CM-producing cell type, cell culture, confluence and stimulation, influence CM and EV quality and quantity [341]. The resulting EV heterogeneity and differences in EV cargo impedes reproducibility and comparability of studies [342]. Another big obstacle when comparing CM and its subfraction is the standardization strategy for studies, the optimal dosage of the treatment and the number of doses [343]. The most common way to

determine the therapeutic dose of an EV treatment is by quantifying the number of particles using NTA in an isolate [16].

Another topic that needs to be investigated is the route of administration. Potential therapeutic effects of secretomes, EVs or soluble proteins influenced by their absorption characteristics, the distribution in the body, the metabolic status of the patient and the clearance [338]. In particular, clearance of EVs is a big problem - e.g it was shown that EVs are quickly cleared from the circulating blood and discharged from the body [338,339].

Finally, studies focusing on an optimal administration frequency are essential to implement the successful translation of secretome- based treatments into the clinical setting.

10 References

1. Walden, G. *et al.* A Clinical, Biological, and Biomaterials Perspective into Tendon Injuries and Regeneration. *Tissue Eng. Part B. Rev.* **23**, 44–58 (2017).

2. Thomopoulos, S., Parks, W. C., Rifkin, D. B. & Derwin, K. A. Mechanisms of tendon injury and repair. *J. Orthop. Res.* **33**, 832–839 (2015).

3. Pinchbeck, G. L. *et al.* Horse injuries and racing practices in National Hunt racehorses in the UK: the results of a prospective cohort study. *Vet. J.* **167**, 45–52 (2004).

4. Dowling, B. A., Dart, A. J., Hodgson, D. R. & Smith, R. K. W. Superficial digital flexor tendonitis in the horse. *Equine Vet. J.* **32**, 369–378 (2000).

5. SMITH, R. K. W., KORDA, M., BLUNN, G. W. & GOODSHIP, A. E. Isolation and implantation of autologous equine mesenchymal stem cells from bone marrow into the superficial digital flexor tendon as a potential novel treatment. *Equine Vet. J.* **35**, 99–102 (2003).

6. Voga, M., Adamic, N., Vengust, M. & Majdic, G. Stem Cells in Veterinary Medicine-Current State and Treatment Options. *Front. Vet. Sci.* **7**, 278 (2020).

7. Van Loon, V. J. F., Scheffer, C. J. W., Genn, H. J., Hoogendoorn, A. C. & Greve, J. W. Clinical follow-up of horses treated with allogeneic equine mesenchymal stem cells derived from umbilical cord blood for different tendon and ligament disorders. *Vet. Q.* **34**, 92–97 (2014).

8. Beerts, C. *et al.* Tenogenically Induced Allogeneic Peripheral Blood Mesenchymal Stem Cells in Allogeneic Platelet-Rich Plasma: 2-Year Follow-up after Tendon or Ligament Treatment in Horses. *Front. Vet. Sci.* **4**, (2017).

9. VIDAL, M. A. *et al.* Comparison of Chondrogenic Potential in Equine Mesenchymal Stromal Cells Derived from Adipose Tissue and Bone Marrow. *Vet. Surg.* **37**, 713–724 (2008).

10. Ferris, D. J. *et al.* Clinical outcome after intra-articular administration of bone marrow derived mesenchymal stem cells in 33 horses with stifle injury. *Vet. Surg.* **43**, 255–265 (2014).

11. Hosseini, S., Taghiyar, L., Safari, F. & Baghaban Eslaminejad, M. Regenerative

Medicine Applications of Mesenchymal Stem Cells BT - Cell Biology and Translational Medicine, Volume 2: Approaches for Diverse Diseases and Conditions. in (ed. Turksen, K.) 115–141 (Springer International Publishing, 2018). doi:10.1007/5584_2018_213.

12. Torricelli, P. *et al.* Regenerative medicine for the treatment of musculoskeletal overuse injuries in competition horses. *Int. Orthop. 2011 3510* **35**, 1569–1576 (2011).

13. Ricco, S. *et al.* Allogeneic Adipose Tissue-Derived Mesenchymal Stem Cells in Combination with Platelet Rich Plasma are Safe and Effective in the Therapy of Superficial Digital Flexor Tendonitis in the Horse: *http://dx.doi.org/10.1177/03946320130260S108* **26**, 61–68 (2013).

14. GODWIN, E. E., YOUNG, N. J., DUDHIA, J., BEAMISH, I. C. & SMITH, R. K. W. Implantation of bone marrow-derived mesenchymal stem cells demonstrates improved outcome in horses with overstrain injury of the superficial digital flexor tendon. *Equine Vet. J.* **44**, 25–32 (2012).

15. Dyson, S. J. Medical management of superficial digital flexor tendonitis: A comparative study in 219 horses (1992-2000). *Equine Vet. J.* **36**, 415–419 (2004).

16. Théry, C. *et al.* Minimal information for studies of extracellular vesicles 2018 (MISEV2018): a position statement of the International Society for Extracellular Vesicles and update of the MISEV2014 guidelines. *https://doi.org/10.1080/20013078.2018.1535750* **7**, (2018).

17. Brandt, L. *et al.* Tenogenic Properties of Mesenchymal Progenitor Cells Are Compromised in an Inflammatory Environment. *Int. J. Mol. Sci. 2018, Vol. 19, Page 2549* **19**, 2549 (2018).

18. Frank, C. B. & Hart, D. A. The Biology of Tendons and Ligaments. in *Biomechanics of Diarthrodial Joints* (eds. Ratcliffe, A., Woo, S. L.-Y. & Mow, V. C.) 39–62 (Springer New York, 1990).

19. Canty, E. G. & Kadler, K. E. Procollagen trafficking, processing and fibrillogenesis. *J. Cell Sci.* **118**, 1341–1353 (2005).

20. Barnard, K., Light, N. D., Sims, T. J. & Bailey, A. J. Chemistry of the collagen cross-links. Origin and partial characterization of a putative mature cross-link of collagen. *Biochem. J.* **244**, 303–309 (1987).

21. Thorpe, C. T. *et al.* Helical sub-structures in energy-storing tendons provide a possible mechanism for efficient energy storage and return. *Acta Biomater.* **9**, 7948–7956 (2013).

22. Thorpe, C. T., Udeze, C. P., Birch, H. L., Clegg, P. D. & Screen, H. R. C. Specialization of tendon mechanical properties results from interfascicular differences. *J. R. Soc. Interface* **9**, 3108–3117 (2012).

23. Ahtikoski, A. M. *et al.* Synthesis and degradation of type IV collagen in rat skeletal muscle during immobilization in shortened and lengthened positions. *Acta Physiol. Scand.* **177**, 473–481 (2003).

24. Hanson, A. N. & Bentley, J. P. Quantitation of Type I to type III collagen ratios in small samples of human tendon, blood vessels, and atherosclerotic plaque. *Anal. Biochem.* **130**, 32–40 (1983).

25. BIRCH, H. L., BAILEY, A. J. & GOODSHIP, A. E. Macroscopic 'degeneration' of equine superficial digital flexor tendon is accompanied by a change in extracellular matrix composition. *Equine Vet. J.* **30**, 534–539 (1998).

26. Kleiner, D. M. Human Tendons: Anatomy, Physiology and Pathology. *J. Athl. Train.* **33**, 185–186 (1998).

27. Thorpe, C. T., Birch, H. L., Clegg, P. D. & Screen, H. R. C. The role of the non-collagenous matrix in tendon function. *Int. J. Exp. Pathol.* **94**, 248–259 (2013).

28. Jarvinen, T. A. *et al.* Mechanical loading regulates tenascin-C expression in the osteotendinous junction. *J. Cell Sci.* **112**, 3157–3166 (1999).

29. REES, S. G. *et al.* Catabolism of aggrecan, decorin and biglycan in tendon. *Biochem. J.* **350**, 181–188 (2000).

30. BAILEY, A. J., SHELLSWELL, G. B. & DUANCE, V. C. Identification and change of collagen types in differentiating myoblasts and developing chick muscle. *Nature* **278**, 67–69 (1979).31. Alexander, R. M. Energy-saving mechanisms in walking and running. *J. Exp. Biol.* **160**, 55–69 (1991).

32. Alexander, R. M. & Bennet-Clark, H. C. Storage of elastic strain energy in muscle and other tissues. *Nature* **265**, 114–117 (1977).

33. Brakebusch, C., Bouvard, D., Stanchi, F., Sakai, T. & Fässler, R. Integrins in invasive

growth. *J. Clin. Invest.* **109**, 999–1006 (2002).

34. Ingber, D. E. *et al.* Cellular Tensegrity: Exploring How Mechanical Changes in the Cytoskeleton Regulate Cell Growth, Migration, and Tissue Pattern during Morphogenesis. in *Mechanical Engineering of the Cytoskeleton in Developmental Biology* (ed. Gordon, R. B. T.-I. R. of C.) vol. 150 173–224 (Academic Press, 1994).

35. Banes, A. J. *et al.* Gap Junctions Regulate Responses of Tendon Cells Ex Vivo to Mechanical Loading. *Clin. Orthop. Relat. Res.* **367**, (1999).

36. Bloch, R. J. *et al.* Costameres: Repeating Structures at the Sarcolemma of Skeletal Muscle. *Clin. Orthop. Relat. Res.* **403**, (2002).

37. Carragher, N. O., Levkau, B., Ross, R. & Raines, E. W. Degraded Collagen Fragments Promote Rapid Disassembly of Smooth Muscle Focal Adhesions That Correlates with Cleavage of Pp125FAK, Paxillin, and Talin. *J. Cell Biol.* **147**, 619–630 (1999).

38. Burridge, K. & Chrzanowska-Wodnicka, M. FOCAL ADHESIONS, CONTRACTILITY, AND SIGNALING. *Annu. Rev. Cell Dev. Biol.* **12**, 463–519 (1996).

39. Reynolds, S. D. *et al.* Cloning of the chick BMP1/Tolloid cDNA and expression in skeletal tissues. *Gene* **248**, 233–243 (2000).

40. Ning, W. *et al.* Mechanical behavior in living cells consistent with the tensegrity model. *Proc. Natl. Acad. Sci.* **98**, 7765–7770 (2001).

41. WANG, J. H.-C. Substrate Deformation Determines Actin Cytoskeleton Reorganization: A Mathematical Modeling and Experimental Study. *J. Theor. Biol.* **202**, 33–41 (2000).

42. Chiquet, M., Renedo, A. S., Huber, F. & Flück, M. How do fibroblasts translate mechanical signals into changes in extracellular matrix production? *Matrix Biol.* **22**, 73–80 (2003).

43. Abraham, A. C. *et al.* Targeting the NF-κB signaling pathway in chronic tendon disease. *Sci. Transl. Med.* **11**, eaav4319 (2019).

44. Millar, N. L. *et al.* Tendinopathy. *Nat. Rev. Dis. Prim.* **7**, 1 (2021).

45. Herod, T. W. & Veres, S. P. Development of overuse tendinopathy: A new descriptive model for the initiation of tendon damage during cyclic loading. *J. Orthop. Res.* **36**, 467–476 (2018).

46. Tran, P. H. T. *et al.* Early development of tendinopathy in humans: Sequence of pathological changes in structure and tissue turnover signaling. *FASEB J.* **34**, 776–788 (2020).

47. Nichols, A. E. C., Best, K. T. & Loiselle, A. E. The cellular basis of fibrotic tendon healing: challenges and opportunities. *Transl. Res.* **209**, 156–168 (2019).

48. Lin, T. W., Cardenas, L. & Soslowsky, L. J. Biomechanics of tendon injury and repair. *J. Biomech.* **37**, 865–877 (2004).

49. Yang, G., Rothrauff, B. B. & Tuan, R. S. Tendon and ligament regeneration and repair: clinical relevance and developmental paradigm. *Birth Defects Res. C. Embryo Today* **99**, 203–222 (2013).

50. Schulze-Tanzil, G. *et al.* The role of pro-inflammatory and immunoregulatory cytokines in tendon healing and rupture: new insights. *Scand. J. Med. Sci. Sports* **21**, 337–351 (2011).

51. Cambré, I. *et al.* Mechanical strain determines the site-specific localization of inflammation and tissue damage in arthritis. *Nat. Commun.* **9**, 4613 (2018).

52. Maffulli, N., Ewen, S. W. B., Waterston, S. W., Reaper, J. & Barrass, V. Tenocytes from Ruptured and Tendinopathic Achilles Tendons Produce Greater Quantities of Type III Collagen than Tenocytes from Normal Achilles Tendons: An in Vitro Model of Human Tendon Healing. *Am. J. Sports Med.* **28**, 499–505 (2000).

53. Tang, C. *et al.* The roles of inflammatory mediators and immunocytes in tendinopathy. *J. Orthop. Transl.* **14**, 23–33 (2018).

54. Dakin, S. G. *et al.* Chronic inflammation is a feature of Achilles tendinopathy and rupture. *Br. J. Sports Med.* **52**, 359 LP – 367 (2018).

55. Dakin, S. G. Inflammation or damage: Fibroblasts decide. *Sci. Transl. Med.* **11**, eaax9562 (2019).

56. Docheva, D., Müller, S. A., Majewski, M. & Evans, C. H. Biologics for tendon repair. *Adv. Drug Deliv. Rev.* **84**, 222–239 (2015).

57. Review of Treatment Options for Equine Tendon and Ligament Injuries: What's New and How Do They Work? | IVIS. https://www.ivis.org/library/aaep/aaep-annual-

convention-seattle-2005/review-of-treatment-options-for-equine-tendon-and-ligament-injuries-whats-new-and-how-do-they-work.

58. Villalba, J., Molina-Corbacho, M., García, R. & Martínez-Carreres, L. Home-Based Intravenous Analgesia With an Elastomeric Pump After Medial Patellofemoral Ligament Repair: A Case Series. *J. PeriAnesthesia Nurs.* **36**, 690–694 (2021).

59. Kainth, G. S. & Goel, A. A useful technique of using anterior cruciate ligament reconstruction jig for preparing patellar tunnel in surgical repair of extensor tendon ruptures. *Ann. R. Coll. Surg. Engl.* **103**, 142–143 (2021).

60. Lim, W. L., Liau, L. L., Ng, M. H., Chowdhury, S. R. & Law, J. X. Current Progress in Tendon and Ligament Tissue Engineering. *Tissue Eng. Regen. Med.* **16**, 549–571 (2019).

61. Sudhakar, N. *et al.* Chapter 4 - Omics Approaches in Fungal Biotechnology: Industrial and Medical Point of View. in (eds. Barh, D. & Azevedo, V. B. T.-O. T. and B.-E.) 53–70 (Academic Press, 2018). doi:https://doi.org/10.1016/B978-0-12-815870-8.00004-8.

62. Timmers, L. *et al.* Human mesenchymal stem cell-conditioned medium improves cardiac function following myocardial infarction. *Stem Cell Res.* **6**, 206–214 (2011).

63. Gnecchi, M. *et al.* Paracrine action accounts for marked protection of ischemic heart by Akt-modified mesenchymal stem cells. *Nat. Med.* **11**, 367–368 (2005).

64. Caplan, A. I. & Correa, D. The MSC: an injury drugstore. *Cell Stem Cell* **9**, 11–15 (2011).

65. Caplan, A. I. & Dennis, J. E. Mesenchymal stem cells as trophic mediators. *J. Cell. Biochem.* **98**, 1076–1084 (2006).

66. Kupcova Skalnikova, H. Proteomic techniques for characterisation of mesenchymal stem cell secretome. *Biochimie* **95**, 2196–2211 (2013).

67. Lai, R. C. *et al.* Proteolytic Potential of the MSC Exosome Proteome: Implications for an Exosome-Mediated Delivery of Therapeutic Proteasome. *Int. J. Proteomics* **2012**, 971907 (2012).

68. Alessio, N. *et al.* The secretome of MUSE cells contains factors that may play a role in regulation of stemness, apoptosis and immunomodulation. *Cell Cycle* **16**, 33–44 (2017).

69. Kološa, K., Motaln, H., Herold-Mende, C., Koršič, M. & Lah, T. T. Paracrine Effects of

Mesenchymal Stem Cells Induce Senescence and Differentiation of Glioblastoma Stem-Like Cells. *Cell Transplant.* **24**, 631–644 (2015).

70. Equine Surgery - Jorg A. Auer, John A. Stick - Google Books. https://books.google.at/books?hl=en&lr=&id=0mRgDwAAQBAJ&oi=fnd&pg=PP1&ots=sdrpeWZc60&sig=lCLJMQzIOukmlIYCJKST3v6ELzs&redir_esc=y#v=onepage&q&f=false.

71. Mageed, M. *et al.* Influence of cryopreservation and mechanical stimulation on equine Autologous Conditioned Plasma (ACP®). *Tierarztl. Prax. Ausg. G. Grosstiere. Nutztiere.* **43**, 97–104 (2015).

72. Hessel, L. N., Bosch, G., van Weeren, P. R. & Ionita, J.-C. Equine autologous platelet concentrates: A comparative study between different available systems. *Equine Vet. J.* **47**, 319–325 (2015).

73. Ionita, C. R. *et al.* Comparison of humoral insulin-like growth factor-1, platelet-derived growth factor-BB, transforming growth factor-β1, and interleukin-1 receptor antagonist concentrations among equine autologous blood-derived preparations. *Am. J. Vet. Res.* **77**, 898–905 (2016).

74. Kümmerle, J. M., Theiss, F. & Smith, R. K. W. Chapter 84 - Diagnosis and Management of Tendon and Ligament Disorders. in (eds. Auer, J. A., Stick, J. A., Kümmerle, J. M. & Prange, T. B. T.-E. S. (Fifth E.) 1411–1445 (W.B. Saunders, 2019). doi:https://doi.org/10.1016/B978-0-323-48420-6.00084-3.

75. Hauschild, G. *et al.* Short term storage stability at room temperature of two different platelet-rich plasma preparations from equine donors and potential impact on growth factor concentrations. *BMC Vet. Res.* **13**, 1–9 (2017).

76. McClain, A. K. & McCarrel, T. M. The effect of four different freezing conditions and time in frozen storage on the concentration of commonly measured growth factors and enzymes in equine platelet-rich plasma over six months. *BMC Vet. Res.* **15**, 1–9 (2019).

77. Young, R. G. *et al.* Use of mesenchymal stem cells in a collagen matrix for achilles tendon repair. *J. Orthop. Res.* **16**, 406–413 (1998).

78. Smith, R. K. W. Mesenchymal stem cell therapy for equine tendinopathy. *Disabil. Rehabil.* **30**, 1752–1758 (2008).

79. Smith, R. K. W. & Webbon, P. M. Harnessing the stem cell for the treatment of tendon injuries: heralding a new dawn? *Br. J. Sports Med.* **39**, 582 LP – 584 (2005).

80. Smith, R. K. W. *et al.* Beneficial Effects of Autologous Bone Marrow-Derived Mesenchymal Stem Cells in Naturally Occurring Tendinopathy. *PLoS One* **8**, e75697 (2013).

81. Costa-Almeida, R., Calejo, I. & Gomes, M. E. Mesenchymal Stem Cells Empowering Tendon Regenerative Therapies. *Int. J. Mol. Sci.* **20**, (2019).

82. Horwitz, E. M. *et al.* Isolated allogeneic bone marrow-derived mesenchymal cells engraft and stimulate growth in children with osteogenesis imperfecta: Implications for cell therapy of bone. *Proc. Natl. Acad. Sci.* **99**, 8932 LP – 8937 (2002).

83. Prochazkova, M. *et al.* Chapter 18 - Embryonic Versus Adult Stem Cells. in (eds. Vishwakarma, A., Sharpe, P., Shi, S. & Ramalingam, M. B. T.-S. C. B. and T. E. in D. S.) 249–262 (Academic Press, 2015). doi:https://doi.org/10.1016/B978-0-12-397157-9.00020-5.

84. Dulak, J., Szade, K., Szade, A., Nowak, W. N. & Józkowicz, A. Adult stem cells: hopes and hypes of regenerative medicine. *Acta Biochim. Pol.* **62 3**, 329–337 (2015).

85. Dominici, M. *et al.* Minimal criteria for defining multipotent mesenchymal stromal cells. The International Society for Cellular Therapy position statement. *Cytotherapy* **8**, 315–317 (2006).

86. Nixon, A. J., Dahlgren, L. A., Haupt, J. L., Yeager, A. E. & Ward, D. L. Effect of adipose-derived nucleated cell fractions on tendon repair in horses with collagenase-induced tendinitis. *Am. J. Vet. Res.* **69**, 928–937 (2008).

87. de Mattos Carvalho, A. *et al.* Use of Adipose Tissue-Derived Mesenchymal Stem Cells for Experimental Tendinitis Therapy in Equines. *J. Equine Vet. Sci.* **31**, 26–34 (2011).

88. Kang, J.-G. *et al.* Characterization and clinical application of mesenchymal stem cells from equine umbilical cord blood. *J. Vet. Sci.* **14**, 367–371 (2013).

89. Longhini, A. L. F. *et al.* Peripheral blood-derived mesenchymal stem cells demonstrate immunomodulatory potential for therapeutic use in horses. *PLoS One* **14**, e0212642 (2019).

90. Prado, A. A. F. *et al.* Characterization of mesenchymal stem cells derived from the equine synovial fluid and membrane. *BMC Vet. Res.* **11**, 281 (2015).

91. Beerts, C. *et al.* Tenogenically Induced Allogeneic Peripheral Blood Mesenchymal Stem Cells in Allogeneic Platelet-Rich Plasma: 2-Year Follow-up after Tendon or Ligament Treatment in Horses . *Frontiers in Veterinary Science* vol. 4 158 (2017).

92. Gugjoo, M. B., Amarpal, Makhdoomi, D. M. & Sharma, G. T. Equine Mesenchymal Stem Cells: Properties, Sources, Characterization, and Potential Therapeutic Applications. *J. Equine Vet. Sci.* **72**, 16–27 (2019).

93. Secunda, R. *et al.* Isolation, expansion and characterisation of mesenchymal stem cells from human bone marrow, adipose tissue, umbilical cord blood and matrix: a comparative study. *Cytotechnology* **67**, 793–807 (2015).

94. Carrade, D. D. *et al.* Intradermal injections of equine allogeneic umbilical cord-derived mesenchymal stem cells are well tolerated and do not elicit immediate or delayed hypersensitivity reactions. *Cytotherapy* **13**, 1180–1192 (2011).

95. Koch, T. G., Heerkens, T., Thomsen, P. D. & Betts, D. H. Isolation of mesenchymal stem cells from equine umbilical cord blood. *BMC Biotechnol.* **7**, 26 (2007).

96. Murata, D. *et al.* Multipotency of equine mesenchymal stem cells derived from synovial fluid. *Vet. J.* **202**, 53–61 (2014).

97. Ishikawa, S. *et al.* Isolation of equine peripheral blood stem cells from a Japanese native horse. *J. equine Sci.* **28**, 153–158 (2017).

98. Valtieri, M. & Sorrentino, A. The mesenchymal stromal cell contribution to homeostasis. *J. Cell. Physiol.* **217**, 296–300 (2008).

99. Yin, F. *et al.* Transplantation of mesenchymal stem cells exerts anti-apoptotic effects in adult rats after spinal cord ischemia-reperfusion injury. *Brain Res.* **1561**, 1–10 (2014).

100. Stagg, J. & Galipeau, J. Mechanisms of Immune Modulation by Mesenchymal Stromal Cells and Clinical Translation. *Current Molecular Medicine* vol. 13 856–867.

101. Maumus, M., Jorgensen, C. & Noël, D. Mesenchymal stem cells in regenerative medicine applied to rheumatic diseases: Role of secretome and exosomes. *Biochimie* **95**, 2229–2234 (2013).

102. Bartosh, T. J., Ullah, M., Zeitouni, S., Beaver, J. & Prockop, D. J. Cancer cells enter dormancy after cannibalizing mesenchymal stem/stromal cells (MSCs). *Proc. Natl. Acad. Sci.* **113**, E6447 LP-E6456 (2016).

103. Krampera, M. *et al.* Role for Interferon-γ in the Immunomodulatory Activity of Human Bone Marrow Mesenchymal Stem Cells. *Stem Cells* **24**, 386–398 (2006).

104. Mancheño-Corvo, P. *et al.* T Lymphocyte Prestimulation Impairs in a Time-Dependent Manner the Capacity of Adipose Mesenchymal Stem Cells to Inhibit Proliferation: Role of Interferon γ, Poly I:C, and Tryptophan Metabolism in Restoring Adipose Mesenchymal Stem Cell Inhibitory Effect. *Stem Cells Dev.* **24**, 2158–2170 (2015).

105. Hoogduijn, M. J. *et al.* Human Heart, Spleen, and Perirenal Fat-Derived Mesenchymal Stem Cells Have Immunomodulatory Capacities. *Stem Cells Dev.* **16**, 597–604 (2007).

106. Jorgensen, C., Deschaseaux, F., Planat-Benard, V. & Gabison, E. [Mesenchymal stem cells: A therapeutic update]. *Med. Sci. (Paris).* **27**, 275–284 (2011).

107. Zaher, W., Harkness, L., Jafari, A. & Kassem, M. An update of human mesenchymal stem cell biology and their clinical uses. *Arch. Toxicol.* **88**, 1069–1082 (2014).

108. Kandoi, S. *et al.* Evaluation of platelet lysate as a substitute for FBS in explant and enzymatic isolation methods of human umbilical cord MSCs. *Sci. Rep.* **8**, 12439 (2018).

109. Schrepfer, S. *et al.* Stem Cell Transplantation: The Lung Barrier. *Transplant. Proc.* **39**, 573–576 (2007).

110. Mäkelä, T. *et al.* Safety and biodistribution study of bone marrow–derived mesenchymal stromal cells and mononuclear cells and the impact of the administration route in an intact porcine model. *Cytotherapy* **17**, 392–402 (2015).

111. von Bahr, L. *et al.* Analysis of Tissues Following Mesenchymal Stromal Cell Therapy in Humans Indicates Limited Long-Term Engraftment and No Ectopic Tissue Formation. *Stem Cells* **30**, 1575–1578 (2012).

112. Baldari, S. *et al.* Challenges and Strategies for Improving the Regenerative Effects of Mesenchymal Stromal Cell-Based Therapies. *Int. J. Mol. Sci.* **18**, 2087 (2017).

113. Lohan, P., Treacy, O., Griffin, M. D., Ritter, T. & Ryan, A. E. Anti-Donor Immune Responses Elicited by Allogeneic Mesenchymal Stem Cells and Their Extracellular

Vesicles: Are We Still Learning? . *Frontiers in Immunology* vol. 8 1626 (2017).

114. Koniusz, S. *et al.* Extracellular Vesicles in Physiology, Pathology, and Therapy of the Immune and Central Nervous System, with Focus on Extracellular Vesicles Derived from Mesenchymal Stem Cells as Therapeutic Tools. *Front. Cell. Neurosci.* **10**, (2016).

115. Phinney, D. G. & Pittenger, M. F. Concise Review: MSC-Derived Exosomes for Cell-Free Therapy. *Stem Cells* **35**, 851–858 (2017).

116. Tran, C. & Damaser, M. S. Stem cells as drug delivery methods: application of stem cell secretome for regeneration. *Adv. Drug Deliv. Rev.* **82**–**83**, 1–11 (2015).

117. Li, Z. *et al.* Epigenetic Dysregulation in Mesenchymal Stem Cell Aging and Spontaneous Differentiation. *PLoS One* **6**, e20526 (2011).

118. Severino, V. *et al.* Insulin-like growth factor binding proteins 4 and 7 released by senescent cells promote premature senescence in mesenchymal stem cells. *Cell Death Dis.* **4**, e911–e911 (2013).

119. Nauta, A. J. *et al.* Donor-derived mesenchymal stem cells are immunogenic in an allogeneic host and stimulate donor graft rejection in a nonmyeloablative setting. *Blood* **108**, 2114–2120 (2006).

120. Zangi, L. *et al.* Direct Imaging of Immune Rejection and Memory Induction by Allogeneic Mesenchymal Stromal Cells. *Stem Cells* **27**, 2865–2874 (2009).

121. Hoynowski, S. M. *et al.* Characterization and differentiation of equine umbilical cord-derived matrix cells. *Biochem. Biophys. Res. Commun.* **362**, 347–353 (2007).

122. Hass, R., Kasper, C., Böhm, S. & Jacobs, R. Different populations and sources of human mesenchymal stem cells (MSC): A comparison of adult and neonatal tissue-derived MSC. *Cell Commun. Signal.* **9**, 12 (2011).

123. Barlow, S. *et al.* Comparison of Human Placenta- and Bone Marrow–Derived Multipotent Mesenchymal Stem Cells. *Stem Cells Dev.* **17**, 1095–1108 (2008).

124. Zhang, Y., Khan, D., Delling, J. & Tobiasch, E. Mechanisms underlying the osteo- and adipo-differentiation of human mesenchymal stem cells. *ScientificWorldJournal.* **2012**, 793823 (2012).

125. Rogers, I. & Casper, R. F. Umbilical cord blood stem cells. *Best Pract. Res. Clin. Obstet.*

Gynaecol. **18**, 893–908 (2004).

126. Siennicka, K., Zołocińska, A., Dębski, T. & Pojda, Z. Comparison of the Donor Age-Dependent and in Vitro Culture-Dependent Mesenchymal Stem Cell Aging in Rat Model. *Stem Cells Int.* **2021**, (2021).

127. Xu, L. *et al.* Tissue source determines the differentiation potentials of mesenchymal stem cells: a comparative study of human mesenchymal stem cells from bone marrow and adipose tissue. *Stem Cell Res. Ther.* **8**, 275 (2017).

128. Ma, Y. *et al.* The tissue origin of human mesenchymal stem cells dictates their therapeutic efficacy on glucose and lipid metabolic disorders in type II diabetic mice. *Stem Cell Res. Ther.* **12**, 385 (2021).

129. Lopez-Verrilli, M. A. *et al.* Mesenchymal stem cell-derived exosomes from different sources selectively promote neuritic outgrowth. *Neuroscience* **320**, 129–139 (2016).

130. Yi, T. *et al.* Manufacture of Clinical-Grade Human Clonal Mesenchymal Stem Cell Products from Single Colony Forming Unit-Derived Colonies Based on the Subfractionation Culturing Method. *Tissue Eng. Part C Methods* **21**, 1251–1262 (2015).

131. Van Loon, V. J. F., Scheffer, C. J. W., Genn, H. J., Hoogendoorn, A. C. & Greve, J. W. Clinical follow-up of horses treated with allogeneic equine mesenchymal stem cells derived from umbilical cord blood for different tendon and ligament disorders. *Vet. Q.* **34**, 92–97 (2014).

132. Geburek, F. *et al.* Effect of single intralesional treatment of surgically induced equine superficial digital flexor tendon core lesions with adipose-derived mesenchymal stromal cells: a controlled experimental trial. *Stem Cell Res. Ther.* **8**, 129 (2017).

133. Carvalho, A. M. *et al.* Equine tendonitis therapy using mesenchymal stem cells and platelet concentrates: a randomized controlled trial. *Stem Cell Res. Ther.* **4**, 85 (2013).

134. Depuydt, E. *et al.* The Evaluation of Equine Allogeneic Tenogenic Primed Mesenchymal Stem Cells in a Surgically Induced Superficial Digital Flexor Tendon Lesion Model . *Frontiers in Veterinary Science* vol. 8 (2021).

135. Ahrberg, A. B. *et al.* Effects of mesenchymal stromal cells versus serum on tendon healing in a controlled experimental trial in an equine model. *BMC Musculoskelet. Disord.* **19**, 230 (2018).

136. Hmadcha, A., Martin-Montalvo, A., Gauthier, B. R., Soria, B. & Capilla-Gonzalez, V. Therapeutic Potential of Mesenchymal Stem Cells for Cancer Therapy . *Frontiers in Bioengineering and Biotechnology* vol. 8 (2020).

137. Espinosa, G. *et al.* Equine bone marrow-derived mesenchymal stromal cells inhibit reactive oxygen species production by neutrophils. *Vet. Immunol. Immunopathol.* **221**, 109975 (2020).

138. Bastos, F. Z. *et al.* Quality control and immunomodulatory potential for clinical-grade equine bone marrow-derived mesenchymal stromal cells and conditioned medium. *Res. Vet. Sci.* **132**, 407–415 (2020).

139. Khatab, S. *et al.* Mesenchymal stem cell secretome reduces pain and subchondral bone alterations in a mouse osteoarthritis model. *Osteoarthr. Cartil.* **26**, S15–S16 (2018).

140. Bartekova, M., Radosinska, J., Jelemensky, M. & Dhalla, N. S. Role of cytokines and inflammation in heart function during health and disease. *Heart Fail. Rev.* **23**, 733–758 (2018).

141. Beohar, N., Rapp, J., Pandya, S. & Losordo, D. W. Rebuilding the Damaged Heart: The Potential of Cytokines and Growth Factors in the Treatment of Ischemic Heart Disease. *J. Am. Coll. Cardiol.* **56**, 1287–1297 (2010).

142. Gnecchi, M. *et al.* Evidence supporting paracrine hypothesis for Akt-modified mesenchymal stem cell-mediated cardiac protection and functional improvement. *FASEB J.* **20**, 661–669 (2006).

143. Tögel, F. *et al.* Vasculotropic, paracrine actions of infused mesenchymal stem cells are important to the recovery from acute kidney injury. *Am. J. Physiol. Physiol.* **292**, F1626–F1635 (2007).

144. Reis, L. A. *et al.* Bone Marrow-Derived Mesenchymal Stem Cells Repaired but Did Not Prevent Gentamicin-Induced Acute Kidney Injury through Paracrine Effects in Rats. *PLoS One* **7**, e44092 (2012).

145. Changjin, L. *et al.* Exosomes Mediate the Cytoprotective Action of Mesenchymal Stromal Cells on Hypoxia-Induced Pulmonary Hypertension. *Circulation* **126**, 2601–2611 (2012).

146. Zanotti, L. *et al.* Encapsulated mesenchymal stem cells for in vivo immunomodulation.

Leukemia **27**, 500–503 (2013).

147. Xia, X. *et al.* Secretome from hypoxia-conditioned adipose-derived mesenchymal stem cells promotes the healing of gastric mucosal injury in a rodent model. *Biochim. Biophys. Acta - Mol. Basis Dis.* **1864**, 178–188 (2018).

148. van Buul, G. M. *et al.* Mesenchymal stem cells secrete factors that inhibit inflammatory processes in short-term osteoarthritic synovium and cartilage explant culture. *Osteoarthr. Cartil.* **20**, 1186–1196 (2012).

149. Pouya, S. *et al.* Study the effects of mesenchymal stem cell conditioned medium injection in mouse model of acute colitis. *Int. Immunopharmacol.* **54**, 86–94 (2018).

150. Ranganath, S. H., Levy, O., Inamdar, M. S. & Karp, J. M. Harnessing the Mesenchymal Stem Cell Secretome for the Treatment of Cardiovascular Disease. *Cell Stem Cell* **10**, 244–258 (2012).

151. Park, S.-R. *et al.* Stem Cell Secretome and Its Effect on Cellular Mechanisms Relevant to Wound Healing. *Mol. Ther.* **26**, 606–617 (2018).

152. Guo, Z. Y. *et al.* Human umbilical cord mesenchymal stem cells promote peripheral nerve repair via paracrine mechanisms. *Neural Regen. Res.* **10**, 651–658 (2015).

153. Martins, L. F. *et al.* Mesenchymal stem cells secretome-induced axonal outgrowth is mediated by BDNF. *Sci. Rep.* **7**, 4153 (2017).

154. Guo, L. *et al.* Rescuing macrophage normal function in spinal cord injury with embryonic stem cell conditioned media. *Mol. Brain* **9**, 48 (2016).

155. Kay, A. G. *et al.* Mesenchymal Stem Cell-Conditioned Medium Reduces Disease Severity and Immune Responses in Inflammatory Arthritis. *Sci. Rep.* **7**, 18019 (2017).

156. Chen, Z.-Y., Hu, Y.-Y., Hu, X.-F. & Cheng, L.-X. The conditioned medium of human mesenchymal stromal cells reduces irradiation-induced damage in cardiac fibroblast cells. *J. Radiat. Res.* **59**, 555–564 (2018).

157. Niu, Y. *et al.* Bone mesenchymal stem cell-conditioned medium attenuates the effect of oxidative stress injury on NSCs by inhibiting the Notch1 signaling pathway. *Cell Biol. Int.* **43**, 1267–1275 (2019).

158. Xu, X., Li, D., Li, X., Shi, Q. & Ju, X. Mesenchymal stem cell conditioned medium

alleviates oxidative stress injury induced by hydrogen peroxide via regulating miR143 and its target protein in hepatocytes. *BMC Immunol.* **18**, 51 (2017).

159. Wang, B. *et al.* Secretome of Human Fetal Mesenchymal Stem Cell Ameliorates Replicative Senescence. *Stem Cells Dev.* **25**, 1755–1766 (2016).

160. Zhu, B. *et al.* Stem Cell-Derived Exosomes Prevent Aging-Induced Cardiac Dysfunction through a Novel Exosome/lncRNA MALAT1/NF-*κ*B/TNF-*α* Signaling Pathway. *Oxid. Med. Cell. Longev.* **2019**, 9739258 (2019).

161. Chen, W. *et al.* Conditioned medium of human bone marrow-derived stem cells promotes tendon-bone healing of the rotator cuff in a rat model. *Biomaterials* **271**, 120714 (2021).

162. Chen, Q. *et al.* Tenocyte proliferation and migration promoted by rat bone marrow mesenchymal stem cell-derived conditioned medium. *Biotechnol. Lett.* **40**, 215–224 (2018).

163. Lange-Consiglio, A. *et al.* Conditioned Medium from Horse Amniotic Membrane-Derived Multipotent Progenitor Cells: Immunomodulatory Activity In Vitro and First Clinical Application in Tendon and Ligament Injuries In Vivo. *Stem Cells Dev.* **22**, 3015–3024 (2013).

164. Gurunathan, S., Kang, M.-H., Jeyaraj, M., Qasim, M. & Kim, J.-H. Review of the Isolation, Characterization, Biological Function, and Multifarious Therapeutic Approaches of Exosomes. *Cells* **8**, 307 (2019).

165. Kalluri, R. The biology and function of exosomes in cancer. *J. Clin. Invest.* **126**, 1208–1215 (2016).

166. Moghadasi, S. *et al.* A paradigm shift in cell-free approach: the emerging role of MSCs-derived exosomes in regenerative medicine. *J. Transl. Med. 2021 191* **19**, 1–21 (2021).

167. Zhang, Y., Liu, Y., Liu, H. & Tang, W. H. Exosomes: biogenesis, biologic function and clinical potential. *Cell Biosci.* **9**, 19 (2019).

168. Garcia, N. A., Ontoria-Oviedo, I., González-King, H., Diez-Juan, A. & Sepúlveda, P. Glucose Starvation in Cardiomyocytes Enhances Exosome Secretion and Promotes Angiogenesis in Endothelial Cells. *PLoS One* **10**, e0138849 (2015).

169. Pegtel, D. M. & Gould, S. J. Exosomes. *Annu. Rev. Biochem.* **88**, 487–514 (2019).

170. Khalyfa, A. & Gozal, D. Exosomal miRNAs as potential biomarkers of cardiovascular risk in children. *J. Transl. Med.* **12**, 162 (2014).

171. Pegtel, D. M. *et al.* Functional delivery of viral miRNAs via exosomes. *Proc. Natl. Acad. Sci.* **107**, 6328 LP – 6333 (2010).

172. Squadrito, M. L. *et al.* Endogenous RNAs Modulate MicroRNA Sorting to Exosomes and Transfer to Acceptor Cells. *Cell Rep.* **8**, 1432–1446 (2014).

173. Vagner, T. *et al.* Protein Composition Reflects Extracellular Vesicle Heterogeneity. *Proteomics* **19**, e1800167–e1800167 (2019).

174. Greening, D. W. & Simpson, R. J. Understanding extracellular vesicle diversity – current status. *Expert Rev. Proteomics* **15**, 887–910 (2018).

175. Carayon, K. *et al.* Proteolipidic composition of exosomes changes during reticulocyte maturation. *J. Biol. Chem.* **286**, 34426–34439 (2011).

176. Segura, E., Amigorena, S. & Théry, C. Mature dendritic cells secrete exosomes with strong ability to induce antigen-specific effector immune responses. *Blood Cells, Mol. Dis.* **35**, 89–93 (2005).

177. Christ, L., Raiborg, C., Wenzel, E. M., Campsteijn, C. & Stenmark, H. Cellular Functions and Molecular Mechanisms of the ESCRT Membrane-Scission Machinery. *Trends Biochem. Sci.* **42**, 42–56 (2017).

178. Chiaruttini, N. *et al.* Relaxation of Loaded ESCRT-III Spiral Springs Drives Membrane Deformation. *Cell* **163**, 866–879 (2015).

179. John, M. *et al.* Structure and membrane remodeling activity of ESCRT-III helical polymers. *Science (80-.).* **350**, 1548–1551 (2015).

180. Lee, I.-H., Kai, H., Carlson, L.-A., Groves, J. T. & Hurley, J. H. Negative membrane curvature catalyzes nucleation of endosomal sorting complex required for transport (ESCRT)-III assembly. *Proc. Natl. Acad. Sci.* **112**, 15892 LP – 15897 (2015).

181. Raiborg, C. & Stenmark, H. The ESCRT machinery in endosomal sorting of ubiquitylated membrane proteins. *Nature* **458**, 445–452 (2009).

182. Hurley, J. H. The ESCRT complexes. *Crit. Rev. Biochem. Mol. Biol.* **45**, 463–487 (2010).

183. Joo, H. S., Suh, J. H., Lee, H. J., Bang, E. S. & Lee, J. M. Current Knowledge and Future Perspectives on Mesenchymal Stem Cell-Derived Exosomes as a New Therapeutic Agent. *International Journal of Molecular Sciences* vol. 21 (2020).

184. Katarina, T. *et al.* Ceramide Triggers Budding of Exosome Vesicles into Multivesicular Endosomes. *Science (80-.).* **319**, 1244–1247 (2008).

185. van Niel, G. *et al.* The Tetraspanin CD63 Regulates ESCRT-Independent and -Dependent Endosomal Sorting during Melanogenesis. *Dev. Cell* **21**, 708–721 (2011).

186. Rana, S., Yue, S., Stadel, D. & Zöller, M. Toward tailored exosomes: The exosomal tetraspanin web contributes to target cell selection. *Int. J. Biochem. Cell Biol.* **44**, 1574–1584 (2012).

187. Zech, D., Rana, S., Büchler, M. W. & Zöller, M. Tumor-exosomes and leukocyte activation: an ambivalent crosstalk. *Cell Commun. Signal.* **10**, 37 (2012).

188. Kooijmans, S. A. A. *et al.* Display of GPI-anchored anti-EGFR nanobodies on extracellular vesicles promotes tumour cell targeting. *J. Extracell. Vesicles* **5**, 31053 (2016).

189. Laulagnier, K. *et al.* Amyloid precursor protein products concentrate in a subset of exosomes specifically endocytosed by neurons. *Cell. Mol. Life Sci.* **75**, 757–773 (2018).

190. Sancho-Albero, M. *et al.* Exosome origin determines cell targeting and the transfer of therapeutic nanoparticles towards target cells. *J. Nanobiotechnology* **17**, 16 (2019).

191. Jurgielewicz, B. J., Yao, Y. & Stice, S. L. Kinetics and Specificity of HEK293T Extracellular Vesicle Uptake using Imaging Flow Cytometry. *Nanoscale Res. Lett.* **15**, 170 (2020).

192. Mulcahy, L. A., Pink, R. C. & Carter, D. R. F. Routes and mechanisms of extracellular vesicle uptake. *J. Extracell. Vesicles* **3**, 24641 (2014).

193. Abels, E. R. & Breakefield, X. O. Introduction to Extracellular Vesicles: Biogenesis, RNA Cargo Selection, Content, Release, and Uptake. *Cell. Mol. Neurobiol.* **36**, 301–312 (2016).

194. Teng, F. & Fussenegger, M. Shedding Light on Extracellular Vesicle Biogenesis and

Bioengineering. *Adv. Sci.* **8**, 2003505 (2021).

195. Jahn, R. & Scheller, R. H. SNAREs — engines for membrane fusion. *Nat. Rev. Mol. Cell Biol.* **7**, 631–643 (2006).

196. Montecalvo, A. *et al.* Mechanism of transfer of functional microRNAs between mouse dendritic cells via exosomes. *Blood* **119**, 756–766 (2012).

197. Morelli, A. E. *et al.* Endocytosis, intracellular sorting, and processing of exosomes by dendritic cells. *Blood* **104**, 3257–3266 (2004).

198. Joshi, B. S., de Beer, M. A., Giepmans, B. N. G. & Zuhorn, I. S. Endocytosis of Extracellular Vesicles and Release of Their Cargo from Endosomes. *ACS Nano* **14**, 4444–4455 (2020).

199. Delenclos, M. *et al.* Investigation of Endocytic Pathways for the Internalization of Exosome-Associated Oligomeric Alpha-Synuclein. *Front. Neurosci.* **11**, (2017).

200. Chen, C. *et al.* Visualization and intracellular dynamic tracking of exosomes and exosomal miRNAs using single molecule localization microscopy. *Nanoscale* **10**, 5154–5162 (2018).

201. Parolini, I. *et al.* Microenvironmental pH Is a Key Factor for Exosome Traffic in Tumor Cells*. *J. Biol. Chem.* **284**, 34211–34222 (2009).

202. Mercer, J., Schelhaas, M. & Helenius, A. Virus Entry by Endocytosis. *Annu. Rev. Biochem.* **79**, 803–833 (2010).

203. Shelke, G. V. *et al.* Endosomal signalling via exosome surface TGFβ-1. *J. Extracell. Vesicles* **8**, 1650458 (2019).

204. Tian, T. *et al.* Dynamics of exosome internalization and trafficking. *J. Cell. Physiol.* **228**, 1487–1495 (2013).

205. Tian, T., Wang, Y., Wang, H., Zhu, Z. & Xiao, Z. Visualizing of the cellular uptake and intracellular trafficking of exosomes by live-cell microscopy. *J. Cell. Biochem.* **111**, 488–496 (2010).

206. Ha, D., Yang, N. & Nadithe, V. Exosomes as therapeutic drug carriers and delivery vehicles across biological membranes: current perspectives and future challenges. *Acta Pharm. Sin. B* **6**, 287–296 (2016).

207. Heusermann, W. *et al.* Exosomes surf on filopodia to enter cells at endocytic hot spots, traffic within endosomes, and are targeted to the ER. *J. Cell Biol.* **213**, 173–184 (2016).

208. Leavitt, R. J., Limoli, C. L. & Baulch, J. E. miRNA-based therapeutic potential of stem cell-derived extracellular vesicles: a safe cell-free treatment to ameliorate radiation-induced brain injury. *Int. J. Radiat. Biol.* **95**, 427–435 (2019).

209. Vasudevan, S. Posttranscriptional Upregulation by MicroRNAs. *WIREs RNA* **3**, 311–330 (2012).

210. Makarova, J. A. *et al.* Intracellular and extracellular microRNA: An update on localization and biological role. *Prog. Histochem. Cytochem.* **51**, 33–49 (2016).

211. Godoy, P. M. *et al.* Large Differences in Small RNA Composition Between Human Biofluids. *Cell Rep.* **25**, 1346–1358 (2018).

212. Griffiths-Jones, S., Grocock, R. J., van Dongen, S., Bateman, A. & Enright, A. J. miRBase: microRNA sequences, targets and gene nomenclature. *Nucleic Acids Res.* **34**, D140–D144 (2006).

213. Malhas, A., Goulbourne, C. & Vaux, D. J. The nucleoplasmic reticulum: form and function. *Trends Cell Biol.* **21**, 362–373 (2011).

214. Santos, M. F. *et al.* VAMP-associated protein-A and oxysterol-binding protein-related protein 3 promote the entry of late endosomes into the nucleoplasmic reticulum. *J. Biol. Chem.* **293**, 13834–13848 (2018).

215. Spooner, R. A., Smith, D. C., Easton, A. J., Roberts, L. M. & Lord, J. M. Retrograde transport pathways utilised by viruses and protein toxins. *Virol. J.* **3**, (2006).

216. Izquierdo-Useros, N. *et al.* Capture and transfer of HIV-1 particles by mature dendritic cells converges with the exosome-dissemination pathway. *Blood* **113**, 2732–2741 (2009).

217. Royo, F., Théry, C., Falcón-Pérez, J. M., Nieuwland, R. & Witwer, K. W. Methods for Separation and Characterization of Extracellular Vesicles: Results of a Worldwide Survey Performed by the ISEV Rigor and Standardization Subcommittee. *Cells* vol. 9 (2020).

218. Livshits, M. A. *et al.* Isolation of exosomes by differential centrifugation: Theoretical

analysis of a commonly used protocol. *Sci. Rep.* **5**, 17319 (2015).

219. Théry, C., Amigorena, S., Raposo, G. & Clayton, A. Isolation and Characterization of Exosomes from Cell Culture Supernatants and Biological Fluids. *Curr. Protoc. Cell Biol.* **30**, 3.22.1-3.22.29 (2006).

220. Yoo, Y. K. *et al.* Toward Exosome-Based Neuronal Diagnostic Devices. *Micromachines* **9**, 634 (2018).

221. Cvjetkovic, A., Lötvall, J. & Lässer, C. The influence of rotor type and centrifugation time on the yield and purity of extracellular vesicles. *J. Extracell. vesicles* **3**, 10.3402/jev.v3.23111 (2014).

222. Sidhom, K., Obi, P. O. & Saleem, A. A Review of Exosomal Isolation Methods: Is Size Exclusion Chromatography the Best Option? *International Journal of Molecular Sciences* vol. 21 (2020).

223. Merchant, M. L. *et al.* Microfiltration isolation of human urinary exosomes for characterization by MS. *PROTEOMICS – Clin. Appl.* **4**, 84–96 (2010).

224. Konoshenko, M. Y., Lekchnov, E. A., Vlassov, A. V & Laktionov, P. P. Isolation of Extracellular Vesicles: General Methodologies and Latest Trends. *Biomed Res. Int.* **2018**, 8545347 (2018).

225. Rood, I. M. *et al.* Comparison of three methods for isolation of urinary microvesicles to identify biomarkers of nephrotic syndrome. *Kidney Int.* **78**, 810–816 (2010).

226. McNamara, R. P. *et al.* Large-scale, cross-flow based isolation of highly pure and endocytosis-competent extracellular vesicles. *J. Extracell. Vesicles* **7**, 1541396 (2018).

227. Busatto, S. *et al.* Tangential Flow Filtration for Highly Efficient Concentration of Extracellular Vesicles from Large Volumes of Fluid. *Cells* vol. 7 (2018).

228. Deregibus Chiara, M. *et al.* Charge-based precipitation of extracellular vesicles. *Int J Mol Med* **38**, 1359–1366 (2016).

229. Morani, M. *et al.* Electrokinetic characterization of extracellular vesicles with capillary electrophoresis: A new tool for their identification and quantification. *Anal. Chim. Acta* **1128**, 42–51 (2020).

230. Gascoyne, P. R. C. & Vykoukal, J. Particle separation by dielectrophoresis.

Electrophoresis **23**, 1973–1983 (2002).

231. Heath, N. *et al.* Rapid isolation and enrichment of extracellular vesicle preparations using anion exchange chromatography. *Sci. Rep.* **8**, 5730 (2018).

232. Wang, J. *et al.* The Novel Methods for Analysis of Exosomes Released from Endothelial Cells and Endothelial Progenitor Cells. *Stem Cells Int.* **2016**, 2639728 (2016).

233. Shao, H. *et al.* Protein typing of circulating microvesicles allows real-time monitoring of glioblastoma therapy. *Nat. Med.* **18**, 1835–1840 (2012).

234. Choi, H. & Mun, J. Y. Structural Analysis of Exosomes Using Different Types of Electron Microscopy. *Appl. Microsc.* **47**, 171–175 (2017).

235. YUANA, Y. *et al.* Atomic force microscopy: a novel approach to the detection of nanosized blood microparticles. *J. Thromb. Haemost.* **8**, 315–323 (2010).

236. Peak, T. C. *et al.* Exosomes secreted by placental stem cells selectively inhibit growth of aggressive prostate cancer cells. *Biochem. Biophys. Res. Commun.* **499**, 1004–1010 (2018).

237. Fuhrmann, G., Serio, A., Mazo, M., Nair, R. & Stevens, M. M. Active loading into extracellular vesicles significantly improves the cellular uptake and photodynamic effect of porphyrins. *J. Control. Release* **205**, 35–44 (2015).

238. Wang, S. *et al.* Recent advances in single extracellular vesicle detection methods. *Biosens. Bioelectron.* **154**, 112056 (2020).

239. Dehghani, M. & Gaborski, T. R. Chapter Two - Fluorescent labeling of extracellular vesicles. in *Extracellular vesicles* (eds. Spada, S. & Galluzzi, L. B. T.-M. in E.) vol. 645 15–42 (Academic Press, 2020).

240. Li, Y.-J., Wu, J.-Y., Wang, J.-M., Hu, X.-B. & Xiang, D.-X. Emerging strategies for labeling and tracking of extracellular vesicles. *J. Control. Release* **328**, 141–159 (2020).

241. Carnell-Morris, P., Tannetta, D., Siupa, A., Hole, P. & Dragovic, R. Analysis of Extracellular Vesicles Using Fluorescence Nanoparticle Tracking Analysis BT - Extracellular Vesicles: Methods and Protocols. in (eds. Kuo, W. P. & Jia, S.) 153–173 (Springer New York, 2017). doi:10.1007/978-1-4939-7253-1_13.

242. Rath, A., Glibowicka, M., Nadeau, V. G., Chen, G. & Deber, C. M. Detergent binding

explains anomalous SDS-PAGE migration of membrane proteins. *Proc. Natl. Acad. Sci.* **106**, 1760 LP – 1765 (2009).

243. Orozco, A. F. & Lewis, D. E. Flow cytometric analysis of circulating microparticles in plasma. *Cytom. Part A* **77A**, 502–514 (2010).

244. Oesterreicher, J. *et al.* Fluorescence-Based Nanoparticle Tracking Analysis and Flow Cytometry for Characterization of Endothelial Extracellular Vesicle Release. *Int. J. Mol. Sci.* **21**, 9278 (2020).

245. Ingato, D., Edson, J. A., Zakharian, M. & Kwon, Y. J. Cancer Cell-Derived, Drug-Loaded Nanovesicles Induced by Sulfhydryl-Blocking for Effective and Safe Cancer Therapy. *ACS Nano* **12**, 9568–9577 (2018).

246. Cho, S., Yang, H. C. & Rhee, W. J. Simultaneous multiplexed detection of exosomal microRNAs and surface proteins for prostate cancer diagnosis. *Biosens. Bioelectron.* **146**, 111749 (2019).

247. Fitts, C. A., Ji, N., Li, Y. & Tan, C. Exploiting Exosomes in Cancer Liquid Biopsies and Drug Delivery. *Adv. Healthc. Mater.* **8**, 1801268 (2019).

248. Santos, A. G., da Rocha, G. O. & de Andrade, J. B. Occurrence of the potent mutagens 2- nitrobenzanthrone and 3-nitrobenzanthrone in fine airborne particles. *Sci. Rep.* **9**, (2019).

249. Wu, L. *et al.* Exosomes derived from gastric cancer cells activate NF-κB pathway in macrophages to promote cancer progression. *Tumor Biol.* **37**, 12169–12180 (2016).

250. Waldenström, A. & Ronquist, G. Role of exosomes in myocardial remodeling. *Circ. Res.* **114**, 315–324 (2014).

251. Kitai, Y. *et al.* DNA-Containing Exosomes Derived from Cancer Cells Treated with Topotecan Activate a STING-Dependent Pathway and Reinforce Antitumor Immunity. *J. Immunol.* **198**, 1649–1659 (2017).

252. Jiang, L. *et al.* EpCAM-dependent extracellular vesicles from intestinal epithelial cells maintain intestinal tract immune balance. *Nat. Commun. 2016 71* **7**, 1–16 (2016).

253. Howitt, J. & Hill, A. F. Exosomes in the Pathology of Neurodegenerative Diseases. *J. Biol. Chem.* **291**, 26589–26597 (2016).

254. Mohammed, E., Khalil, E. & Sabry, D. Effect of Adipose-Derived Stem Cells and Their Exo as Adjunctive Therapy to Nonsurgical Periodontal Treatment: A Histologic and Histomorphometric Study in Rats. *Biomol. 2018, Vol. 8, Page 167* **8**, 167 (2018).

255. Harrell, C. R., Jovicic, N., Djonov, V. & Volarevic, V. Therapeutic Use of Mesenchymal Stem Cell-Derived Exosomes: From Basic Science to Clinics. *Pharm. 2020, Vol. 12, Page 474* **12**, 474 (2020).

256. Lai, P. *et al.* A potent immunomodulatory role of exosomes derived from mesenchymal stromal cells in preventing cGVHD 11 Medical and Health Sciences 1107 Immunology. *J. Hematol. Oncol.* **11**, 1–15 (2018).

257. Yu, B., Li, X.-R. & Zhang, X.-M. Mesenchymal stem cell-derived extracellular vesicles as a new therapeutic strategy for ocular diseases. *World J. Stem Cells* **12**, 178–187 (2020).

258. Yang, J., Zhang, X., Chen, X., Wang, L. & Yang, G. Exosome Mediated Delivery of miR-124 Promotes Neurogenesis after Ischemia. *Mol. Ther. - Nucleic Acids* **7**, 278–287 (2017).

259. Kamerkar, S. *et al.* Exosomes facilitate therapeutic targeting of oncogenic KRAS in pancreatic cancer. *Nat. 2017 5467659* **546**, 498–503 (2017).

260. Besse, B. *et al.* Dendritic cell-derived exosomes as maintenance immunotherapy after first line chemotherapy in NSCLC. *Oncoimmunology* **5**, (2016).

261. Shi, Z., Wang, Q. & Jiang, D. Extracellular vesicles from bone marrow-derived multipotent mesenchymal stromal cells regulate inflammation and enhance tendon healing. *J. Transl. Med.* **17**, 211 (2019).

262. Shi, Y. *et al.* Exosomes Derived from Bone Marrow Stromal Cells (BMSCs) Enhance Tendon-Bone Healing by Regulating Macrophage Polarization. *Med. Sci. Monit.* **26**, e923328–e923328 (2020).

263. Huang, Y. *et al.* Bone marrow mesenchymal stem cell-derived exosomes promote rotator cuff tendon-bone healing by promoting angiogenesis and regulating M1 macrophages in rats. *Stem Cell Res. Ther.* **11**, 496 (2020).

264. Wang, C., Hu, Q., Song, W., Yu, W. & He, Y. Adipose Stem Cell–Derived Exosomes Decrease Fatty Infiltration and Enhance Rotator Cuff Healing in a Rabbit Model of

Chronic Tears. *Am. J. Sports Med.* **48**, 1456–1464 (2020).

265. Shen, H., Yoneda, S., Abu-Amer, Y., Guilak, F. & Gelberman, R. H. Stem cell-derived extracellular vesicles attenuate the early inflammatory response after tendon injury and repair. *J. Orthop. Res.* **38**, 117–127 (2020).

266. Iraci, N., Leonardi, T., Gessler, F., Vega, B. & Pluchino, S. Focus on Extracellular Vesicles: Physiological Role and Signalling Properties of Extracellular Membrane Vesicles. *Int. J. Mol. Sci.* **17**, (2016).

267. Pascucci, L. *et al.* Membrane vesicles mediate pro-angiogenic activity of equine adipose-derived mesenchymal stromal cells. *Vet. J.* **202**, 361–366 (2014).

268. Lange-Consiglio, A. *et al.* Equine Amniotic Microvesicles and Their Anti-Inflammatory Potential in a Tenocyte Model In Vitro. *Stem Cells Dev.* **25**, 610–621 (2016).

269. Perrini, C. *et al.* Microvesicles secreted from equine amniotic-derived cells and their potential role in reducing inflammation in endometrial cells in an in-vitro model. *Stem Cell Res. Ther.* **7**, 169 (2016).

270. Hosseinkhani, B., Kuypers, S., van den Akker, N. M. S., Molin, D. G. M. & Michiels, L. Extracellular Vesicles Work as a Functional Inflammatory Mediator Between Vascular Endothelial Cells and Immune Cells. *Front. Immunol.* **9**, 1789 (2018).

271. Wolf, M. *et al.* A functional corona around extracellular vesicles enhances angiogenesis during skin regeneration and signals in immune cells. *bioRxiv* 808808 (2021) doi:10.1101/808808.

272. Liu, Y. *et al.* Conditioned Medium From the Stem Cells of Human Exfoliated Deciduous Teeth Ameliorates Neuropathic Pain in a Partial Sciatic Nerve Ligation Model . *Frontiers in Pharmacology* vol. 13 (2022).

273. Sevivas, N. *et al.* Mesenchymal Stem Cell Secretome: A Potential Tool for the Prevention of Muscle Degenerative Changes Associated With Chronic Rotator Cuff Tears. *Am. J. Sports Med.* **45**, 179–188 (2016).

274. Yu, H. *et al.* Bone marrow mesenchymal stem cell-derived exosomes promote tendon regeneration by facilitating the proliferation and migration of endogenous tendon stem/progenitor cells. *Acta Biomater.* **106**, 328–341 (2020).

275. Gissi, C. *et al.* Extracellular vesicles from rat-bone-marrow mesenchymal stromal/stem cells improve tendon repair in rat Achilles tendon injury model in dose-dependent manner: A pilot study. *PLoS One* **15**, e0229914 (2020).

276. Li, J. *et al.* Extracellular vesicles from hydroxycamptothecin primed umbilical cord stem cells enhance anti-adhesion potential for treatment of tendon injury. *Stem Cell Res. Ther.* **11**, 500 (2020).

277. Wang, Y. *et al.* Exosomes from tendon stem cells promote injury tendon healing through balancing synthesis and degradation of the tendon extracellular matrix. *J. Cell. Mol. Med.* **23**, 5475–5485 (2019).

278. Lange-Consiglio, A. *et al.* MicroRNAs of Equine Amniotic Mesenchymal Cell-derived Microvesicles and Their Involvement in Anti-inflammatory Processes. *Cell Transplant.* **27**, 45–54 (2018).

279. Kim, K. H., Park, T. S., Cho, B. W. & Kim, T. M. Nanoparticles from equine fetal bone marrow-derived cells enhance the survival of injured chondrocytes. *Animals* **10**, 1–17 (2020).

280. Arévalo-Turrubiarte, M., Baratta, M., Ponti, G., Chiaradia, E. & Martignani, E. Extracellular vesicles from equine mesenchymal stem cells decrease inflammation markers in chondrocytes in vitro. *Equine Vet. J.* **54**, 1133–1143 (2022).

281. Yeo, R. W. Y. *et al.* Mesenchymal stem cell: an efficient mass producer of exosomes for drug delivery. *Adv. Drug Deliv. Rev.* **65**, 336–341 (2013).

282. Niada, S., Giannasi, C., Magagnotti, C., Andolfo, A. & Brini, A. T. Proteomic analysis of extracellular vesicles and conditioned medium from human adipose-derived stem/stromal cells and dermal fibroblasts. *J. Proteomics* **232**, 104069 (2021).

283. Villatoro, A. J., Martín-Astorga, M. D. C., Alcoholado, C., Sánchez-Martín, M. D. M. & Becerra, J. Proteomic Analysis of the Secretome and Exosomes of Feline Adipose-Derived Mesenchymal Stem Cells. *Anim. an open access J. from MDPI* **11**, 295 (2021).

284. Gnecchi, M., Danieli, P., Malpasso, G. & Ciuffreda, M. C. Paracrine Mechanisms of Mesenchymal Stem Cells in Tissue Repair BT - Mesenchymal Stem Cells: Methods and Protocols. in (ed. Gnecchi, M.) 123–146 (Springer New York, 2016). doi:10.1007/978-1-4939-3584-0_7.

285. Skalnikova, H., Motlik, J., Gadher, S. J. & Kovarova, H. Mapping of the secretome of primary isolates of mammalian cells, stem cells and derived cell lines. *Proteomics* **11**, 691–708 (2011).

286. Baberg, F. *et al.* Secretome analysis of human bone marrow derived mesenchymal stromal cells. *Biochim. Biophys. Acta - Proteins Proteomics* **1867**, 434–441 (2019).

287. Islam, A., Urbarova, I., Bruun, J.-A. & Martinez-Zubiaurre, I. Large-scale secretome analyses unveil the superior immunosuppressive phenotype of umbilical cord stromal cells as compared to other adult mesenchymal stromal cells. *Eur. cells \& Mater.* **37**, 153–174 (2019).

288. Korf-Klingebiel, M. *et al.* Bone marrow cells are a rich source of growth factors and cytokines: implications for cell therapy trials after myocardial infarction. *Eur. Heart J.* **29**, 2851–2858 (2008).

289. Korf-Klingebiel, M. *et al.* Myeloid-derived growth factor (C19orf10) mediates cardiac repair following myocardial infarction. *Nat. Med.* **21**, 140–149 (2015).

290. Beer, L. *et al.* Analysis of the Secretome of Apoptotic Peripheral Blood Mononuclear Cells: Impact of Released Proteins and Exosomes for Tissue Regeneration. *Sci. Rep.* **5**, 16662 (2015).

291. Al-Sadi, O. *et al.* Tenocytes, pro-inflammatory cytokines and leukocytes: a relationship? *Muscles. Ligaments Tendons J.* **1**, 68–76 (2012).

292. John, T. *et al.* Effect of pro-inflammatory and immunoregulatory cytokines on human tenocytes. *J. Orthop. Res.* **28**, 1071–1077 (2010).

293. Podbielska, M. *et al.* Cytokine-induced release of ceramide-enriched exosomes as a mediator of cell death signaling in an oligodendroglioma cell line. *J. Lipid Res.* **57**, 2028–2039 (2016).

294. Lauber, K. *et al.* Apoptotic Cells Induce Migration of Phagocytes via Caspase-3-Mediated Release of a Lipid Attraction Signal. *Cell* **113**, 717–730 (2003).

295. Sunshine, H. & Iruela-Arispe, M. L. Membrane Lipids and Cell Signaling. *Curr. Opin. Lipidol.* **28**, 408 (2017).

296. Németh, K. *et al.* Bone marrow stromal cells attenuate sepsis via prostaglandin E2–

dependent reprogramming of host macrophages to increase their interleukin-10 production. *Nat. Med.* **15**, 42–49 (2009).

297. Zagoura, D. S. *et al.* Therapeutic potential of a distinct population of human amniotic fluid mesenchymal stem cells and their secreted molecules in mice with acute hepatic failure. *Gut* **61**, 894 LP – 906 (2012).

298. Turner, J.-E. *et al.* IL-9–mediated survival of type 2 innate lymphoid cells promotes damage control in helminth-induced lung inflammation. *J. Exp. Med.* **210**, 2951–2965 (2013).

299. Lee, R. H., Oh, J. Y., Choi, H. & Bazhanov, N. Therapeutic factors secreted by mesenchymal stromal cells and tissue repair. *J. Cell. Biochem.* **112**, 3073–3078 (2011).

300. Mirabella, T., Cilli, M., Carlone, S., Cancedda, R. & Gentili, C. Amniotic liquid derived stem cells as reservoir of secreted angiogenic factors capable of stimulating neo-arteriogenesis in an ischemic model. *Biomaterials* **32**, 3689–3699 (2011).

301. Giampà, C. *et al.* Conditioned medium from amniotic cells protects striatal degeneration and ameliorates motor deficits in the R6/2 mouse model of Huntington's disease. *J. Cell. Mol. Med.* **23**, 1581–1592 (2019).

302. Jenner, F. *et al.* Evaluation of the Potential of Umbilical Cord Mesenchymal Stromal Cell–Derived Small Extracellular Vesicles to Improve Rotator Cuff Healing: A Pilot Ovine Study. *Am. J. Sports Med.* **51**, 331–342 (2023).

303. Mol, E. A., Goumans, M. J., Doevendans, P. A., Sluijter, J. P. G. & Vader, P. Higher functionality of extracellular vesicles isolated using size-exclusion chromatography compared to ultracentrifugation. *Nanomedicine Nanotechnology, Biol. Med.* **13**, 2061–2065 (2017).

304. Kennedy, T. L., Russell, A. J. & Riley, P. Experimental limitations of extracellular vesicle-based therapies for the treatment of myocardial infarction. *Trends Cardiovasc. Med.* **31**, 405–415 (2021).

305. Zhao, Z., Wijerathne, H., Godwin, A. K. & Soper, S. A. Isolation and analysis methods of extracellular vesicles (EVs). *Extracell. vesicles Circ. nucleic acids* **2**, (2021).

306. Veerman, R. E. *et al.* Molecular evaluation of five different isolation methods for extracellular vesicles reveals different clinical applicability and subcellular origin. *J.*

Extracell. Vesicles **10**, e12128 (2021).

307. Lobb, R. J. *et al.* Optimized exosome isolation protocol for cell culture supernatant and human plasma. *J. Extracell. vesicles* **4**, (2015).

308. Nieuwland, R., Falcón-Pérez, J. M., Théry, C. & Witwer, K. W. Rigor and standardization of extracellular vesicle research: Paving the road towards robustness. *J. Extracell. Vesicles* **10**, e12037 (2020).

309. Margolis, L. & Sadovsky, Y. The biology of extracellular vesicles: The known unknowns. *PLoS Biol.* **17**, (2019).

310. Kooijmans, S. A. A., de Jong, O. G. & Schiffelers, R. M. Exploring interactions between extracellular vesicles and cells for innovative drug delivery system design. *Adv. Drug Deliv. Rev.* **173**, 252–278 (2021).

311. Silva, A. K. A. *et al.* Development of extracellular vesicle-based medicinal products: A position paper of the group 'Extracellular Vesicle translatiOn to clinicaL perspectiVEs - EVOLVE France'. *Adv. Drug Deliv. Rev.* **179**, (2021).

312. Xu, R., Greening, D. W., Zhu, H.-J., Takahashi, N. & Simpson, R. J. Extracellular vesicle isolation and characterization: toward clinical application. *J. Clin. Invest.* **126**, 1152–1162 (2016).

313. Klyachko, N. L., Arzt, C. J., Li, S. M., Gololobova, O. A. & Batrakova, E. V. Extracellular Vesicle-Based Therapeutics: Preclinical and Clinical Investigations. *Pharm. 2020, Vol. 12, Page 1171* **12**, 1171 (2020).

314. Gudbergsson, J. M., Johnsen, K. B., Skov, M. N. & Duroux, M. Systematic review of factors influencing extracellular vesicle yield from cell cultures. *Cytotechnology* **68**, 579 (2016).

315. Gupta, D., Zickler, A. M. & El Andaloussi, S. Dosing extracellular vesicles. *Adv. Drug Deliv. Rev.* **178**, 113961 (2021).

316. Salmond, N. & Williams, K. C. Isolation and characterization of extracellular vesicles for clinical applications in cancer – time for standardization? *Nanoscale Adv.* **3**, 1830–1852 (2021).

317. Lötvall, J. *et al.* Minimal experimental requirements for definition of extracellular vesicles

and their functions: a position statement from the International Society for Extracellular Vesicles. *https://doi.org/10.3402/jev.v3.26913* **3**, (2014).

318. Boulestreau, J., Maumus, M., Rozier, P., Jorgensen, C. & Noël, D. Mesenchymal Stem Cell Derived Extracellular Vesicles in Aging. *Front. Cell Dev. Biol.* **8**, 107 (2020).

319. Zhang, Y., Ravikumar, M., Ling, L., Nurcombe, V. & Cool, S. M. Age-Related Changes in the Inflammatory Status of Human Mesenchymal Stem Cells: Implications for Cell Therapy. *Stem cell reports* **16**, 694–707 (2021).

320. Urbanelli, L., Buratta, S., Sagini, K., Tancini, B. & Emiliani, C. Extracellular Vesicles as New Players in Cellular Senescence. *Int. J. Mol. Sci. 2016, Vol. 17, Page 1408* **17**, 1408 (2016).

321. Lunyak, V. V., Amaro-Ortiz, A. & Gaur, M. Mesenchymal stem cells secretory responses: Senescence messaging secretome and immunomodulation perspective. *Front. Genet.* **8**, 220 (2017).

322. Carlomagno, C. *et al.* Raman Fingerprint of Extracellular Vesicles and Conditioned Media for the Reproducibility Assessment of Cell-Free Therapeutics . *Frontiers in Bioengineering and Biotechnology* vol. 9 (2021).

323. Papait, A. *et al.* Comparison of EV-free fraction, EVs, and total secretome of amniotic mesenchymal stromal cells for their immunomodulatory potential: a translational perspective . *Frontiers in Immunology* vol. 13 (2022).

324. González-Cubero, E., González-Fernández, M. L., Olivera, E. R. & Villar-Suárez, V. Extracellular vesicle and soluble fractions of adipose tissue-derived mesenchymal stem cells secretome induce inflammatory cytokines modulation in an in vitro model of discogenic pain. *Spine J.* **22**, 1222–1234 (2022).

325. Mitchell, R. *et al.* Secretome of adipose-derived mesenchymal stem cells promotes skeletal muscle regeneration through synergistic action of extracellular vesicle cargo and soluble proteins. *Stem Cell Res. Ther.* **10**, 116 (2019).

326. Giannasi, C. *et al.* Comparison of two ASC-derived therapeutics in an in vitro OA model: secretome versus extracellular vesicles. *Stem Cell Res. Ther.* **11**, 521 (2020).

327. Wagner, T. *et al.* Different pro-angiogenic potential of γ-irradiated PBMC-derived secretome and its subfractions. *Sci. Rep.* **8**, 18016 (2018).

328. Sung, B. H., Parent, C. A. & Weaver, A. M. Extracellular vesicles: Critical players during cell migration. *Dev. Cell* **56**, 1861–1874 (2021).

329. Kriebel, P. W. *et al.* Extracellular vesicles direct migration by synthesizing and releasing chemotactic signals. *J. Cell Biol.* **217**, 2891–2910 (2018).

330. Niada, S., Giannasi, C., Gualerzi, A., Banfi, G. & Brini, A. T. Differential Proteomic Analysis Predicts Appropriate Applications for the Secretome of Adipose-Derived Mesenchymal Stem/Stromal Cells and Dermal Fibroblasts. *Stem Cells Int.* **2018**, 7309031 (2018).

331. Monguió-Tortajada, M., Gálvez-Montón, C., Bayes-Genis, A., Roura, S. & Borràs, F. E. Extracellular vesicle isolation methods: rising impact of size-exclusion chromatography. *Cell. Mol. Life Sci.* **76**, 2369–2382 (2019).

332. Van Deun, J. *et al.* The impact of disparate isolation methods for extracellular vesicles on downstream RNA profiling. *J. Extracell. Vesicles* **3**, 24858 (2014).

333. Patel, D. B. *et al.* Impact of cell culture parameters on production and vascularization bioactivity of mesenchymal stem cell-derived extracellular vesicles. *Bioeng. Transl. Med.* **2**, 170–179 (2017).

334. Miclau, K., Hambright, W. S., Huard, J., Stoddart, M. J. & Bahney, C. S. Cellular expansion of MSCs: Shifting the regenerative potential. *Aging Cell* **22**, e13759 (2023).

335. Gualerzi, A. *et al.* Raman spectroscopy uncovers biochemical tissue-related features of extracellular vesicles from mesenchymal stromal cells. *Sci. Rep.* **7**, 9820 (2017).

336. Shin, S. *et al.* Comparative proteomic analysis of the mesenchymal stem cells secretome from adipose, bone marrow, placenta and wharton's jelly. *Int. J. Mol. Sci.* **22**, 1–17 (2021).

337. Zhu, Y. *et al.* A Comprehensive Proteomics Analysis Reveals a Secretory Path- and Status-Dependent Signature of Exosomes Released from Tumor-Associated Macrophages. *J. Proteome Res.* **14**, 4319–4331 (2015).

338. Eddershaw, P. J., Beresford, A. P. & Bayliss, M. K. ADME/PK as part of a rational approach to drug discovery. *Drug Discov. Today* **5**, 409–414 (2000).

339. Charoenviriyakul, C. *et al.* Cell type-specific and common characteristics of exosomes

derived from mouse cell lines: Yield, physicochemical properties, and pharmacokinetics. *Eur. J. Pharm. Sci.* **96**, 316–322 (2017).

340. Smyth, T. *et al.* Biodistribution and delivery efficiency of unmodified tumor-derived exosomes. *J. Control. Release* **199**, 145–155 (2015).

341. Soukup, R. *et al.* Characterisation of Extracellular Vesicles from Equine Mesenchymal Stem Cells. *Int. J. Mol. Sci.* **23**, (2022).

342. Peinado, H. *et al.* Melanoma exosomes educate bone marrow progenitor cells toward a pro-metastatic phenotype through MET. *Nat. Med.* **18**, 883–891 (2012).

343. ATKINSON, A. J. CHAPTER 1 - Introduction to Clinical Pharmacology. in (eds. Atkinson, A. J., Abernethy, D. R., Daniels, C. E., Dedrick, R. L. & Markey, S. P. B. T.-P. of C. P. (Second E.) 1–7 (Academic Press, 2007). doi:https://doi.org/10.1016/B978-012369417-1/50041-9.